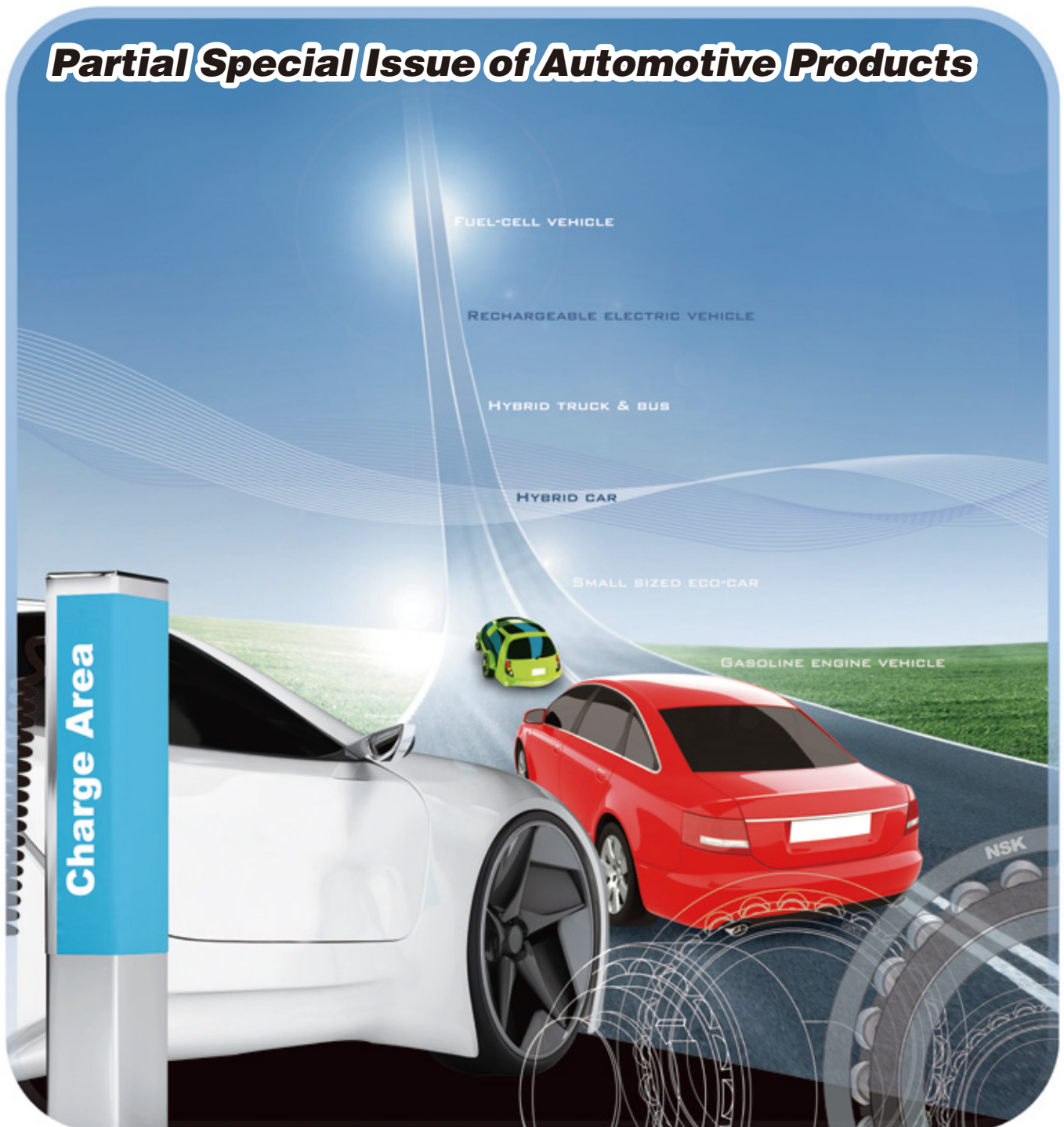


NSK Technical Journal

Motion & Control

No. 24 December 2014

Partial Special Issue of Automotive Products



ISSN1342-3630

NSK

MOTION & CONTROL No. 24

NSK Technical Journal

Printed and Published: December 2014

ISSN1342-3630

Publisher: NSK Ltd., Ohsaki, Shinagawa, Tokyo, JAPAN

Public Relations Department

TEL +81-3-3779-7051

FAX +81-3-3779-7431

Editor: Naoki MITSUE

Managing Editor: Hitoshi EBISAWA

Design, Typesetting & Printing: Kuge Printing Co., Ltd.

© NSK Ltd.

The contents of this journal are the copyright of NSK Ltd.

Contents

Partial Special Issue of Automobile Products

Preface

NSK's Automotive Products	Y. Shoda	1
---------------------------------	----------	---

Technical Articles

Development of Ultrahigh-Speed Ball Bearings for Motors in Next-Generation Hybrid Vehicles	T. Maejima, T. Tanaka	2
Development of New-Generation Low-Frictional-Torque Tapered Roller Bearings	T. Saito, H. Maejima, T. Hiramoto	8
Development of Ultralow-Torque Ball Bearings for Hybrid Vehicles	Y. Tsuchida, S. Tanaka, T. Muraoka	15
Development of Low-Torque Thrust Needle Roller Bearing for Automotive Air Conditioner Compressors	T. Yano, H. Aida, S. Murata	22
Development of Low-Torque Hub Unit Bearings	M. Tanahashi	27
Technological Trends of Bearings for Electric Motors on Board Vehicles	N. Izawa	34

New Products

Ultrahigh-Speed Ball Bearing for Motors and Power Generators in Next-Generation Hybrid Vehicles	38
Ultralow-Torque Sealed-Clean Ball Bearings for Transmissions	40
High-Speed-Type Miniature Roller & Cage Assembly for Planetary Gears	42
Long-Life Thrust Needle Roller Bearings Using Alternative Material to SK85	44
High-Strength, Pressed-Steel Pulley	46
Newly Developed, Highly Durable Clutch Pulley Unit	48
Electric Power Steering System for Excellent On-Center Steering Feel	50
Ball Screw for Motorcycle Brake Systems	52

Technical Articles

Mechanism of Dent Initiated Flaking and Bearing Life Enhancement Technology under Contaminated Lubrication Condition	
Part I: Effect of Tangential Force on Dent Initiated Flaking	T. Ueda, N. Mitamura 54
Part II: Effect of Rolling Element Surface Roughness on Flaking Resulting from Dents, and Life Enhancement Technology of Rolling Bearings under Contaminated Lubrication Condition	T. Ueda, N. Mitamura 64
Oil Film Behavior under Minute Vibrating Conditions in EHL Point Contacts	T. Maruyama, T. Saitoh 72
Development of ROBUSTSLIM Series of Low-Profile Angular Contact Ball Bearings for Swivel Units in Machine Tools	M. Aoki 80

New Products

Smear-Resistant Spherical Roller Bearings for Papermaking Machinery	86
High-Performance Bearings for Satellite Attitude Control Reaction Wheels	88
Slight-Preload Type RA Series Roller Guides of NSK Linear Guides	90

NSK's Automotive Products

Yoshio Shoda
Special Adviser

The Japanese automobile industry has been steadily making developments while overcoming the challenges brought about by restrictions on exhaust emissions and the oil crisis of the 1970s. Subsequently, automakers have pursued improved fuel economy, higher power output, and various comfortable rides since the 1980s. Japanese brand automobiles have been especially excelling at maintaining the best quality levels in the world with respect to higher fuel economy and safety features. Starting with NSK's launch of ball-screw-type steering systems into the market in 1959, NSK also has been launching needle roller bearings and automatic transmission components into the market since the 1960s. Moreover, NSK launched long-life sealed-clean bearings for transmissions, and the third-generation hub unit bearing (HUB3) for automobiles in 1987 in response to demand for reductions in size and weight, and improved fuel economy. In this manner, NSK has been constantly providing the most advanced technology for the automotive market. In addition, NSK released the electric power steering (EPS) into the market in 1989, and was able to fulfill a long-lasting dream of introducing the half-toroidal continuously variable transmission (CVT) to the market in 1999. These components were ahead of their times.

As a consequence of the global financial crisis triggered by the Lehman Brothers collapse in 2008, large changes in the automotive market and related technologies have become prominent. Electric drive, as represented by hybrid vehicles and electric vehicles, has been rapidly developing in response to energy conservation requirements and environmental issues, as automotive markets rapidly expand in developing countries. NSK has been developing transmission bearings and hub unit bearings that have promoted further reductions in size and weight, and performed with lower frictional torque. NSK has also been introducing new products in response to new developments in automotive technology. These include bearings unique to automobiles used for new applications or used under more severe conditions such as the bearings for hybrid vehicles and electric vehicles, and ball screws for electrifying actuators. Consequently, NSK has developed hub unit bearings for the four largest emerging economies of Brazil, Russia, India, and China—so-called BRIC markets—as products that are suitable for the automotive markets in developing countries.

NSK continues to develop bearings that perform with less friction, which contributes to reducing energy consumption, and continues to develop products that promote reductions in size and weight, which contribute to environmental friendliness. These products have been developed on the basis of NSK's four core technologies: tribology, material engineering, analysis technology, and mechatronics. In this special issue on automotive components, some of NSK's recent technological achievements and products are introduced. NSK will further strengthen its research development capabilities and contribute to the progress of automotive technologies for resolving global environmental issues and promoting energy conservation far into the future.



Yoshio Shoda

Development of Ultrahigh-Speed Ball Bearings for Motors in Next-Generation Hybrid Vehicles

Takeshi Maejima, Future Technology Development Center
Takanori Tanaka, Automotive Bearing Technology Center

ABSTRACT

In recent years, issues resulting from the effects of global warming, such as climate change, which is caused by greenhouse gases including carbon dioxide, have been discussed as one of the pressing global environmental issues. In the automotive field, each manufacturer in Japan is strictly required to reduce tailpipe emissions of carbon dioxide, which is one of the greenhouse gases, and is working on improving fuel efficiency in order to reduce the emissions of carbon dioxide. Most major automobile manufacturers have seriously focused on developing hybrid vehicles or electric vehicles to reduce the consumption of fossil fuels. The next generation of hybrid-vehicle motors will need to be smaller and lighter while providing sufficient performance capabilities to endure ultrahigh-speed rotation for increasing power output.

NSK has clarified bearing issues related to ultrahigh-speed rotation and has introduced new ball bearings that provide sufficient performance capabilities to endure conditions of more than 30 000 rpm, which is 1.5 times faster than the performance limits of currently available bearings.

1. Introduction

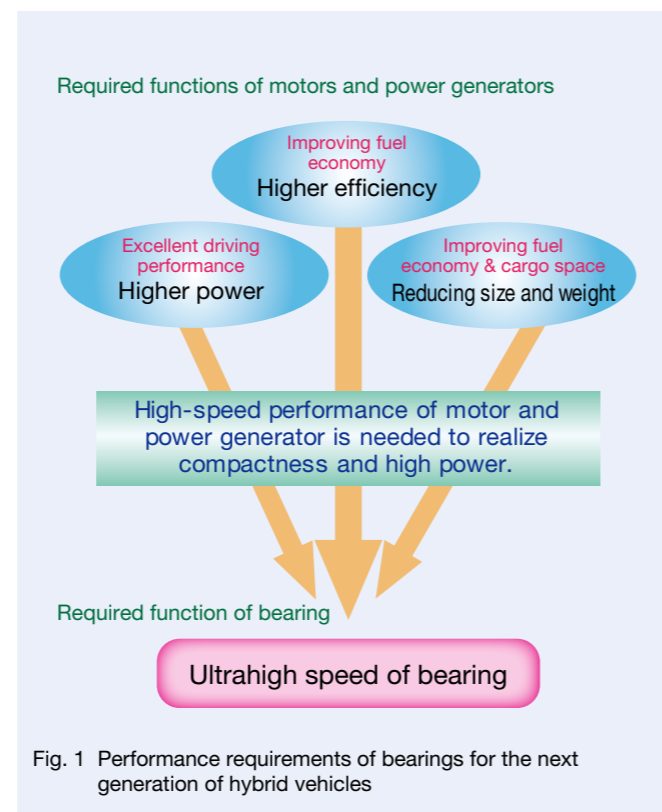
In recent years, issues resulting from the effects of global warming, such as climate change, which is caused by greenhouse gases including carbon dioxide, have been discussed as one of the pressing global environmental issues. In the automotive field, each manufacturer in Japan is strictly required to reduce tailpipe emissions of carbon dioxide, which is one of the greenhouse gases, and is working on improving fuel economy in order to reduce the emissions of carbon dioxide. Therefore, attention has been seriously focused on hybrid vehicles or electric vehicles. Especially, most major automobile manufacturers have seriously focused their attention on hybrid vehicles, for which demand is rapidly increasing, in efforts to improve fuel economy as it is anticipated that total global sales of hybrid vehicles will exceed ten million vehicles in 2020¹⁾, though sales were approximately one million vehicles in 2010. While the motors for next-generation hybrid vehicles have been advanced in term of reduction in size and weight in order to satisfy the requirement for improving fuel economy, assuring sufficient cargo space, and providing excellent driving performance, the need for ultrahigh-speed rotating performance of the motors has been increasing for increased power output.

In this article, NSK has clarified bearing issues related to ultrahigh-speed rotation and has introduced new ball bearings that provide sufficient performance capabilities to endure operating conditions of more than 30 000 rpm, which is 1.5 times faster than the performance limits of currently available bearings.

2. Required Functions and Issues Related to Ultrahigh-Speed Ball Bearings

Figure 1 shows the required functions of motor bearings for the next generation of hybrid vehicles.

As stated above, the next generation of hybrid-vehicle motors will need to be smaller and lighter for improving



fuel economy and enlarging the engine room space for mounting, and at the same time, to increase power output. Since motor power output will be reduced if the motors are made smaller, higher speed rotation is necessary in order to ensure the same amount or a higher amount of power output than that of current motors for the motors to be made smaller.

Deep groove ball bearings are generally used as the support bearing of motors in consideration of low torque and ease of assembly. However, there are problems under high-speed rotation, such as insufficient lubrication by centrifugal force, heat generation and wear by bearing friction, and cage fracturing^{2)–4)}.

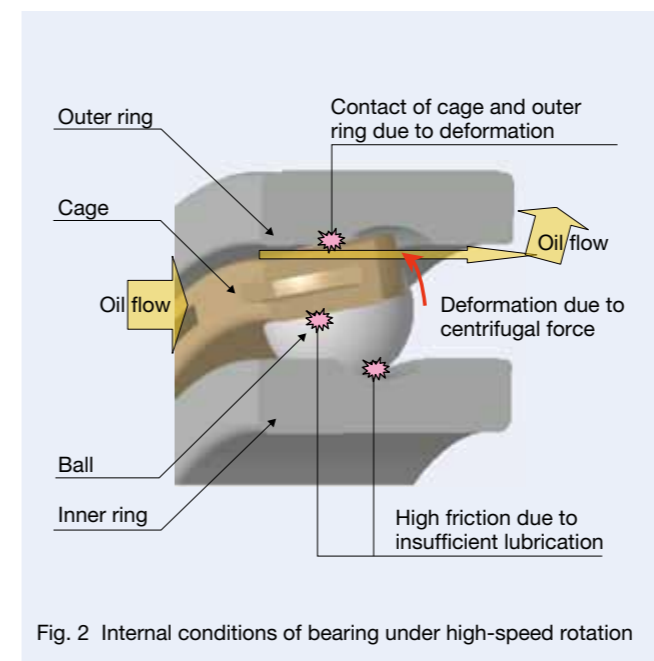
2.1 Lubrication

Figure 2 shows bearing conditions under high-speed rotation.

Though oil lubrication or grease lubrication is generally used for bearings, oil lubrication, which is superior in lubricating properties, needs to be adopted for ultrahigh-speed ball bearings for next-generation hybrid vehicles.

If oil lubrication is used, however, rotational speeds of the rolling elements and the cage are high, a large amount of oil moves towards the outside diameter side of the bearing due to centrifugal force, and insufficient lubrication occurs between the balls and the inner ring, or between the balls and the cage. A bearing with insufficient lubrication leads to seizure of the internal components and then bearing lock, and finally results in motor failure.

In contrast, there is a method to supplement insufficient lubrication by increasing the amount of lubricating oil. However, agitation resistance of oil increases rotational torque of the bearing, and fuel efficiency of the automobiles decreases. This fails to comply with the requirements of bearings for drive motors.



2.2 Bearing friction

It is not enough to address only the issue of insufficient lubrication for achieving ultrahigh-speed rotation of deep groove ball bearings. Other issues such as reducing the amount of friction of the bearing interior are also required. The details of these issues are described in the following sections.

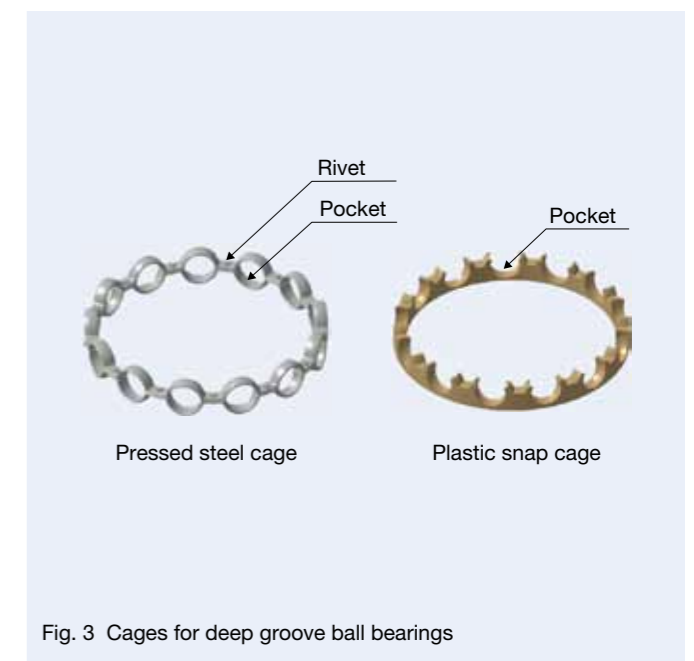
2.2.1 Friction between ball and raceway surface

When a deep groove ball bearing is rotated, sliding friction occurs between the ball and the raceway surface in proportion to the rotational speed of the bearing. Sliding friction is insignificant at general rotational speeds. But it is important to control the sliding friction between the ball and the raceway surface under ultrahigh-speed conditions because heat generation of the bearing becomes high due to the severe increase of friction.

2.2.2 Friction between ball and cage

Figure 3 shows the types of cages.

Pressed steel ribbon cages (pressed steel cage) or plastic snap cages are generally used as the cage for deep groove ball bearings. A pressed steel cage has a structure of two press-formed ribbons (with spherical pressed pocket surfaces) that are riveted together. In addition, a plastic snap cage is formed using nylon resin reinforced with glass fibers. Because both cages have a structure of spherical shaped pocket surfaces for holding balls, friction occurs between the ball and the pocket surface. If operated under normal rotational speeds, and since the force acting at the impact of ball and cage is small, friction at the cage pocket surface is insignificant on par with friction between the ball and the bearing rings. Under ultrahigh-speed rotation (30 000 rpm), however, the circumferential speed of the ball reaches approximately 40 m/s, and moreover,



the force at the point of impact between the ball and the cage increases. Because a plastic snap cage has a self-lubricating property and is lightweight, it is advantageous for high speed compared with a pressed steel cage. Since wear at the pocket surface becomes larger due to friction between the ball and the cage pocket surface when conditions of insufficient lubrication occur under ultrahigh speeds, however, it is possible that the cage could drop out of the bearing interior in the worst-case scenario.

2.3 Cage strength

From the viewpoint of the aforementioned, plastic snap cages have been adopted. However, when a typical plastic snap cage is rotated at high speed, the cage deforms in the direction of the outside surface due to centrifugal force while the circular ring of the cage acts as the pivot point of deformation as shown in Figure 2, and the cage makes contact with the outer ring. When the cage makes contact with the outer ring, the amount of bearing heat generation increases. In addition, the cage breaks into pieces because of the excessive stress that occurs on the circular ring pocket surface of the largely deformed cage.

A strong cage structure that is capable of withstanding centrifugal forces needs to be developed as a measure against the aforementioned cage deformation and breakage. It is possible to increase cage strength by thickening the cage circular ring. However, this would require wider bearings because the cage would spread out of the bearing under current bearing widths, and an increase in bearing width would increase the occupied space area in the motor and add additional weight, which is counterproductive to the need for a compact and lightweight design.

3. Features of Newly Developed Bearing

Optimization of bearing specifications, oil flow control in the bearing interior, and changes to the plastic cage configuration were conducted in an effort to resolve the aforementioned problems under ultrahigh-speed rotation. Further details are described in the following sections.

3.1 Mounting of a control plate for controlling oil flow

Figure 4 shows a cross-sectional view of the bearing and illustration of oil flow within the current bearing and the newly developed bearing.

For the newly developed bearing, a plate to control oil flow was mounted to the lubricant inflow side of the bearing face of rings for addressing the problem of insufficient lubrication on the inner ring side under ultrahigh-speed rotation. Since this plate facilitates the supply of lubricant oil from within the bearing interior, it becomes possible to prevent bearing seizure by supplying oil assuredly to the inner ring side where lubrication tends to become insufficient, even under ultrahigh-speed rotation where large centrifugal forces are generated.

3.2 Reduction of friction

3.2.1 Optimization of bearing specifications

The newly developed bearing reduces the amount of sliding between the ball and bearing rings by optimizing the groove dimensions and ball diameter (bearing internal specifications), and as a result, friction of the developed bearing under ultrahigh-speed rotation is restricted.

Figure 5 shows the calculated results for PV values (P: surface pressure; V: sliding speed) of each bearing. The PV value of the newly developed bearing has been reduced to approximately 30 % that of the current bearing.

3.2.2 Adoption of plastic cage and optimum configuration

As stated above, plastic snap cages are advantageous for high speeds because of their superior self-lubricating properties and lighter weight compared with that of pressed-steel cages. However, the surface of the cage pocket with the current cage structure wears under ultrahigh-speed rotation since ball-rotating speed is very high under ultrahigh-speed rotation.

To prevent wear of the cage pocket surface, there is a method of improving lubrication properties of the pocket surface, and also a method of reducing impact forces

between the balls and the cage. The former is improved by mounting an oil flow control plate as explained in Section 3.1. For the latter, impact forces between the balls and the cage are reduced and wear is controlled by adjusting the amount of clearance between the balls and the cage pockets and the amount of clearance between the inner ring outside surface and the cage bore surface.

3.3 Improvement of cage strength

The cage assembled into the newly developed bearing offers improved cage rigidity as a result of thickening the circular ring in the axial direction in comparison with the thickness of the current cage. This thicker circular ring prevents the cage tips from deforming towards the outer part of the bearing under ultrahigh-speed rotation. In addition, breakage of the circular ring can be prevented because excessive stress is prevented from being generated on the pocket surfaces of the cage circular ring. The dimensions of the circular ring are optimized using FEM analysis, so that bearing width is not unnecessarily extended.

Figure 6 shows a cross-sectional view of the newly developed bearing.

The newly developed bearing secures sufficient space for the cage circular ring by offsetting the balls in the axial direction to maintain the same width of the current bearing.

4. Verification of Effect of Ultrahigh-Speed Ball Bearing

4.1 Heat generation test

The effect of improving lubrication properties using an oil flow plate, and the effect of reducing friction by optimizing bearing specifications of the newly developed bearing were verified with high-speed testing equipment as shown in Figure 7. Outer ring temperatures were

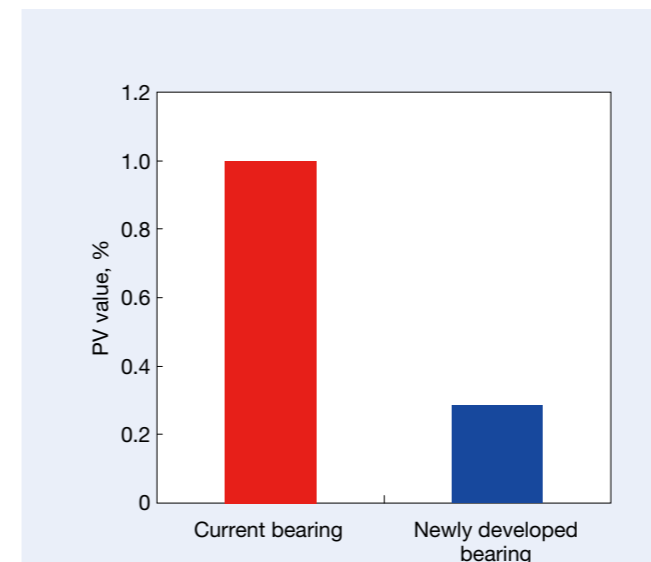


Fig. 5 Calculated results of PV values

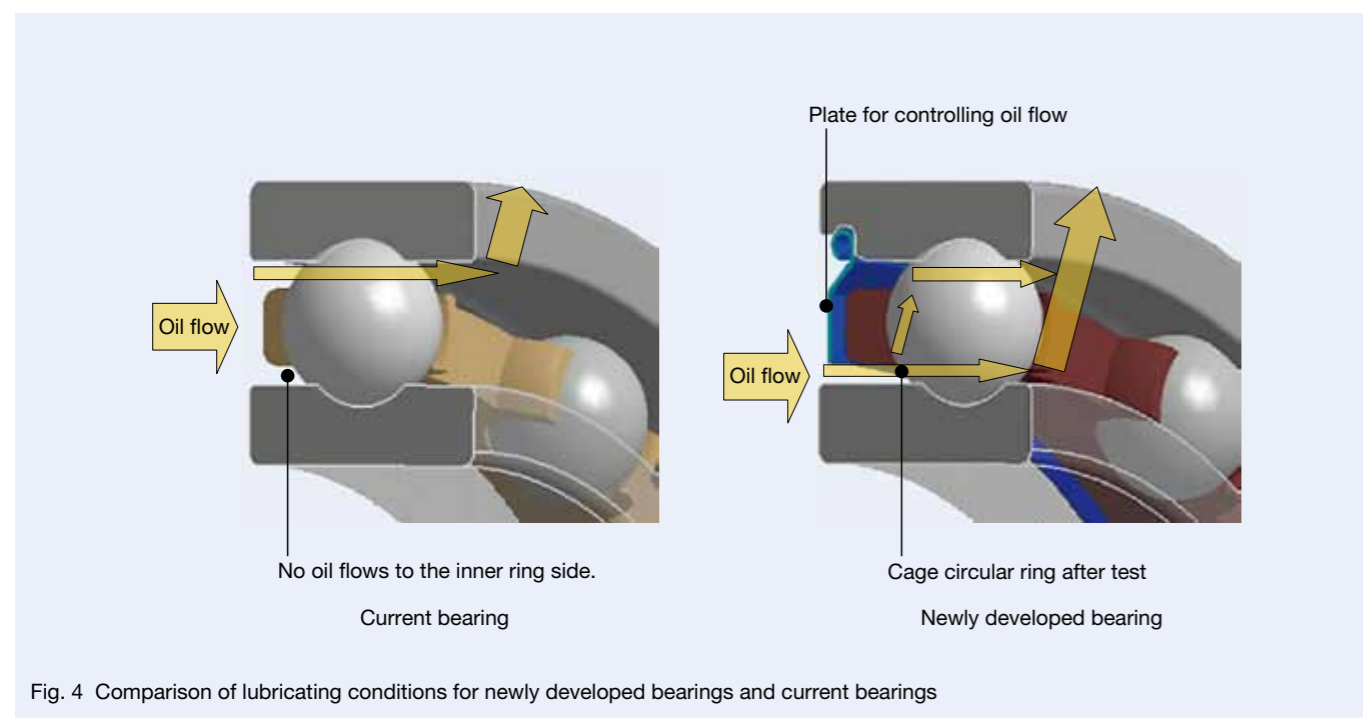


Fig. 4 Comparison of lubricating conditions for newly developed bearings and current bearings

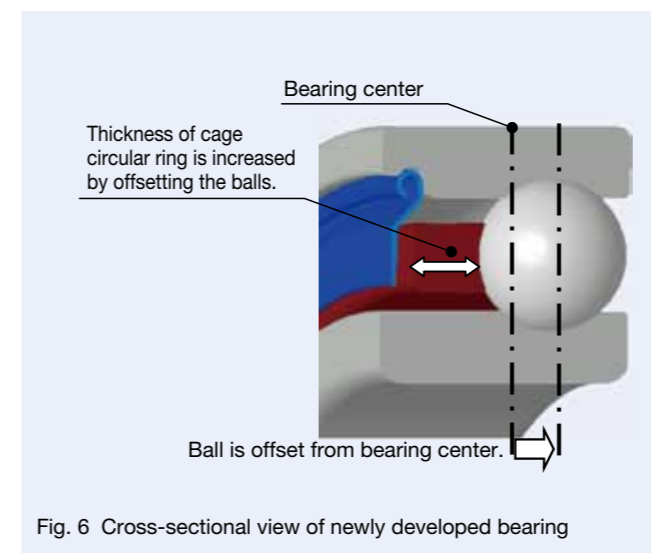


Fig. 6 Cross-sectional view of newly developed bearing

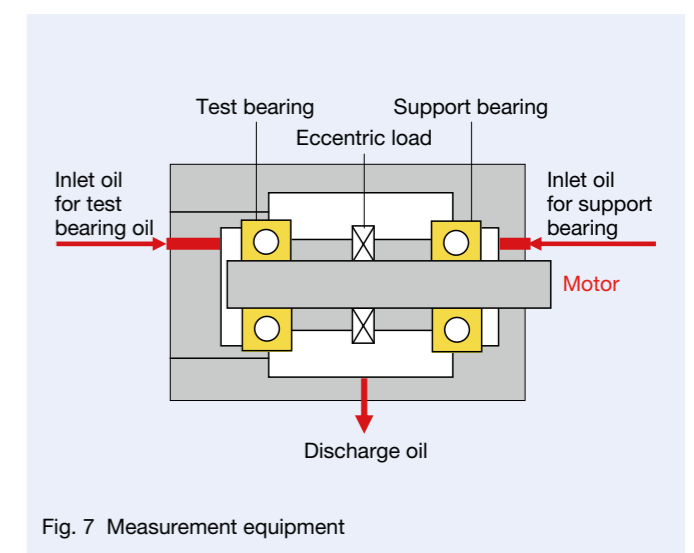


Fig. 7 Measurement equipment

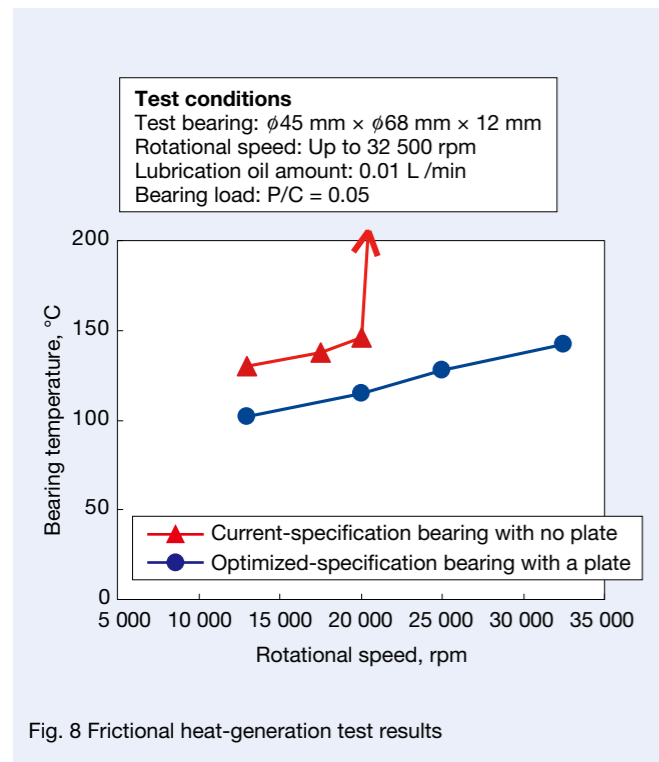
measured at each stage when the inner ring rotational speed was increased for the test.

A deep groove ball bearing (bore: $\phi 45$ mm; outside diameter: $\phi 68$ mm; width: 12 mm) was used for this test. Mineral oil with an approximate VG22 was used for lubrication. The total amount of lubrication oil is pumped to penetrate through the bearing interior by forcibly supplying oil in the amount of 0.01 L/min into the housing on the side of the cage's circular ring using an electric pump. In addition, tests on the current bearing to which the newly developed cage was mounted was also conducted to check the effects of the oil flow plate and optimized bearing specifications.

Figure 8 shows the test results of heat generation. Test results confirmed that the outer ring temperature of the newly developed bearing was over 20 °C lower than that of the current bearing throughout the whole region from the start of testing up to the speed of 20 000 rpm where the current bearing seized. These outcomes are thought to result from the fact that friction in the bearing's interior was reduced and heat generation was limited by the adoption of the oil flow control plate and by the optimization of the bearing specifications.

In addition, the newly developed bearing did not generate any sudden heat generation or suffer from seizure of the outer ring even at 32 500 rpm, though the current bearing generated sudden heat generation of the outer ring at 20 000 rpm, which ultimately resulted in seizure.

This test confirmed that resistance to heat generation and resistance to seizure of the newly developed bearing have greatly increased in comparison with the current bearing.



4.2 High-speed durability test

Comparison testing of the current bearing and the newly developed bearing was conducted to confirm durability using the test equipment shown in Figure 7.

The same deep groove ball bearing (bore: $\phi 45$ mm; outside diameter: $\phi 68$ mm; width: 12 mm) was used for this test as well as the heat generation test with the inner ring being rotated at 30 000 rpm. Mineral oil of an approximate VG22 was used for lubrication, and the amount of lubrication oil predetermined at 0.03 L/min according to actual conditions of ultrahigh-speed motors. In addition, testing was conducted on the current bearing with the current plastic snap cage mounted to it.

Figure 9 shows the high-speed durability test results.

When rotating the current bearing at 30 000 rpm, seizure occurred immediately from the inner ring raceway surface. Since the lubrication became insufficient and the friction between the balls and the inner ring raceway surface became high, the balls changed color and adhesion occurred, and as a result, the shapes of the balls became severely deformed. In addition, the pocket surfaces of the cage were severely worn and glass fiber became exposed by the wear. Furthermore, a part of the cage circular ring broke, and it became clear that cage strength was insufficient to withstand the excessive centrifugal forces at ultrahigh-speed rotation.

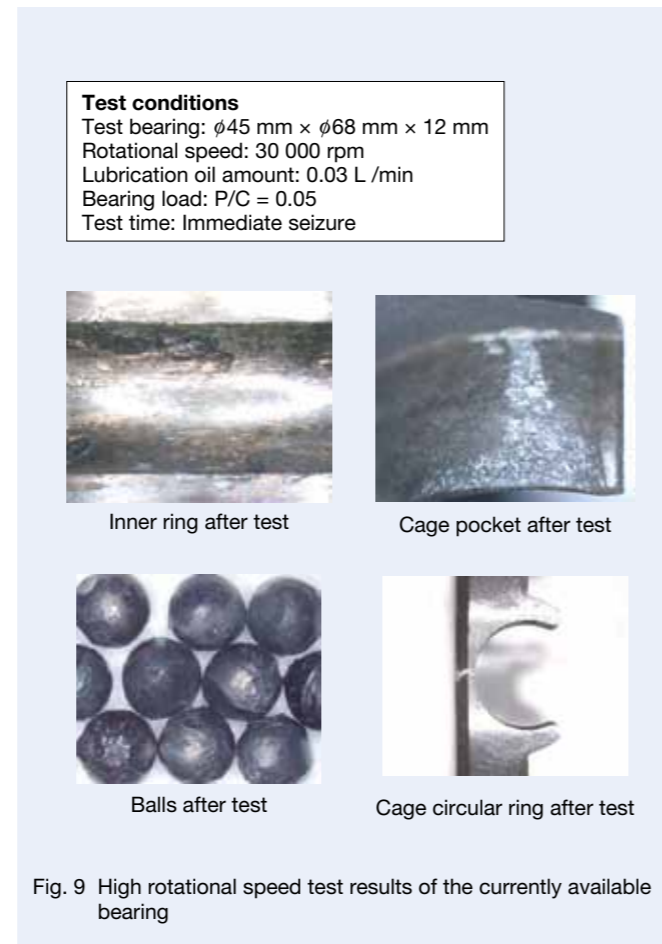


Fig. 9 High rotational speed test results of the currently available bearing

Figure 10 shows the results of high-speed durability testing of the newly developed bearing.

Prominent damage to the balls and the inner ring raceway surface, and exposure of glass fiber from the cage pocket surfaces were not found, nor did breakage of the cage circular ring occur in the newly developed bearing even after 100 hours of testing.

These test results confirmed that the newly developed bearing can withstand ultrahigh-speed rotation of 30 000 rpm for drive motors in next-generation hybrid vehicles.

5. Conclusion

This article reported on the structure and function of ultrahigh-speed ball bearings for motors in next-generation hybrid vehicles.

There is a strong demand for environmental friendliness and fuel economy for automobiles such as hybrid vehicles. In addition to providing this newly developed bearing, NSK will propose new technologies that meet new user needs and contribute to the development of the automobile industry by responding to the requirements of high-speed bearing performance along with facilitating more compact motors.

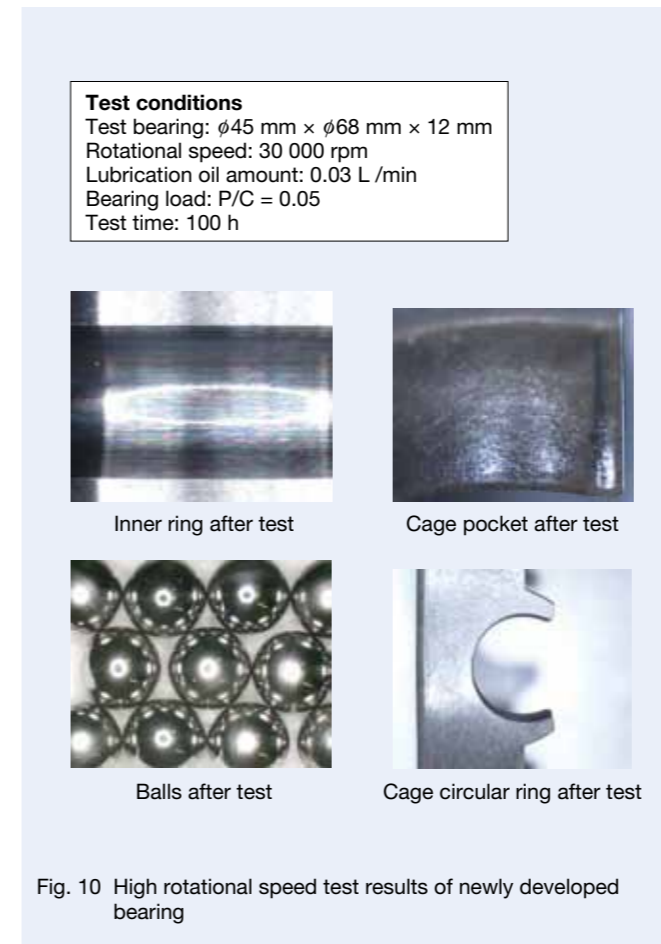


Fig. 10 High rotational speed test results of newly developed bearing

References

- 1) JP-Morgan Securities Japan Co., Ltd. "Global environment series Vol. 3, Reconsideration of hybrid vehicle potential facing an economic crisis."
- 2) S. Sugita, "Ultra High-speed Spindle for Machine Tools," NSK TECHNICAL JOURNAL, No. 676 (2003) 11–15.
- 3) K. Hachiya, K. Yamamura, T. Yamamoto, M. Yamazoe, and H. Yui, "Development of a Hybrid Ball Bearing with Advanced Materials under High-temperature and High-speed Conditions," NSK TECHNICAL JOURNAL, No. 674 (2002) 11–17.
- 4) Y. Miyagawa, K. Seki, and M. Yokoyama, "Research of ball bearing performance under high dn value (First report) — Temperature property of deep groove ball bearing (#6206)," Junkatsu, Vol. 17, No. 10 (1972) 622–632.



Takeshi Maejima



Takanori Tanaka

Development of New-Generation Low-Frictional-Torque Tapered Roller Bearings

Tomoharu Saito and Hiroki Maejima
 Future Technology Development Center
 Takayuki Hiramoto
 Corporate Research & Development Center

ABSTRACT

In terms of the issues of global warming and energy conservation, there has been a growing demand for reduced CO₂ emissions and improved automotive fuel efficiency. Automakers, especially, have been improving fuel efficiency by replacing conventional transmissions, such as manual or automatic transmissions, with CVTs, DCTs, and multi-overdrive ATs. Under these circumstances, there has been a demand for greater reductions in torque and improved durability even for bearings used in power transmission devices.

In this article, we report on a next-generation tapered roller bearing in which the torque is reduced by lowering churning resistance, and lubricating properties are enhanced under severe lubricating conditions. In addition, our newly developed bearing has an easily molded plastic cage, and provides a choice of cage material that matches operating environment, and applications.

1. Introduction

In terms of the issues of global warming and energy conservation, there has been a growing demand for reduced CO₂ emissions and improved automotive fuel efficiency. Especially, there is a need to increase efficiency of the internal combustion engine using fossil fuels, which is a finite resource, because it generates CO₂ in proportion to the amount of fuel that is consumed.

Each automaker aims for improved fuel efficiency by reducing losses or the weight of each component in addition to improving fuel efficiency of internal combustion engines. Automakers, especially, have been improving fuel efficiency by replacing conventional transmissions, such as manual or automatic transmissions, with CVTs, DCTs, and multi-overdrive ATs. Under these circumstances, there has been a demand for greater reductions in torque and improved durability even for bearings used in power transmission components.

In this article, we report on a next-generation tapered roller bearing since we achieved reduced torque by lowering churning resistance, and enhanced lubricating properties under starved lubrication conditions.

2. Low-Torque Technology for Tapered Roller Bearings

2.1 Conventional low-torque technology

The theory of frictional resistance regarding tapered roller bearings has been well established, and developments for achieving lower torque have been conducted based on this theory. Torque factors are classified as follows:

- (1) Rolling friction between inner/outer ring raceway surfaces and roller rolling contact surfaces
 - Frictional loss by elastic hysteresis
 - Viscous resistance of the EHL oil film
- (2) Sliding friction between the inner ring rib and roller heads
 - Friction from metal-to-metal contact
 - Viscous resistance of oil film
- (3) Sliding friction between rollers and cage
- (4) Agitation resistance of lubrication oil

Among these, sliding friction between rollers and the cage in item (3) can be ignored because it is said to be smaller than the friction listed in items (1), (2), and (4).

Measures have already been taken for reducing the friction in items (1) and (2). As a measure for reducing rolling friction between inner/outer ring raceway surfaces and roller rolling contact surfaces in item (1), design specifications such as the number of rollers, roller length, roller diameter, and contact angle have been optimized, and lower torque has been achieved without reducing bearing service life and rigidity to the greatest degree possible. In addition, reduction of sliding friction between the inner ring rib and roller heads in item (2) has been achieved by making improvements with the contact area configuration and surface roughness. For agitation resistance of lubrication oil in item (4), however, lower torque has not yet been achieved. For differential gears where a large amount of high-viscosity lubrication oil is used, it is especially necessary to reduce agitation resistance to achieve lower torque of the bearing because the effect of agitation resistance is large in high-speed areas.

In addition, automakers tend to control agitation resistance of the whole transmission interior by using a lower viscosity and smaller amount of lubrication oil in the transmission for improving fuel efficiency. Furthermore, bearings in hybrid vehicles tend to be operated under starved lubrication conditions such as when the oil pump is not operating when the vehicle is running under electric-only mode. Thus, rich lubricating properties are needed for the bearings.

2.2 Reduction effects of agitation resistance of lubrication oil

We investigated the relationship between the amount of supplied oil and torque for determining the contributing degree of agitation resistance in torque factors of tapered roller bearings. Tapered roller bearings for differential gears were used in the test, and evaluated by the running-torque test rig as shown in Figure 1. After axial load was applied while supplying differential gear oil to the test bearing that was mounted to the test rig, the test bearing

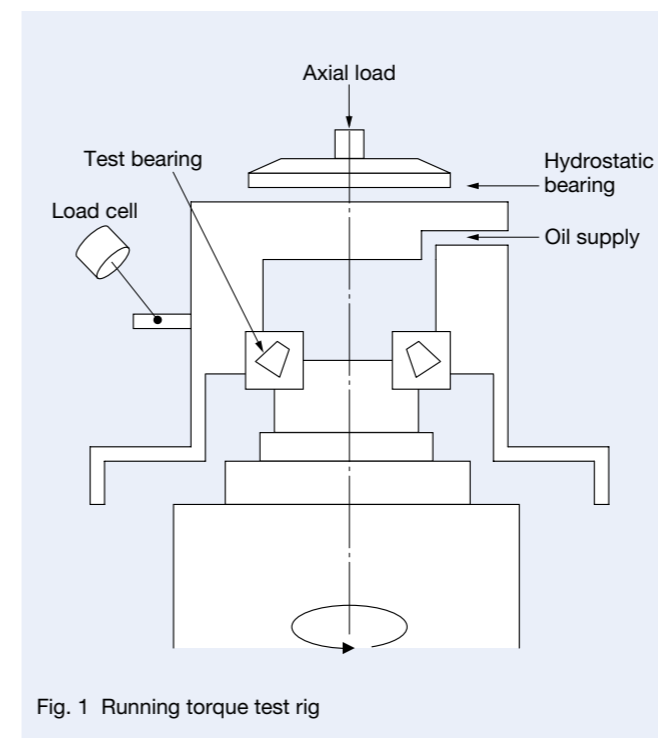


Fig. 1 Running torque test rig

Table 1 Torque test conditions

Bearing size	Bore: $\phi 34.7$ mm; outside diameter: $\phi 88.7$ mm; width: 38 mm
Load conditions	Axial load: 4 000 N
Rotational speed	2 000 rpm
Oil temperature	50 °C
Lubrication oil	Differential gear oil (73 mm ² /s at 40 °C)
Oil supply amount	50 ml/min – 720 ml/min
Lubrication method	Forced lubrication

was rotated (Table 1). Bearing torque was measured by measuring moment force acting on the outer ring of the test bearing that was subjected to axial load through a hydrostatic bearing. Furthermore, we investigated the relationship between torque and the amount of oil with varying amounts of supplied oil in the test rig.

Figure 2 shows the torque test results. It is considered that the reduced amount of torque is the result of agitation resistance when the amount of supplied oil in the test rig is reduced. Accordingly, we were able to confirm that agitation resistance of lubrication oil occupied 26 % of bearing torque. Figure 3 shows the analysis results of torque factors of tapered roller bearings for differential gears based on this result. Not only was rolling friction between inner/outer ring raceway surfaces and roller rolling contact surfaces found, which was conventionally valued, but also the effect of agitation resistance of lubrication oil was found to be high for tapered roller bearings.

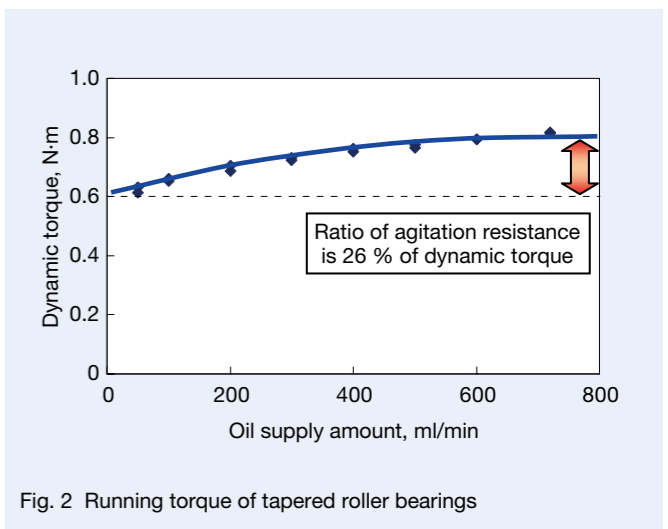


Fig. 2 Running torque of tapered roller bearings

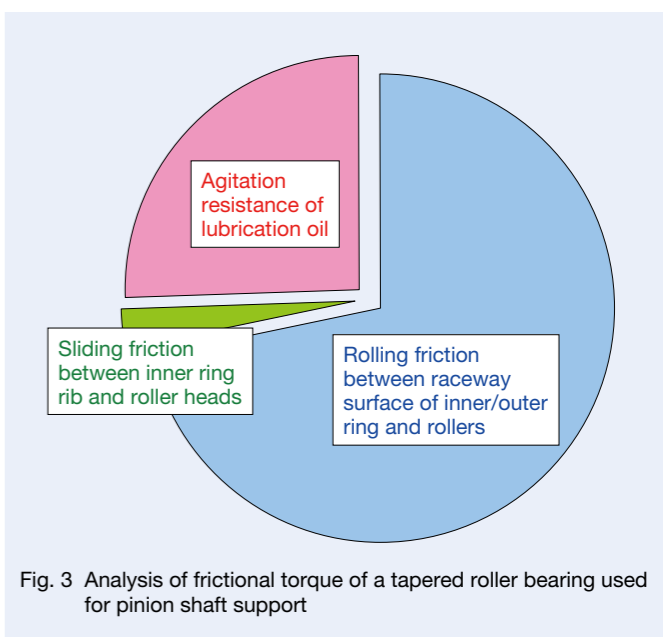


Fig. 3 Analysis of frictional torque of a tapered roller bearing used for pinion shaft support

3. Development Concept of Next-Generation of Low-Frictional-Torque Tapered Roller Bearings

3.1 Reduction of agitation resistance

Controlling the amount of oil in the bearing interior is required in order to reduce the aforementioned agitation resistance. Therefore, we investigated means of decreasing the amount of oil inflow into the bearing interior and a means of increasing the amount of oil outflow from the bearing interior for the next generation of low-torque tapered roller bearings.

Centrifugal force causes a pumping action in tapered roller bearings as shown in Figure 4, and oil flows toward the large rib side from the small rib side of the inner ring while the bearing rotates. Lubrication oil entering into the bearing interior can be controlled by narrowing the clearance between the cage and small rib of the inner ring, which is a flow inlet for reducing the amount of oil inflow into the bearing interior. Though negative pressure occurs in the bearing interior due to bearing rotation, and the force to draw lubrication oil into the bearing is generated, the inflow of lubrication oil into the bearing interior due to this negative pressure can be controlled with the cage by decreasing the interior space.

It is effective to expand the space of the inner ring large rib side, which is the outflow side of oil, for increasing the amount of oil outflow from the bearing interior. In this way, increased agitation resistance of lubrication oil in the bearing interior can be prevented by controlling oil flow of lubrication oil.

Based on the above concept, we evaluated a low-torque cage that was capable of reducing agitation resistance as shown in Figure 4. Because the low-torque cage has a complicated configuration, plastic was adopted for its material to take advantage of injection molding

technology. Figure 5 shows oil flow of the newly developed bearing interior. We consider that the newly developed bearing controls the amount of oil in the bearing interior compared with the conventional bearing by controlling the flow of lubrication oil in the bearing at the inlet and outlet, and, with the plastic cage, by decreasing the amount of interior space.

3.2 Improvement of lubrication property

As stated above, lower viscosity and lower volume of lubrication oil are proceeding for improving fuel economy in transmission bearings, and reduction of agitation resistance has proceeded, but lubrication properties of the bearing have become an issue. Especially, it sometimes generates seizure due to excessive heat generation by sliding friction between the inner ring large rib and roller heads.

Figure 6 shows oil flow in the bearing interior under insufficient lubrication conditions of both the conventional bearing and the newly developed bearing. It is considered that lubrication oil flows to the bearing outside from the rollers through the cage. An oil pool (oil reservoir groove) was configured as shown in Figure 4, and lubrication properties were improved for supplying lubrication oil that flowed outward to the roller heads where seizure tends to occur. Oil pools were configured in a position where the cage pocket and roller heads make contact, and control the flow of lubrication oil. As a result, it was able to retain lubrication oil on the roller heads, though the lubrication oil flowed outward between the rollers in the conventional bearing.

The injection-molded plastic cage is suitable for efficiently configuring an oil pool in the newly developed cage. It is possible to configure an oil pool in a conventional steel cage, but this increases costs due to the complicated configuration. Tapered roller bearings

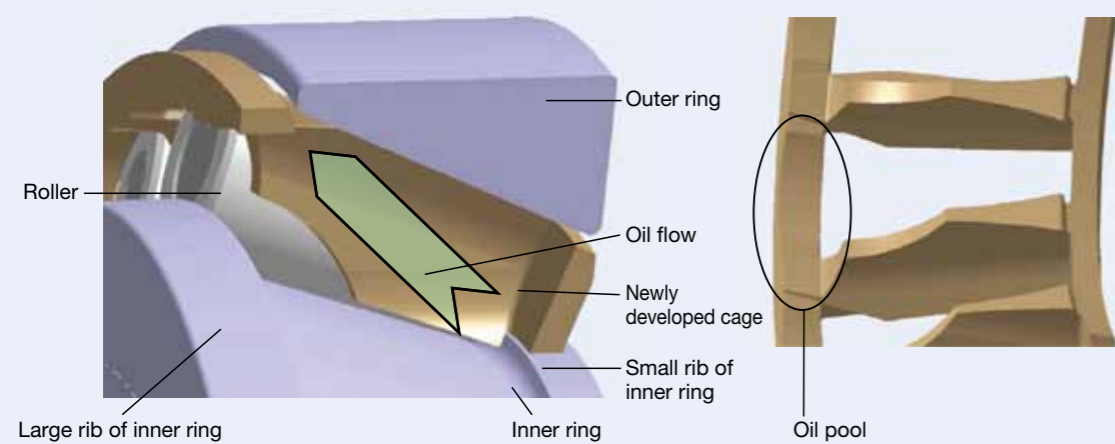


Fig. 4 Highly agitation-resistant plastic cage (Left: assembly; right: view of oil pool on cage)

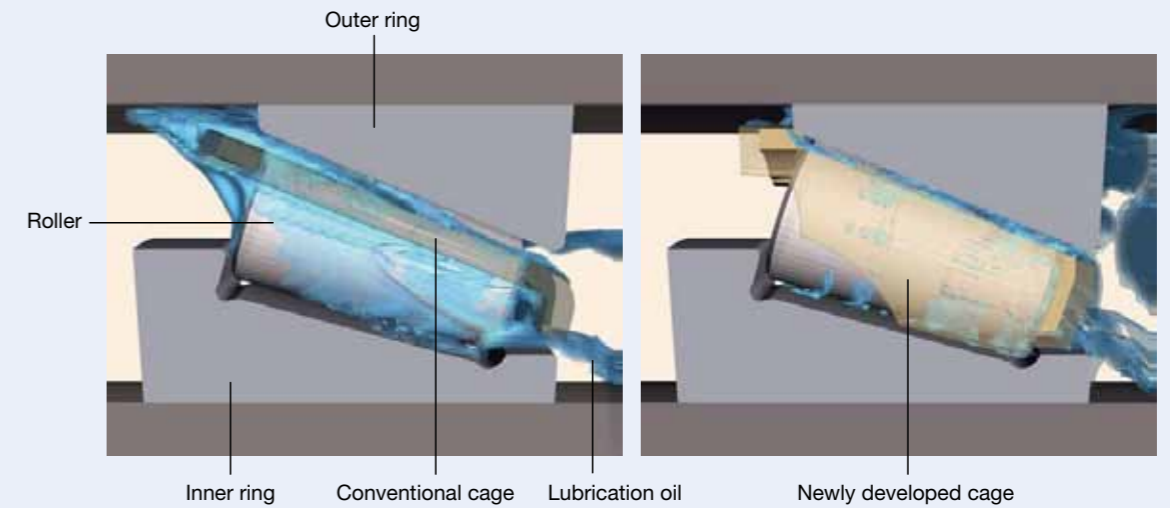


Fig. 5 Oil flow inside tapered roller bearings (Left: conventional bearing; right: newly developed bearing)

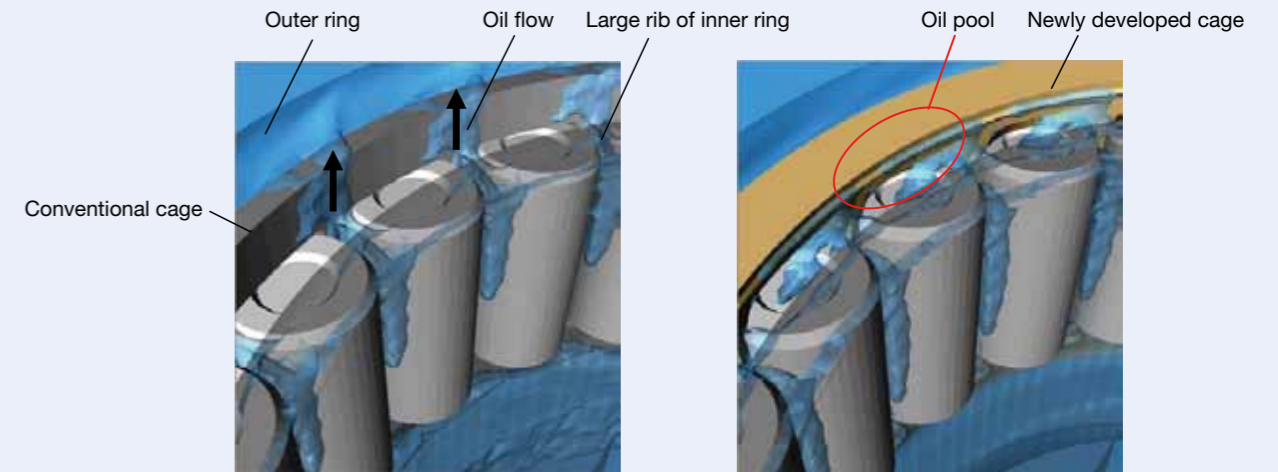


Fig. 6 Oil flow of outflow side of tapered roller bearings (Left: conventional bearing; right: newly developed bearing)

adopting this newly developed cage can contribute to improved fuel economy by responding to severe operating conditions such as in a transmission with a small volume of lubricant and low viscosity for improving fuel economy.

3.3 Plastic material

Material strength of the plastic cage varies due to the influence of the operating environment such as temperature and lubrication oil. Since bearings used in power transmission devices are operated at high temperatures and lubricated by oil mixed with many additives, consideration regarding varying strengths of plastic material is needed for the cage design. Therefore,

distinguishing the application of polyamide 66 or polyamide 46 is required for transmissions in accordance with compatibility between the plastic material and operating temperatures/lubrication oil. In addition, a large amount of extreme pressure additives are contained in the lubrication oil for the differential gears, which creates a very severe operating environment for plastic material. When used in such a severe environment, cage strength can be maintained by adapting NSK's originally developed material (linear polyphenylene sulfide, L-PPS), which is superior in oil resistance. The newly developed bearing can respond to various operating environments for each application by distinguishing the usage of three different kinds of materials.

In addition, it is known that the strength of the position (weld) where the flow of molten plastic meets another flow during molding is generally lower than that of other positions. In this newly developed cage, the weld position is not at the generating position of maximum stress, which prevents cage fracturing.

Moreover, it can achieve approximately 5 % in bearing weight reduction by switching from a steel cage to a plastic cage because the specific gravity of plastic material is lower than that of steel.

4. Performance Evaluation of Next-Generation of Low-Frictional-Torque Tapered Roller Bearings

4.1 Torque evaluation

We mounted the bearing to an actual differential test rig as shown in Figure 7 for evaluating performance of the newly developed bearing including the low-agitation cage, and measured the bearing torque needed to rotate the pinion shaft under the conditions listed in Table 2. We removed the pinion gear teeth in the differential interior to measure bearing torque so as not to engage the pinion

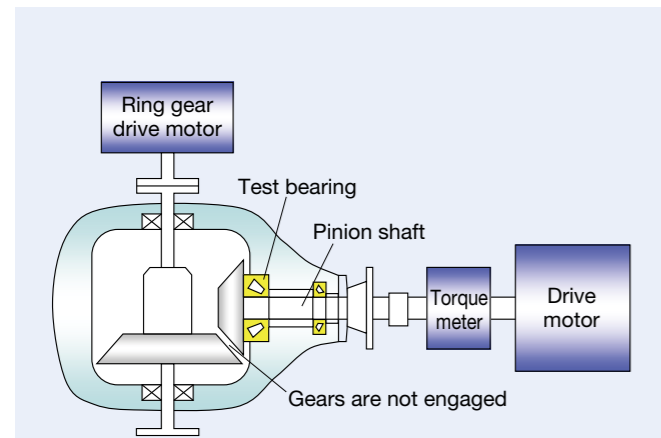


Fig. 7 Torque test rig of rear axle differential

Table 2 Test conditions of rear axle differential

Bearing size	Bore: $\phi 45$ mm; outside diameter: $\phi 95.25$ mm; width: 33 mm
Load conditions	Preload only
Rotational speed	0 rpm – 5 000 rpm
Oil temperature	90 °C
Lubrication oil	Differential gear oil (73 mm ² /s at 40 °C)
Lubrication method	Oil bath lubrication
Cage material	Linear polyphenylene sulfide

gear with the ring gear. In addition, we rotated both the pinion gear and the ring gear shafts at each rotational speed considering the reduction ratio at each shaft by each motor mounted to the pinion gear side and the ring gear side. We evaluated only bearing torque using this test method while recreating lubrication conditions equivalent to an actual test rig.

Figure 8 shows the measurement results. The newly developed bearing had lower torque than the conventional bearing at all speed ranges over 200 rpm. When rotational speed of the pinion was 4 000 rpm (equivalent to a vehicle speed of 120 km/h), the newly developed bearing was able to reduce bearing torque by approximately 20 % compared with the conventional bearing. This means that approximately 80 % of agitation resistance was reduced.

4.2 Evaluation of lubrication property

We compared the period from starting rotation until the generation of seizure in the newly developed bearing with that of the conventional bearing under conditions listed in Table 3 to evaluate lubrication properties of bearings in the case of a small amount of lubrication oil. Figure 9 shows the structure and dimensions of the seizure resistance test rig. Testing was conducted under

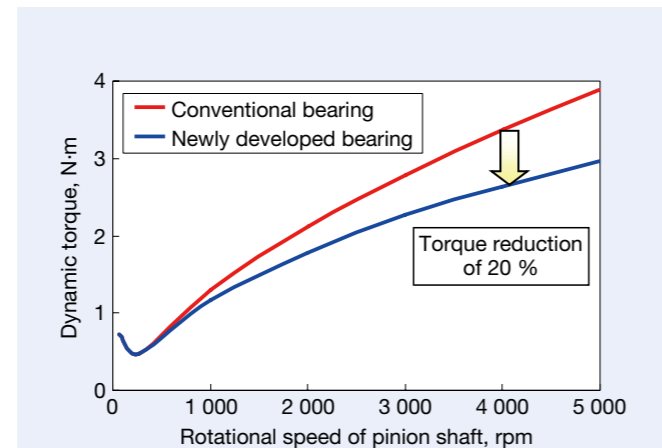


Fig. 8 Frictional torque of rotating pinion shaft

Table 3 Test conditions of lubricating performance

Bearing size	Bore: $\phi 40$ mm; outside diameter: $\phi 68$ mm; width: 19 mm
Load conditions	Axial load: 6 300 N
Rotational speed	3 000 rpm
Ambient temperature	Room temperature
Lubrication oil	VG68 mineral oil
Lubrication method	Oil bath lubrication
Cage material	Polyamide 46
Judgment of seizure	At overcurrent in motor

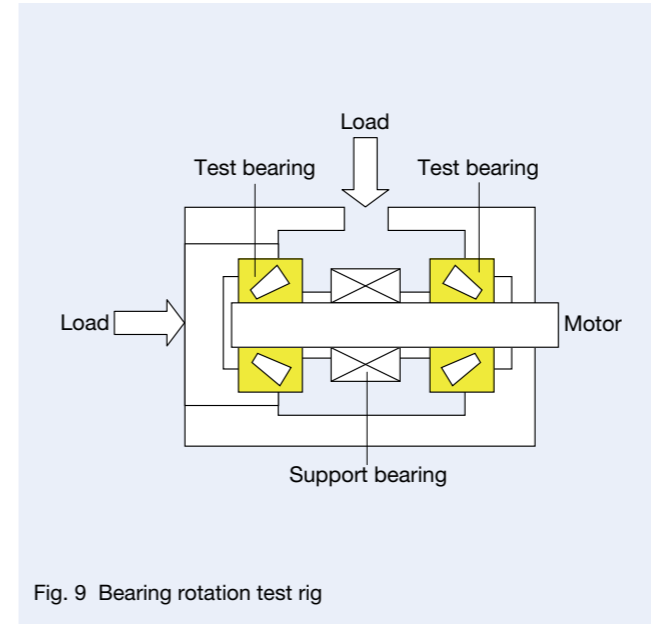


Fig. 9 Bearing rotation test rig

conditions of oil bath lubrication and the height of the oil surface with the stationary bearing was at the height of the lowest roller end of the test bearing. After axial load was applied, the motor was rotated. The moment when overcurrent passed through the motor was defined as the moment of seizure.

Figure 10 shows the test results. If the period from start until seizure of the conventional bearing with a steel cage was defined as 1, the period from start to seizure of the bearing with the newly developed cage increased by more than 26 times using controlled lubrication oil on the roller heads because of the oil pool. This confirms that the newly developed bearing can maintain sufficient lubrication conditions even for transmissions under severe lubrication conditions due to promoting reduced amounts of lubrication oil and lowered viscosity of lubrication oil, and can contribute to improved efficiency of the transmission as a whole.

4.3 Confirmation of durability

Durability testing was conducted under conditions listed in Table 4 for evaluating the durability of the cage with reduced agitation resistance using a bearing with the plastic cage that had been deteriorated from immersion in high-temperature lubrication oil. Specifications of the test rig were almost the same as the seizure resistance test rig in Figure 9. After the oil bath conditions were set to where the oil surface was at the same height of the rotational shaft center, axial load and radial load were applied to the test bearing, and the inner ring was rotated.

As a result, the cage was free of any fractures, breakage, or cracks even at a rotation of 7 800 rpm (equivalent to a vehicle speed of 230 km/h).

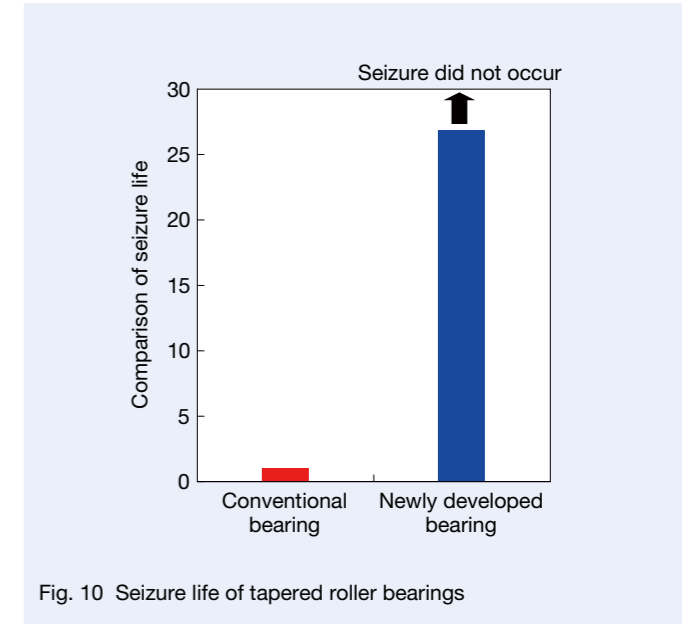


Fig. 10 Seizure life of tapered roller bearings

Table 4 Test conditions of cage strength

Bearing size	Bore: $\phi 45$ mm; outside diameter: $\phi 95.25$ mm; width: 33 mm
Load conditions	Axial load: 12.2 kN; radial load: 11.8 kN
Rotational speed	7 800 rpm
Outer ring temperature	135 °C
Lubrication oil	VG68 mineral oil
Lubrication method	Oil bath lubrication
Cage material	Linear polyphenylene sulfide
Immersion conditions	Differential gear oil (1 200 h at 135 °C)
Test time	250 h

5. Conclusion

This article reported on the next-generation low-frictional-torque tapered roller bearing that controls oil flow in the bearing interior. The newly developed bearing, for controlling oil flow, adopts a plastic cage that is superior in formability, and is capable of both reducing agitation resistance and improving lubrication properties. In addition, it is possible to select a cage material that is suitable for the operating environment.

For the needs of automotive power transmission devices, NSK has responded with this newly developed bearing, and will propose new technologies in response to new user needs, and expects to contribute to the development of the automotive industry.

References

- 1) S. Aihara, "Friction of Roller Bearings and EHL Viscous Rolling Resistance," *NSK TECHNICAL JOURNAL*, No. 649 (1988) 1-5.
- 2) H. Aramaki, "Low Frictional Torque Technology of Rolling Bearings," *NSK Technical Journal Motion & Control*, No. 17 (2005) 25-31.
- 3) H. Suzuki and K. Takei, "NSK Products and Technologies Contribute to Energy Conservation," *NSK Technical Journal Motion & Control*, No. 12 (2002) 5-10.
- 4) H. Suzuki, "Technical Trend of Bearings for Automotive Drive-Trains," *Monthly Tribology*, 8 (1998) 34-35.
- 5) H. Fujita, "Technology for improving property of lubrication oil in a drive system for fuel economy," *Tribologist*, Vol. 53 (2008) 456-461.
- 6) M. Aoki, "Design of plastic molded product," (1988) 85, Institute for Industrial Research.



Tomoharu Saito



Hiroki Maejima



Takayuki Hiramoto

Development of Ultralow-Torque Ball Bearings for Hybrid Vehicles

Yuuki Tsuchida, Susumu Tanaka, and Toshimi Muraoka
Automotive Bearing Technology Center

ABSTRACT

In order to further improve fuel economy, there is a growing need to reduce torque losses in the bearings that are used in the transmissions of hybrid vehicles. To date, it has been considered overly difficult to reduce torque losses further in the ball bearings. However, NSK successfully cut rolling friction losses and agitation losses associated with the lubricant through use of various analysis technologies and experiments. Both the number of balls has been significantly reduced and the internal design has been optimized so that rolling friction losses can be cut. The agitation losses associated with the lubricant have also been cut as a result of introducing a specially shaped plastic cage. In this article, we present an ultralow-torque ball bearing for hybrid vehicles, which has been newly developed to significantly cut torque in comparison with conventional products.

1. Introduction

To further improve fuel economy, lower torque is in demand for the bearings used in transmissions of hybrid vehicles in which an engine and a motor are efficiently combined. Ball bearings with low torque loss are increasingly being used as bearings to support motors and power transmission gears, which are components of transmissions in hybrid vehicles. Meanwhile, it is known that agitation resistance of the supplied lubrication oil greatly affects bearing torque when the bearing is used under oil lubrication conditions.

In this article, we present an ultralow-torque ball bearing for hybrid vehicles that takes on the challenge of advancing the low-torque performance of ball bearings,

which has been conventionally considered to be difficult. The ultralow-torque ball bearings for hybrid vehicles have been newly developed to successfully cut rolling friction losses and agitation losses associated with lubrication oil during bearing rotation through the use of various analysis technologies and experiments for bearings operating under oil lubrication conditions.

2. Required Performance of Bearings for Hybrid Vehicles

An example of how bearings are used for hybrid vehicles is shown in Figure 1, which illustrates the cross-sectional view of a transmission in a front engine, front-wheel (FF)

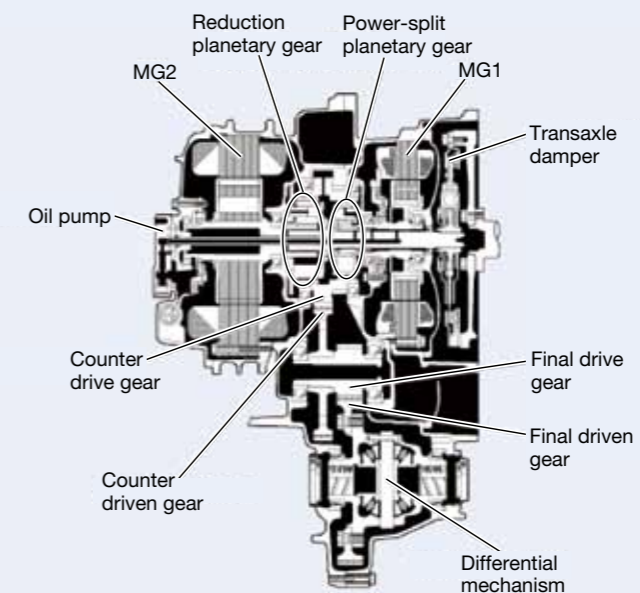


Fig. 1 Cross-sectional view of a transmission for FF hybrid vehicle¹⁾

drive train of a hybrid vehicle. Many ball bearings are used in the motor and power transmission gear support components in this manner.

Although the conditions such as rotational speeds and load conditions differ between ball bearings supporting motors and ball bearings supporting power transmission gears, both bearings decidedly demand lower torque as well as a compact and lightweight design, and sufficient durability.

Principal friction factors of ball bearings include friction between the inner and outer rings and the rolling elements, agitation resistance of the lubrication oil, sliding friction between the seal and the inner ring, and sliding friction between the cage and the rolling elements.

Sometimes, there are cases where the ingress of foreign debris in the lubrication oil invades the bearing interior generating reduced bearing life while operating under oil lubrication conditions. Therefore, seals are mounted to the bearings in some cases as a preventative measure. However, seals are unnecessary and sliding friction between the seal and inner ring can be avoided if oil cleanliness is improved and an open-type ball bearing can fully maintain sufficient durability.

In addition, sliding friction between the cage and rolling elements can be more or less reduced by adopting plastic as a cage material, which is lighter than conventional steel and has low-torque properties.

These low-torque technologies have been partially used in bearings for various transmissions in the past. To further improve fuel economy, low-torque performance exceeding highly conventional performance is in demand for bearings for hybrid vehicles. Further achieving low bearing torque requires a reduction of friction between the inner and outer rings and rolling elements, and agitation resistance of the lubrication oil is essential, in addition to conventional

technologies, which occupy most of the bearing torque. Therefore, it is highly important to reduce both losses with respect to determining low-torque performance.

3. Technology for Ultralow Torque

3.1 Optimization of internal specifications

Generally, ball bearings are designed to be assembled using a greater number of balls of a larger size within certain dimensional constraints for increasing load ratings. However, loss torque due to friction between the inner and outer rings and balls increases if the number of balls increases. Therefore, lower torque is possible, if the number of balls can be reduced while maintaining the necessary load rating under operating conditions shown in Figure 2.

It is possible to optimize bearing design according to operating conditions using NSK's original bearing analysis program (BRAIN). Using BRAIN enables a design with an optimal number of balls, ball diameter, ball pitch circle diameter, raceway groove radius of the inner and outer rings, and internal clearance. In addition, it is possible to further lower torque by incorporating NSK's long-life technology as represented by TF technology.

Balls of between 22 pieces and 24 pieces are mounted in large-size ball bearings that support the counter-drive gear as shown in Figure 1 in standard designs. This is a good example of having successfully reduced the large number of balls by as much as 6 or 7 through the application of analysis technology.

Although it has been conventionally difficult to manufacture bearings with a fewer number of balls, this challenge in manufacturing has been overcome by devising a more suitable manufacturing method.

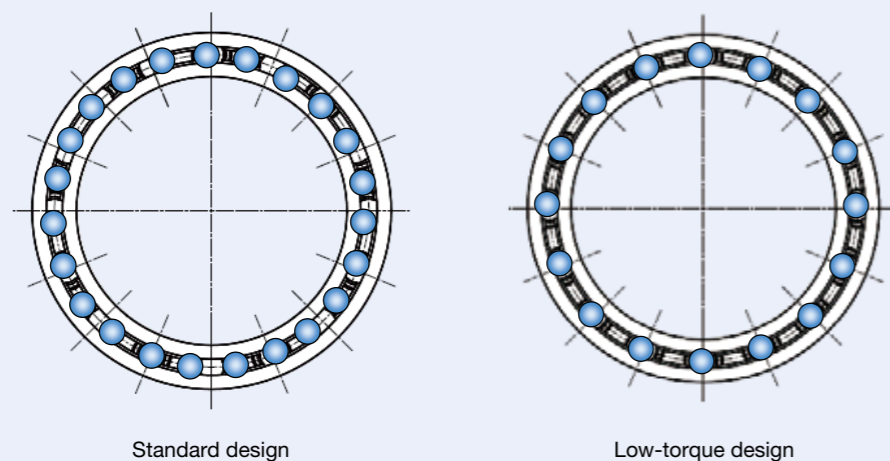


Fig. 2 Example of ball bearing designs

3.2 Optimization of cage shape

When bearings are operating under oil lubrication conditions, the oil is agitated by the orbital motion of rolling elements and the cage, and loss torque is generated by the resistance that occurs at that moment.

Figure 3 shows typical cages that are used in deep groove ball bearings. Cages are generally distinguished between the symmetrical shape of pressed steel cages in the axial direction, and the unsymmetrical shape of plastic-snap cages.

The authors attempted to optimize the shape of the plastic-snap cage while focusing on the effects of cage shape on agitation loss associated with lubrication oil. As a result, we succeeded in developing a low-torque plastic cage that was superior in oil flow control, and drastically reduced agitation loss associated with lubrication oil. Figure 4 illustrates the developed cage and lists its features.

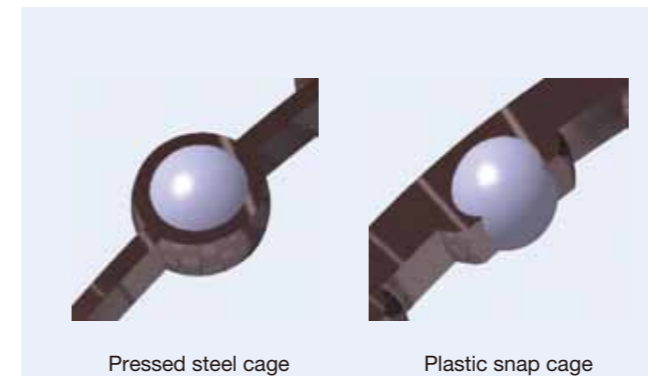


Fig. 3 Standard-type cages for ball bearings

Features of low-torque plastic cage

- Reducing sliding friction between balls and cage using synthetic resin
- Reducing agitation loss by flattening the indented shape in the rotational direction
- Ensuring ease of assembly (reducing stress during assembly)
- Ensuring optimum cage strength

Flattening the indented shape in the rotational direction can have a significant impact on reducing agitation loss. Therefore, it is adopted for the rib side where thinning is generally applied in consideration of formability as well as the pocket tab side where the balls are mounted, and it aims for complete reduction of agitation loss.

Meanwhile, it is known that the pocket portion of a plastic-snap cage deforms at high-speed rotation due to its particular shape. Though the mass increase due to flattening the cage shape furthers the deformation, the low-torque plastic cage is sufficient for high-speed rotation by applying high-strength design through simulation of actual usage environments.

3.3 Validation of lower torque mechanism

We measured torque and recorded the agitation situations of the lubrication oil with a camcorder under the following operating conditions, and compared the developed product with a standard product in order to quantitatively measure the effects of loss reductions on ultralow-torque ball bearings and in order to validate the mechanism of loss reductions.

The newly developed product adopts specifications with an extended flat area of the cage for obtaining high reductions of agitation loss of the lubrication oil by

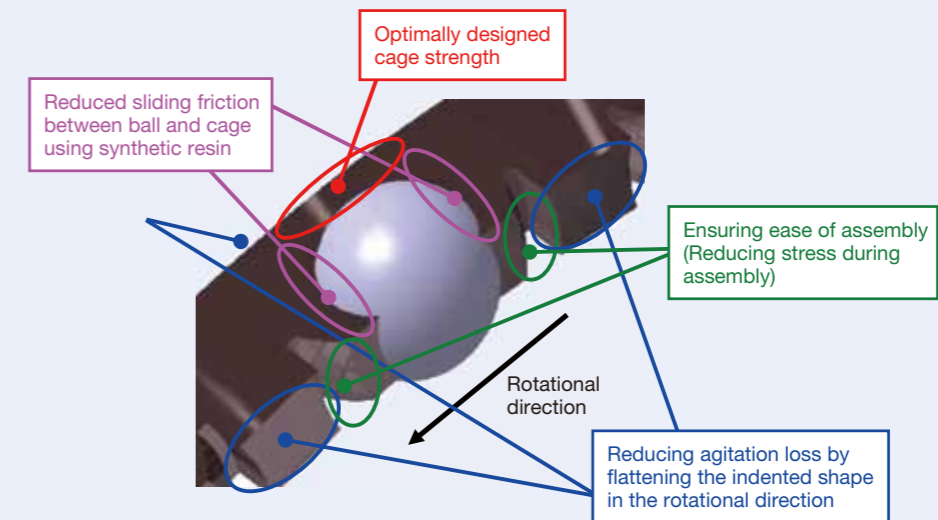


Fig. 4 Low-torque plastic cage

decreasing the number of balls by two in comparison with the standard product (Figure 5).

Operating conditions for torque measurement

Test bearing: Deep groove ball bearing
(Bore: $\phi 35$ mm; outside diameter: $\phi 80$ mm; width: 21 mm)

Number of balls: Standard product: 8 balls
Newly developed product: 6 balls

Cage type: Standard product: pressed steel cage
Newly developed product: low-torque plastic cage

Load: $0.06 C_r$
(C_r : basic dynamic load rating of standard product)

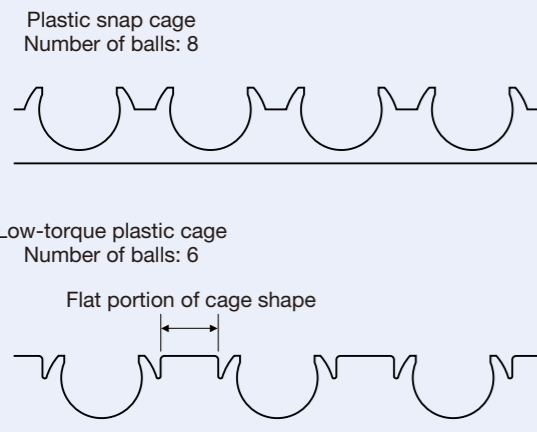


Fig. 5 Flat portion of low-torque plastic cage

Rotational speed: 3 000 rpm
Lubrication oil: ATF
Lubrication oil amount: 1 000 ml/min

Figure 6 shows the results of measured torque, and Figure 7 shows the observed results of agitating conditions of the lubrication oil.

Torque of the newly developed product was reduced by more than 30 % compared with the standard product. Torque reduction in the newly developed product is mainly based on the reduction of loss torque resulting from friction between the inner and outer rings and the balls, and the agitation of lubrication oil. This can be verified by

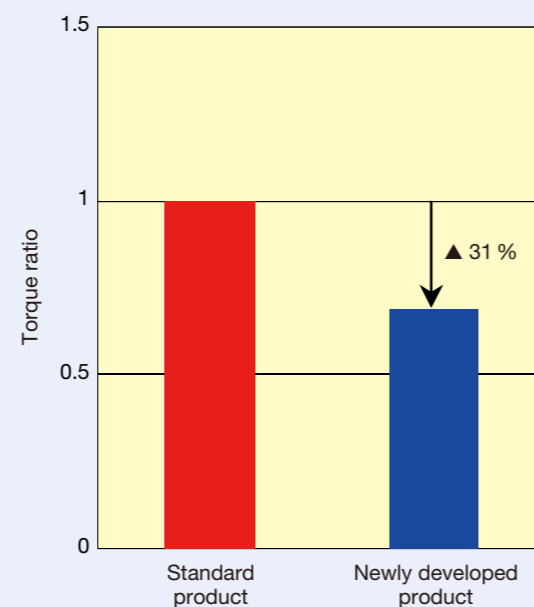


Fig. 6 Torque measurement results



Standard product



Newly developed product

Fig. 7 Observation results of lubricant agitation

the difference in agitating conditions of lubrication oil as shown in Figure 7.

It is striking that the two oil levels are very different. Because the agitation of lubrication oil is large in a standard product, the oil has difficulty passing through the bearing interior. As a result, the oil level is high. Conversely, oil levels in the developed product are lower than that in the standard product because the lubrication oil easily penetrates into bearing interior in addition to commutative action of the lubrication oil. It is considered that this achieves significant torque reduction because the ratio of balls and cage that are immersed in the oil endure very little resistance.

4. Validation of Loss Reduction Effect of Ultralow-Torque Ball Bearings

We quantitatively verified the effect on reduction of loss by differences in operating conditions and sizes of ultralow-torque ball bearings. We measured torque of both standard products and the newly developed product by changing the operating conditions based on the description in Section 3.3.

4.1 Influence of rotational speed

Figure 8 shows the measured results of torque under each rotational speed. Torque of the newly developed product was reduced to a lower level than that of the standard product for all rotational ranges. Though the torque reduction effect of the developed product seems to tend towards a small increase at low-speed rotation, it is almost the same for all rotational ranges and its degree of effect is small.

4.2 Influence of lubricant amount

Figure 9 shows the measured results of torque under conditions of certain amounts of lubricant. Torque of the

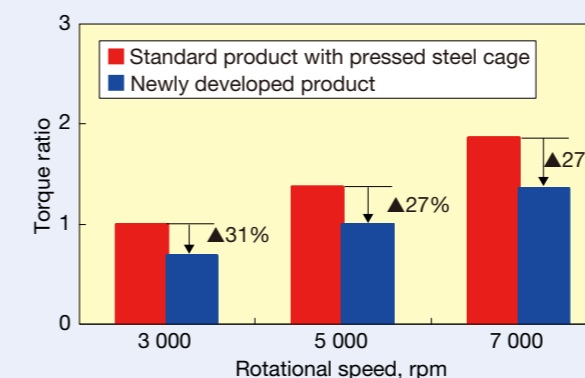


Fig. 8 Torque measurement results for specific rotating speeds

newly developed product is significantly reduced to lower levels than those of standard products under conditions for all lubricant amount conditions.

Torque difference between both bearings as shown in Figure 9, represents the difference of agitation resistance of lubrication oil at each lubricant amount. In the case of small amounts of lubricant, the difference in torque is larger and the difference of agitation resistance becomes larger as well. This shows that the reduction effect on the agitation resistance of the newly developed product with a small amount of lubricant tends to be large. For example, torque of the newly developed product is significantly reduced, and the effect on torque reduction of approximately 48 % can be obtained at the maximum with the lubricant amount of 50 ml/min compared with that of the standard product. This indicates that drops in oil levels and the ratio of balls and cage that are immersed in lubrication oil decreases when compared with standard products if the amount of lubricant in the newly developed product is small. However, the difference between the newly developed product and the standard product is small because most portions of the newly developed product is immersed into oil if the lubricant amount is large. It is considered that the difference of oil level is large and the degree of effects on agitation loss is large if the lubricant amount is smaller.

4.3 Influence of load

Figure 10 shows the measurement results of torque under each load condition. Torque reduction effect of the developed product increases if the load becomes lighter, and approximately 50 % of torque is reduced at the load of $0.02 C_r$. It is considered that this is because the ratio of agitation loss of lubrication oil in bearing torque becomes larger if the load becomes lighter, and why the torque reduction effect becomes small in case of high load is because that friction between the inner and outer rings and rolling element becomes higher and the ratio of agitation loss among whole loss torque becomes smaller.

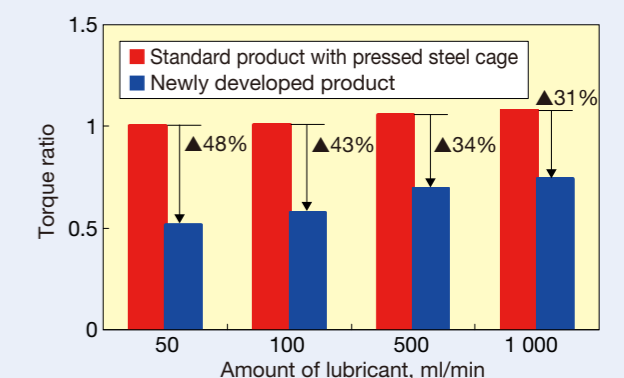


Fig. 9 Torque measurement results for specific amounts of lubricant

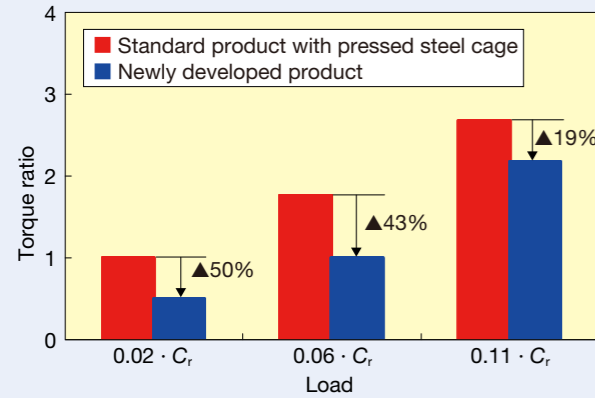


Fig. 10 Torque measurement results for specific loads

4.4 Influence of cage shape regarding flat portion

It is considered that agitation loss can be further reduced by increasing the ratio of the flat portion of the pocket tab side of the low-torque plastic cage. Therefore, we measured torque for specifications with an enlarged flat portion removing 1 or 2 balls from the standard product to verify its effect with the change in ratio of the flat portion of the pocket tab side. We verified the degree of effect on the flat portion while analyzing the effect on the change in number of balls.

As shown in Figure 11, we were able to obtain a torque reduction results by 8% after removing 1 ball, and by 22% after removing 2 balls from the product with the same number of balls as the standard product using a low-torque plastic cage. The analytical value of dynamic frictional torque reveals a predictable reduction of loss torque of 5% after removing 1 ball, and a reduction of 10% after removing 2 balls. The difference between measured results and analytical values increases in line with reduction of the numbers of balls. Thus, it is

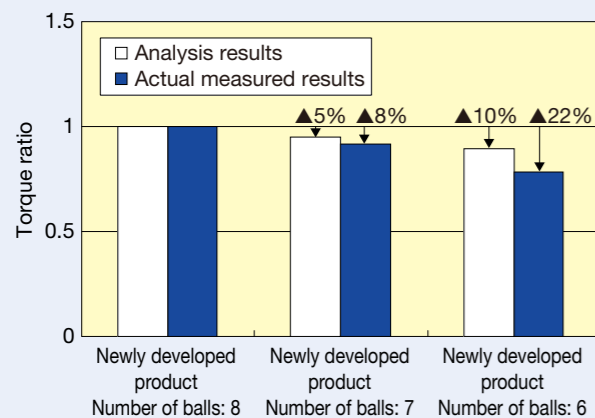


Fig. 11 Torque measurement results for each cage design

considered that agitation resistance of the lubrication oil decreases and the effect of torque reduction increases when the cage flat portion is enlarged.

4.5 Influence of bearing diameter (bearing size)

We verified the same influences of cage shape as stated previously with respect to a large-diameter deep-groove ball bearing with a bore of $\phi 137$ mm, outside diameter of $\phi 172$ mm, and width of 16 mm. This verification is performed with the standard product using a pressed steel cage and the newly developed product using the low-torque plastic cage without changing the number of balls under a load of $0.02 C_r$ at a speed of 2 800 rpm.

Approximately a 45% reduction in torque was obtained even for large-size bearings as shown in Figure 12. As a result of observing agitation conditions of the lubrication oil, we can verify a clear difference of agitation conditions between the standard product and the newly developed product, which was the same as mentioned in section 3.3 and as shown in Figure 13.

In addition, it is possible to further reduce agitation loss by significantly reducing the number of balls and by fully enlarging the flat portion of the pocket side depending on operating conditions because a large number of balls are generally assembled into large-size bearings. For example, this newly developed product consisted of an optimized internal specification and cage shape, which was adopted for a large-size ball bearing that supports a counter drive gear in Figure 1 and achieves significant torque reduction (50% to 65% reduction compared with a conventional product) by decreasing the number of balls by 6 or 7 compared with the number used in a conventional product with standard design.

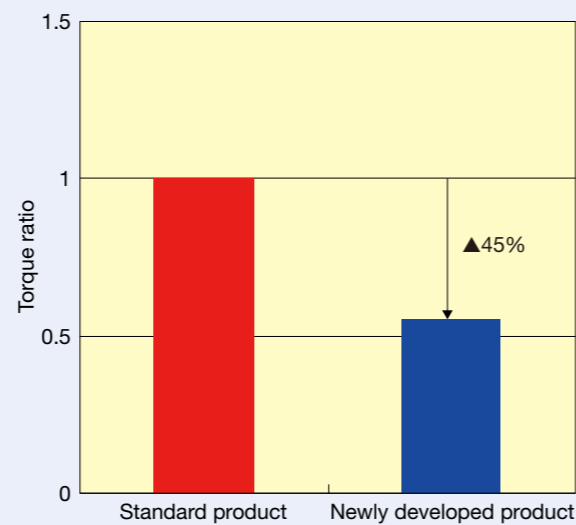


Fig. 12 Torque measurement results for large bearings



Standard product



Newly developed product

Fig. 13 Observation results of lubricant agitation

5. Conclusion

This article introduces an ultralow-torque technology of ball bearings for hybrid vehicles.

Because it is anticipated that further improvement of fuel economy in hybrid vehicles will proceed in the future, we will contribute to improving fuel economy in hybrid vehicles with the application of NSK's four core technologies: tribology, material technology, analysis technology, and mechatronics technology.

References

- 1) Toyota Motor Corporation, "Electronics Manual No. SC12B1J," PRIUS ZVW30 series, (2009).
- 2) H. Aramaki, "Low Frictional Torque Technology of Rolling Bearings," NSK Technical Journal Motion & Control No. 17 (2005) 25-31.
- 3) H. Aramaki, "Rolling Bearing Analysis Program Package BRAIN," NSK Technical Journal Motion & Control No. 3 (1997) 15-24.
- 4) S. Natsumeda, "Computer Simulation Technique for Predicting Performance of Rolling Bearings," NSK TECHNICAL JOURNAL No. 673 (2002) 31-35.
- 5) Y. Murakami, "Long Life Bearing Technology by Carbo-Nitriding," NSK Technical Journal Motion & Control No. 15 (2003) 10-14.



Yuuki Tsuchida



Susumu Tanaka



Toshimi Muraoka

Development of Low-Torque Thrust Needle Roller Bearing for Automotive Air Conditioner Compressors

Takashi Yano, Hiroshi Aida, and Shigenori Murata
Automotive Bearing Technology Center

ABSTRACT

In recent years, reducing CO₂ emissions has become an imperative issue due to global warming concerns. One of the most important issues to be addressed for each vehicle manufacturer is the improvement of fuel economy. This article describes NSK's low-torque thrust needle roller bearing, which achieves a 40 % reduction in torque for the compressor of automotive air conditioners.

1. Introduction

At present, global warming has been viewed as a problem on a global scale, and the reduction of CO₂ emissions has become an imperative issue. Especially for the automotive industry, targets have been set for higher reductions in CO₂ emissions. Each vehicle manufacturer has been developing technologies for improving fuel economy as one of the most important issues they face.

Energy generated by an internal combustion engine in an automobile is distributed to not only the powertrain, but also to components with a certain capability and functionality required for a comfortable passenger compartment. One component that has a large influence is the air conditioner. One example, described in a report, is that when an air conditioner is being operated, vehicle fuel economy is reduced by 15 % to 20 % under normal driving conditions, and reduced by more than 25 % if the vehicle is moving slowly or stopped in a traffic jam. Most of these reductions in fuel economy are directly

caused by compressor operation. Therefore, the needs of frictional reduction at each component of a compressor are increasing.

This article describes NSK's low-torque thrust needle roller bearing, which achieves a 40 % reduction in torque for the compressor of automotive air conditioners.

2. Location and Structure of Bearing

Low torque is in demand for automotive air conditioner compressor bearings to restrict the reduction of fuel economy when the air conditioner is being operated.

Figure 1 shows an example of where bearings are used in an automotive air conditioner compressor, including a cross-sectional view of a swash-plate type of variable capacity compressor, which controls the discharge capacity of refrigerant by varying the angle of the rotating swash plate and offers higher efficiency. Thrust needle roller bearings are located at both ends of the shaft and are used to bear the reactionary forces generated by piston compression.

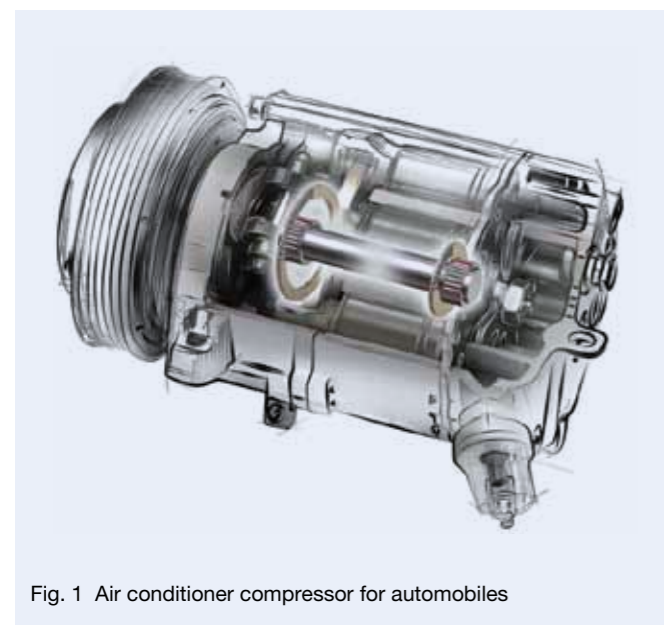


Fig. 1 Air conditioner compressor for automobiles



Photo 1 Low-torque thrust needle roller bearing

The newly developed low-torque thrust needle roller bearing is assembled with a pressed, thin, steel cage and rollers contained within cage pockets, and has a component structure where a pressed, thin, steel bearing washer is positioned on one side.

Photo 1 provides an interior and exterior view of the low-torque thrust needle roller bearing, and Photo 2 shows the internal structure of the bearing.

3. Features of Low-Torque Thrust Needle Roller Bearing

Next, this section describes features of the low-torque thrust needle roller bearing and compares them to a conventional product (Figure 2).

(1) Reduced friction between rollers and raceway washer

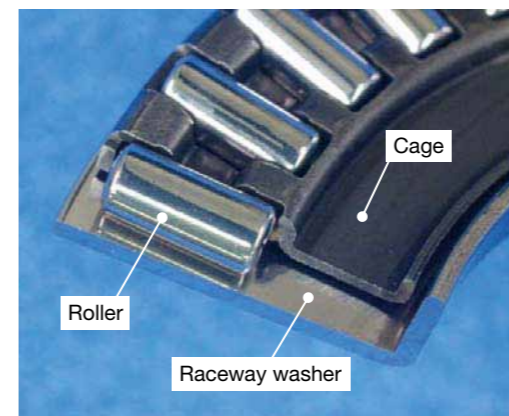


Photo 2 Cutaway view of low-torque thrust needle roller bearing

This reduction is achieved by using fully crowned rollers and by designing a convex raceway surface that reduces friction due to differential slip near the roller end surface, which is generated during bearing rotation (Figure 3).

(2) Reduced friction between rollers and cage
The shape of the cage pocket was reexamined, and a construction where the roller end surface contacts the outer-flanged portion of the cage under high-speed rotation was adopted (Figure 4).

(3) Decreased frictional areas between cage and raceway washer
The guide was constructed so that the side surface of the cage eliminated some contact with the raceway washer (Figure 5).

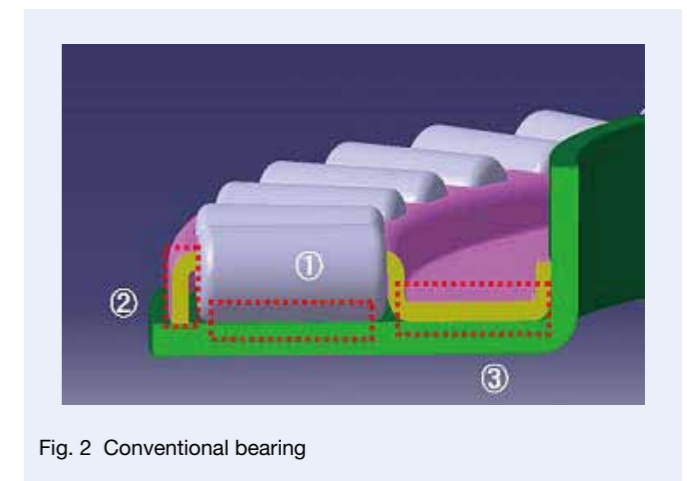


Fig. 2 Conventional bearing

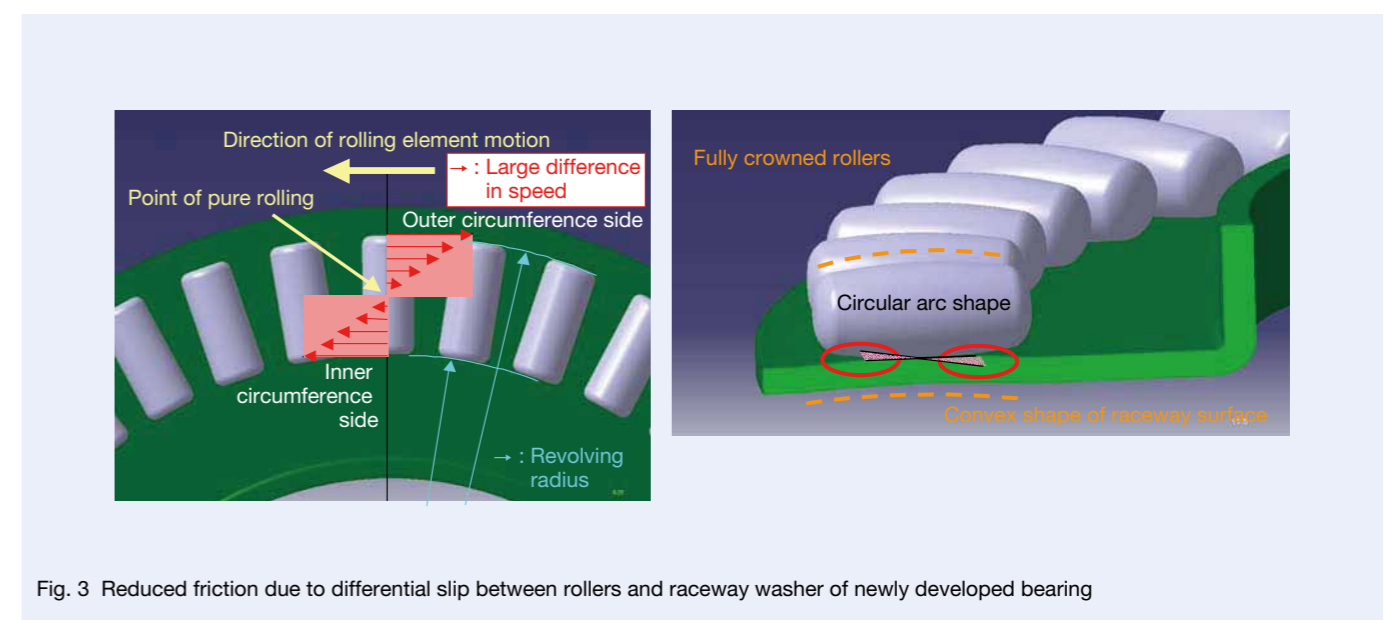


Fig. 3 Reduced friction due to differential slip between rollers and raceway washer of newly developed bearing

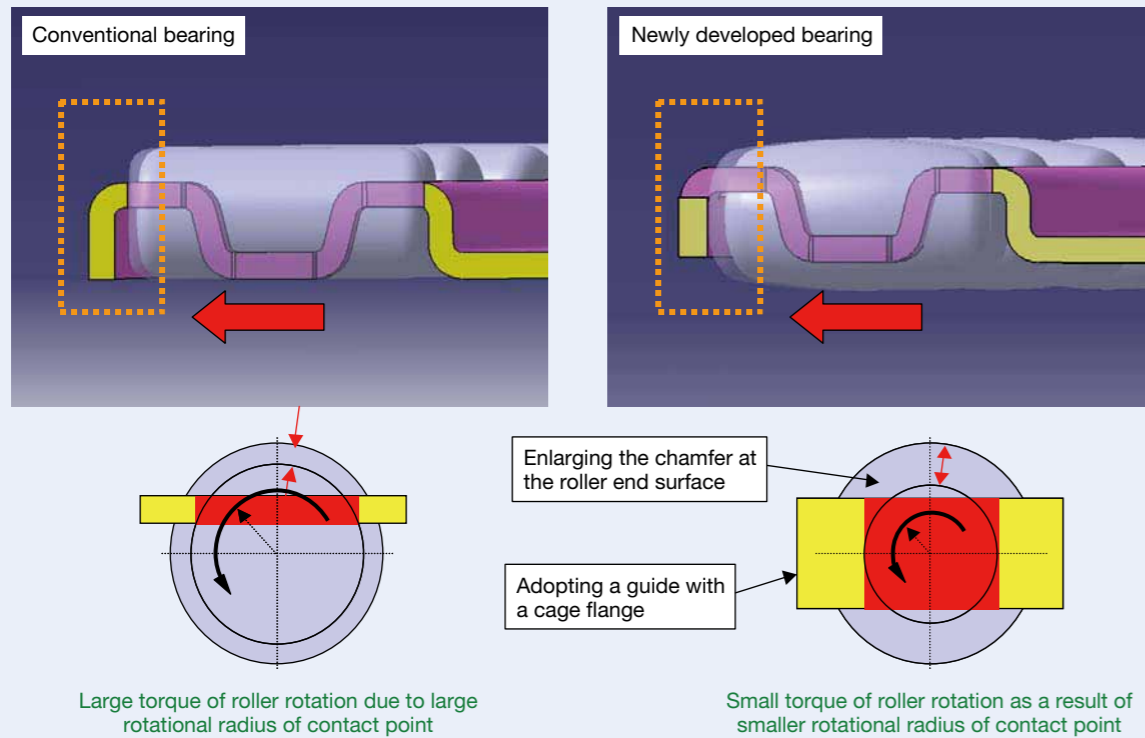


Fig. 4 Reduced friction between rollers and cage

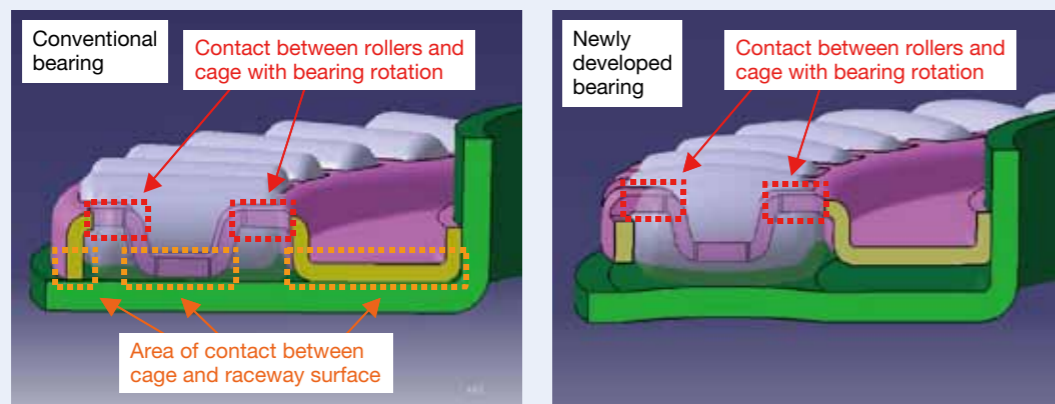


Fig. 5 Decreased frictional areas between cage and raceway washer

4. Torque Measurement

4.1 Torque measurement method

We measured torque of the low-torque thrust needle roller bearing and verified the results. Figure 6 shows a schematic view of torque measurement equipment.

Rotational drag torque at the moment when shaft rotation was changed under conditions of applying axial load to the test bearing was measured as torque. In addition, a constant amount of low-viscosity oil was supplied through the shaft center for lubrication of the bearing. Table 1 lists the measurement conditions.

4.2 Torque measurement results

As a result of reductions made for each slip factor, overall torque reduction of 47% at 1 000 rpm and 39% at 7 000 rpm was observed, and a torque reduction of approximately 40% was achieved for all rotational speeds.

Figure 7 and Figure 8 show the factors contributing to reduced rotational torque. By examining the influence of each item listed in Figure 8, we confirmed that fully crowned rollers have a profound effect on reduction of rotational torque under low rotational speed. This is likely due to the ratio of torque caused by differential slip, which is large in the thrust bearing under low rotational speeds

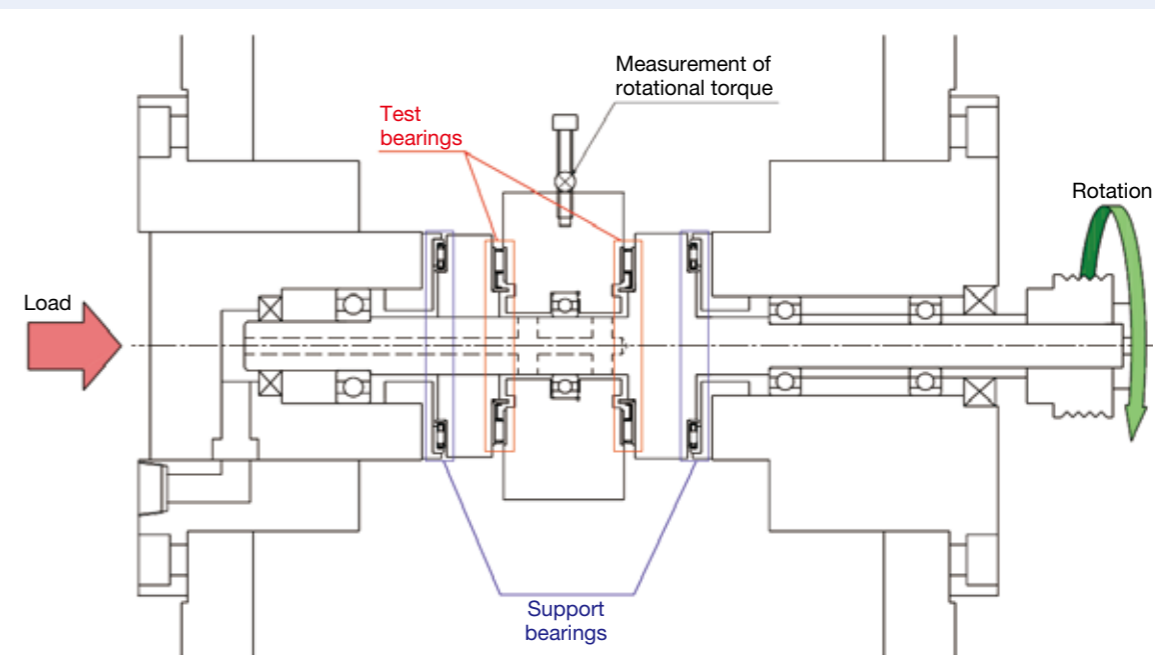


Fig. 6 Torque-measuring equipment

Table 1 Measurement conditions

Axial load	2 000 N
Shaft rotational speed	1 000 rpm to 7 000 rpm
Type of lubrication oil	Low-viscosity oil
Amount of lubrication oil	100 cm ³ /min by oil supply to shaft center
Lubrication oil temperature	60 °C with heater control

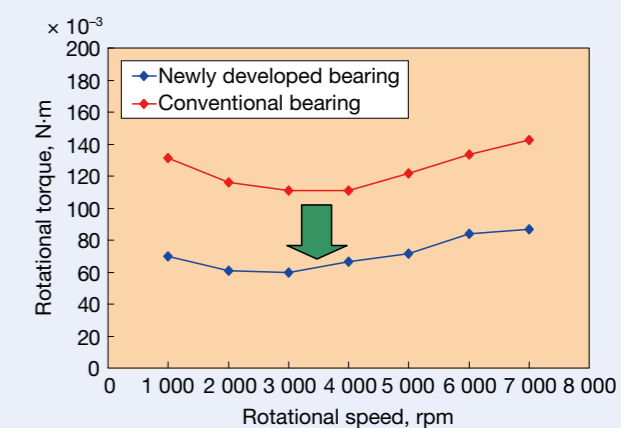


Fig. 7 Measured results of rotational torque

Development of Low-Torque Hub Unit Bearings

Masayoshi Tanahashi
Automotive Bearing Technology Center

ABSTRACT

To address automotive issues related to the global environment, greater focus on reducing driving resistance, reducing weight, and further developing energy regeneration systems is expanding, and as such, demand by automakers for low-torque hub unit bearings is increasing.

As for hub unit bearings, the generation of torque can be evenly split between two portions of the bearing: bearing interior components and the seals. Primary design factors related to torque generation are bearing internal design, preload, grease, seal type, and others. However, since there is typically a trade-off between torque reduction and fundamental performance like rolling fatigue life, a technical approach is required to address this issue. At present, NSK has successfully reduced torque by approximately 25 % through the application of technical solutions that address each design factor.

1. Introduction

The reduction of carbon dioxide emissions and improvement of fuel economy are the most important issues that are recently faced by the automotive industry to address global environment issues including global warming. Therefore, environmentally enlightened approaches such as reduction of driving resistance, light weight, and energy regeneration systems have been the present focus points.

When an automobile is running at a speed of 60 km/h, friction resistance of the hub unit bearing occupies 5 % of running resistance of the entire vehicle¹⁾. In recent years, automobile sales in the markets of developing countries such as BRICs are rapidly increasing. When the number of automobiles actually being driven on the roads increases, fuel consumption also increases accordingly, and improved fuel economy becomes a challenge that will need to be addressed. In order to improve fuel economy, it is important to reduce friction resistance at accelerating speeds, and at constant speeds. Thus, lower torque is in demand for hub unit bearings from the viewpoint of improving fuel economy.

Meanwhile, electric vehicles and hybrid vehicles have been rapidly spreading in recent years, and new terms like the “electric economy” have been created. It is important to facilitate the conservation of the “electric economy” in these vehicles whose drive force is provided by electric motors. Energy regeneration braking has appeared as one of these methods. Energy regeneration braking is a method that utilizes a motor as a generator when decelerating, converts rotational energy of the wheel to electrical energy, and reutilizes the generated electric energy for operating the vehicle. Additionally, rotational resistance when generated is utilized as a brake force. Conventionally, the torque of hub unit bearings has been focused on from the viewpoint of loss when accelerating or running at constant speeds, and has not been focused on as a factor that takes effect

during decelerating. However, it is important for energy regeneration braking to efficiently utilize the motor as a generator; therefore, emphasis has been on reduction of hub unit bearing torque more than ever.

In recent years, the degree to which hub unit bearing torque makes contributions has been increasing in response to the needs of both greater fuel economy and “electric economy” as mentioned above. This article describes concrete methods for lowering torque based on components of torque generation in hub unit bearings.

2. Transition of Hub Unit Bearings

When hub unit bearings are used with clearance or under conditions of low rigidity, driving stability is significantly affected. Therefore, operation is generally under constant preload conditions. Though preload is maintained within a constant range as a result of variations within each product line, there is, of course, a much higher difference in the range of preload variation with subsequent series of hub unit bearings.

Figure 1 illustrates the evolution and features of hub unit bearings. NSK refers to the first generation of bearings as HUB I, the second generation as HUB II, and the third generation as HUB III based on the greater degree of unitization for each subsequent series. The number of flange increases for the purpose of improving ease of assembly and thereby fitting surfaces with counterparts such as a knuckle or hub shaft decrease in accordance with the development of each generation. Preload of a hub unit bearing during running depends on the amount of the initial internal clearance of the bearing and on the amount of reduction of internal clearance due to processes such as the fitting to the counterparts and/or nut tightening. Because interference at the fitting surface and the tightening force of a nut fluctuate, reducing the amount of internal clearance fluctuates as a matter

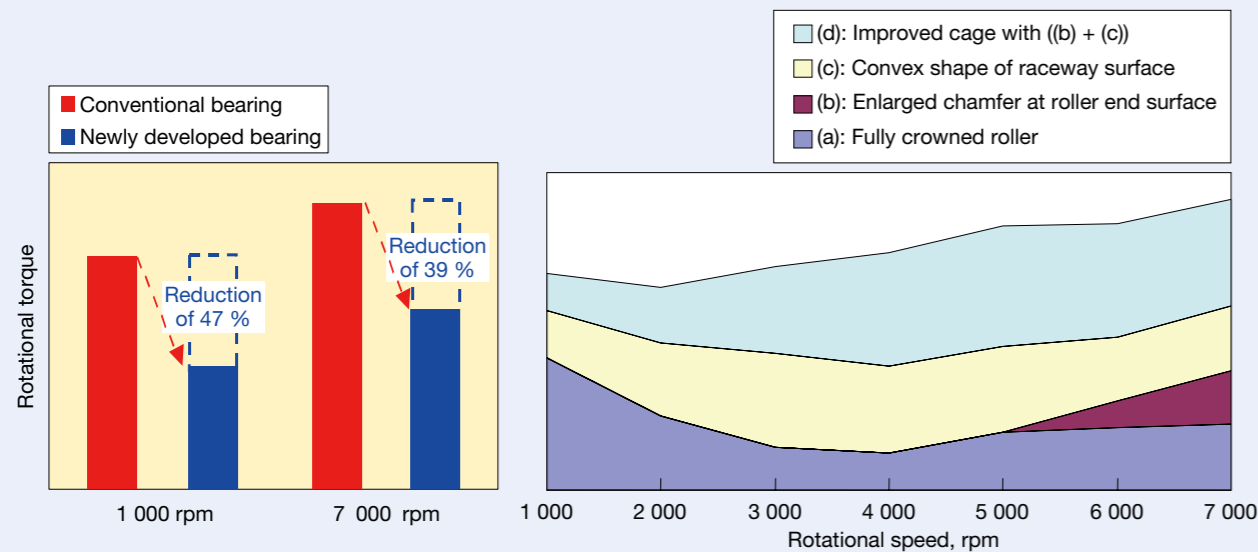


Fig. 8 Analysis of factors contributing to reduced torque

where it is difficult to form and maintain an oil film.

Meanwhile, we verified and achieved better results for reducing rotational torque related to contact between the roller and cage or cage and raceway washer at high rotational speeds. This is likely due to the construction, where contact of the roller end surface with the cage outer flange has been adopted, and improvements in the cage guiding process since the rollers are actively pushed to the outer diameter surface side of the cage by centrifugal force at high rotational speeds. In addition, we verified that the convex shape of the raceway surface also played a role in reducing rotational torque for all rotational speeds.

5. Conclusion

We introduced the construction and results of the low-torque thrust needle roller bearing.

Because this newly developed product can achieve low torque without changing bearing dimensions or boundary dimensions, this bearing can be used to easily retrofit current applications. Use of this bearing can contribute to improved fuel economy when the automotive air conditioner is being operated in line with other advancements made to further enhance fuel economy.

In addition, this product is useful not only for automotive air conditioner compressors but also for the components that are required to reduce rotational torque. The effectiveness of this product is especially anticipated for use in automatic transmissions, which have become increasingly advanced in efficiency, because such transmissions use a large number of thrust needle roller bearings.

We will continue to aggressively develop new products that respond to the many needs of users in the future.



Takashi Yano



Hiroshi Aida



Shigenori Murata

Conventional type	HUB I	HUB II	HUB III
Features Difficult to set preload Complex mounting process	Features (compared with conventional type) Lighter weight Ease of setting preload Improved mounting process Integrated seal	Features (compared with HUB I) Lighter weight Reduced variation in preload Improved mounting of outer ring Enabled mounting to aluminum knuckle	Features (compared with HUB II) Lighter weight Reduced variation in preload Improved mounting of the bearing Higher rigidity

Fig. 1 Evolution and features of hub unit bearings

of course. Therefore, the larger the number of fitting surfaces, the larger the variation of internal clearance reduction, and the preload range becomes broader. That is, the HUB III without a fitting surface can more assiduously limit the preload range. Figure 2 illustrates initial internal clearance and variation of internal clearance reductions using the HUB I and HUB III as examples. The fitting surface with a knuckle and hub shaft is no longer required since the introduction of the HUB III. This bearing reduces variation by approximately 60 % in comparison with the HUB I, and makes it possible to reduce by half the applied preload range.

Details of bearing internal torque will be described later. Figure 3 illustrates the relationship between bearing internal torque and preload. Bearing internal torque becomes large in proportion to preload. Though low torque can be achieved by lowering preload; of course, it is important that the range of preload decreases at the

same time. The ranges of preload for the HUB I, HUB II, and HUB III are shown in the figure with an upper limit preload of 0 kN. It is clear that the HUB III is the most suitable type for achieving low torque. The following information explains the methods of achieving low torque while focusing on the HUB III, which is most suitable for achieving low torque.

3. Components of Torque Generation in Hub Unit Bearings

Torque of a hub unit bearing is considered to be composed of two elements of the bearing. They are torque of the bearing internal components, which support load and rotation of the shaft, and seal torque, which prevents ingress of turbid water into the bearing interior. The ratio of each torque is nearly half. Internal torque of the bearing

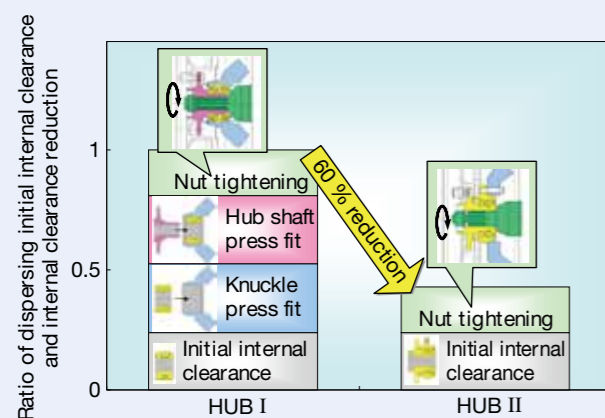


Fig. 2 Dispersion of initial internal clearance and reduction of internal clearance

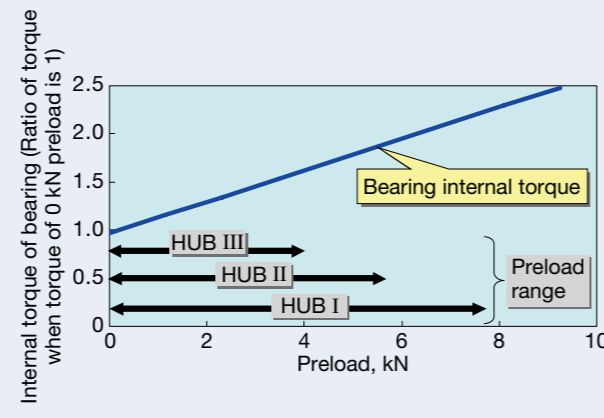


Fig. 3 Relationship between preload and bearing internal torque

is affected by bearing specifications or preload, and seal torque is affected by the type of seal, or by the number of seals (Figure 4).

Figure 5 concludes principal design factors affecting torque of hub unit bearings. Low torque and basic performance such as rolling fatigue life, rigidity, fretting

resistance, and turbid-water resistance of the seal needed for hub unit bearings typically have certain tradeoffs; thus various technological innovations are required²⁾.

This article introduces a method to achieve reduced torque without reducing basic performance, halving both bearing internal torque and seal torque, and provides examples of the aforementioned.

4. Low Torque of Bearing Interior

4.1 Optimization of internal design specifications

Internal design specifications such as ball diameter, number of balls, pitch circle diameter, and raceway groove radius dictate basic bearing performance. If any factor of these specifications is changed for torque reduction, basic bearing performance can be negatively impacted. Therefore, optimum design while considering a balance with basic bearing performance is required when reducing bearing torque.

NSK achieved an approximate 10 % reduction in torque compared with conventional bearings through this optimum design. This article describes the method of torque reduction for each specification.

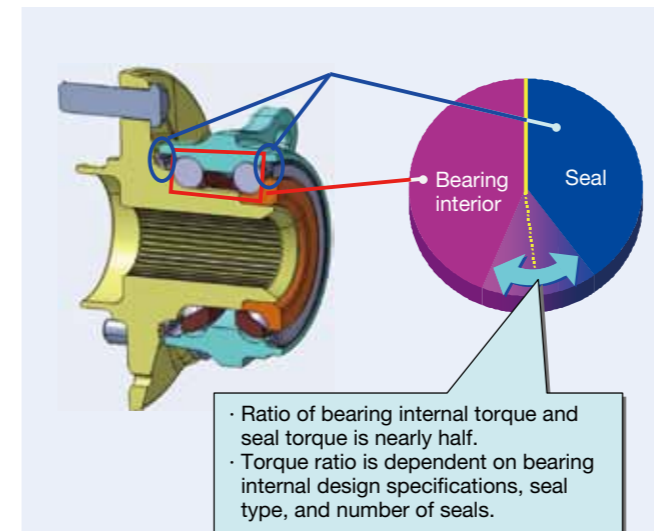


Fig. 4 Ratio of torque of hub unit bearings

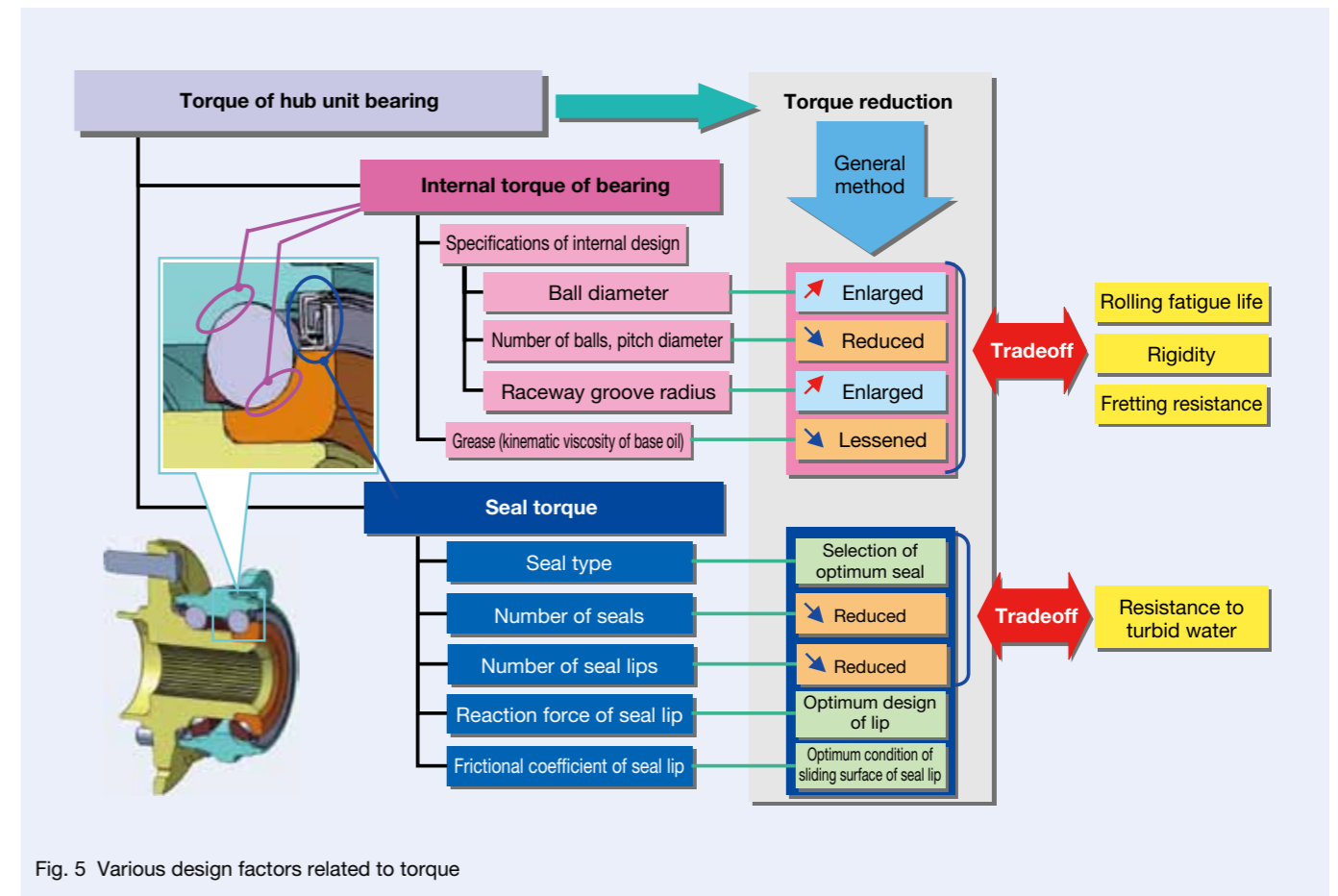


Fig. 5 Various design factors related to torque

4.1.1 Ball diameter

Increasing ball diameter is generally effective for lower torque and increases rolling fatigue life. However, it conversely causes the reduction of rigidity. NSK is developing a design while searching for the optimum solution by combining ball diameter, number of balls, and pitch circle diameter that accordingly fluctuates for balanced performance within a limited space.

4.1.2 Ball number and pitch diameter of ball set

Reducing the number of balls or pitch circle diameter of the ball set is effective in reducing torque. However, it is necessary to pay close attention to such factors, since these factors cause the degradation of basic performance. In recent years, hub unit bearings have been required to drastically reduce weight. Therefore, weight reductions have already reached their limits, and the ball number and pitch diameter of the ball set have already been optimized from the viewpoint of torque.

Conversely, regarding bearings used in markets where the bearings are subjected to severe conditions, such as under water ingress or excessive loads (overloading, impacts) and for developing countries exposed to similarly severe road environments, a greater number of balls and larger pitch diameter of the ball set than that of bearings for developed countries are applied. Such design requirements are in contradiction with the need for reducing torque, and so we have adopted a design that provides a balance with excellent performance by using the method described hereafter.

4.1.3 Raceway groove radius

The raceway groove radius is the most important portion of a bearing where each bearing manufacturer is in possession of original know-how (Figure 6). Enlarging

the raceway groove radius is effective for reducing torque, and it effectively prevents balls from ball overhang (rise over of the ball to the shoulder of the raceway groove) when vehicles turn a corner. Conversely, basic bearing performance reduces due to the increase of contact surface pressure with the balls. At present, NSK balances such complicated performance requirements by adopting an optimum raceway groove radius.

4.2 Selection of optimum grease

Grease is used to lubricate the hub unit bearings. Before hub unit bearings became widely used, grease jobs were often carried out at the time of maintenance and inspection. Presently, however, hub unit bearings are mostly sealed and structurally maintenance free, thus requiring no grease jobs. Therefore, the grease that is initially packed in the bearing is used for the entirety of the bearing's service life. This makes the selection of grease very important.

Grease is basically composed of base oil, a thickener, and additives. Figure 7 shows bearing internal torque when using a single bearing with grease A, grease B, and grease C that contain a base oil with differing kinematic viscosity. From this figure, it is found that internal torque of the bearing correlates with the kinematic viscosity of the grease base oil. When selecting grease A with a minimum kinematic viscosity of base oil in this example, it is found that bearing internal torque can be reduced by approximately 30% compared with that of grease C, which has a maximum kinematic viscosity. Low kinematic viscosity, however, has harmful effects on oil film formation on the rolling surface for reducing rolling fatigue life, and facilitates a greater likelihood of grease leakage. Therefore, reducing internal torque by approximately 15% is a more realistic value in consideration of making a trade off with minimum kinematic viscosity.

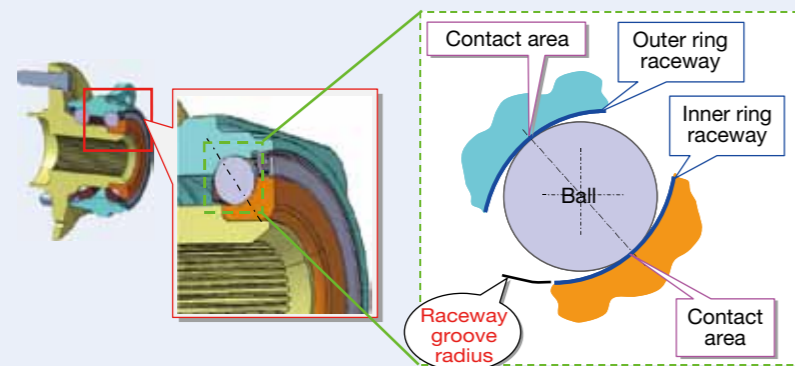


Fig. 6 Optimization of raceway groove radius

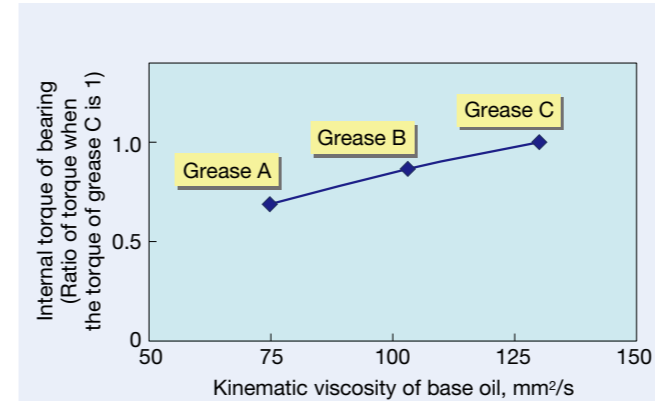


Fig. 7 Relationship between kinematic viscosity of grease base oil and internal torque of bearing

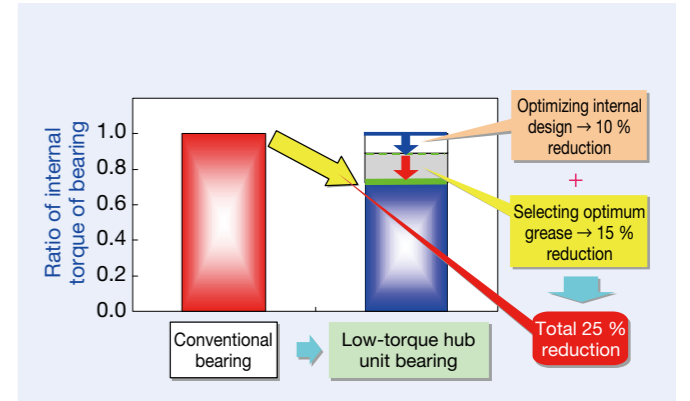


Fig. 8 Reduction of internal torque of hub unit bearing

4.3 Conclusion about bearing internal torque

It is possible to reduce bearing internal torque by 25% compared with that of a conventional bearing by combining the above-mentioned methods (Figure 8). We will explain the reduction of seal torque and finally introduce the torque reduction ratio of a whole bearing in the next section.

5. Low Torque of Seals

Hub unit bearings are used for the chassis of automobiles and are mounted where they are subject to severe environments including exposure to foreign debris such as turbid water. Therefore, excellent turbid-water resistance is required of the seals for hub unit bearings. NSK has prepared various types of seals for each bearing type and each mounting position as shown in Figure 9³⁾.

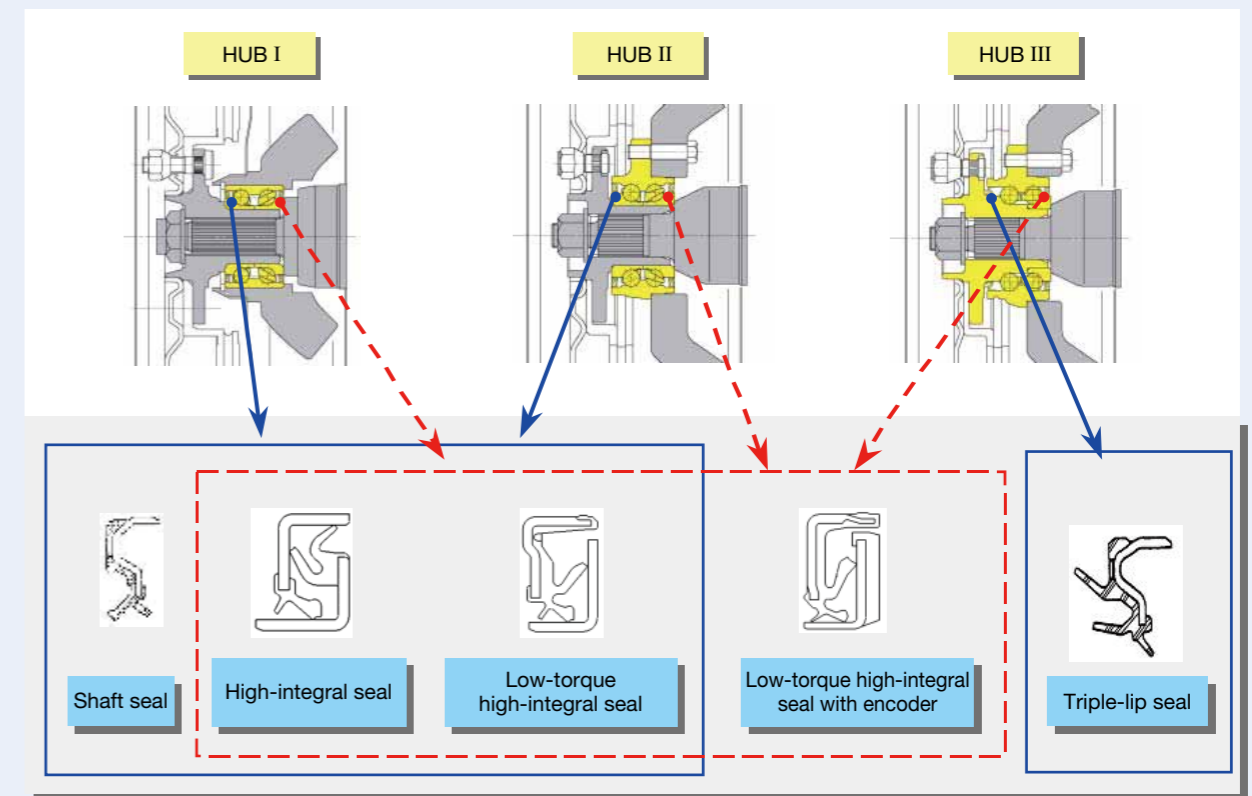


Fig. 9 Seal types for hub unit bearings

The need for turbid-water resistance of hub unit bearings is different between vehicle manufacturers because each vehicle manufacturer has its own approach to addressing issues of turbid-water resistance including the surrounding structure of the bearing, which correlates closely with the structure of the vehicle body. Reducing the number of seals or seal lips is an effective method for lowering torque as shown in Figure 5, but it is necessary to relieve loads acting on the bearing seal by further devising a surrounding structure because turbid-water resistance of the seal itself is adversely impacted. It becomes possible to maintain turbid-water resistance in the system by first avoiding exposure to turbid water during vehicle operation as a result of creating a bearing structure on the vehicle body side which reduces exposure of the bearing, and especially the area surrounding the seal, to the outside environment. However, it is difficult for bearing manufacturers to carry out such an approach on their own, and so a detailed discussion is omitted from this article.

It is necessary to reduce friction force between the seal lip and its sliding surface while ensuring sufficient turbid-water resistance of each seal lip for reducing torque while maintaining turbid-water resistance of the seal itself. It can be considered that this friction force is a product of reaction forces and the friction coefficient of the seal lip. A method for reducing such forces and friction is introduced in the following sections.

5.1 Reduction of reaction forces by optimizing the configuration

Reaction forces of the seal lip correlate with the amount of lip deformation, surface pressure, and contact width. Turbid-water resistance also correlates with the same. Therefore, FEM has been utilized for designing seal lips in recent years. For determining compatibility of low torque and high resistance for turbid water at the design stage, lip configuration has been optimized by utilizing FEM as shown in Figure 10. Giving the same interference as that under actual usage conditions for each lip, reaction forces and contact conditions of the seal lip are verified. As a result, it is possible to maintain high resistance to turbid water by optimizing the contact conditions of the lip as well as the reduction of torque by reducing reaction forces of the lip. In recent years, it has become easy to achieve optimized contact conditions of the lip with smaller reaction forces through greater design freedom of the lip because rubber material with reduced elastic modulus has been developed. Torque of approximately 20 % can be reduced by these methods.

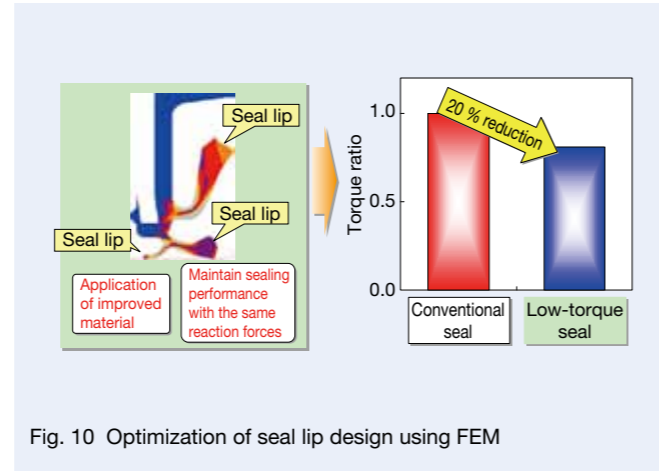


Fig. 10 Optimization of seal lip design using FEM

5.2 Reduction of friction coefficient of seal lip

The friction coefficient of the seal lip varies according to the grease between the seal lip and its sliding surface, and conditions of the seal lip contact surface.

Grease is the same for the bearing interior in that the lower the kinematic viscosity of the grease base oil, the lower the torque. However, it is necessary to consider a balance regarding grease leakage as well, which was described in section 4.2 about the selection of optimum grease.

Factors that influence the condition of the lip contact surface include surface roughness and coefficient of sliding friction. In recent years, research for an optimum value where low torque is compatible with turbid-water resistance has been advanced.

6. Conclusion

We explained the method for reducing hub unit bearing torque.

At present, NSK has succeeded in reducing hub unit bearing torque by approximately 25 % using this method while maintaining high reliability in the market (Figure 11).

However, it is considered that even lower torque will be increasingly in demand for hub unit bearings, in light of the recent growth in sales of automobiles in the markets of developing countries and a significant leap in sales of electric vehicles and hybrid vehicles. Up to the present, hub unit bearings have dramatically progressed in response to market needs. NSK will continue to provide hub unit bearings that respond to market needs and will continue to contribute to society with future developments.

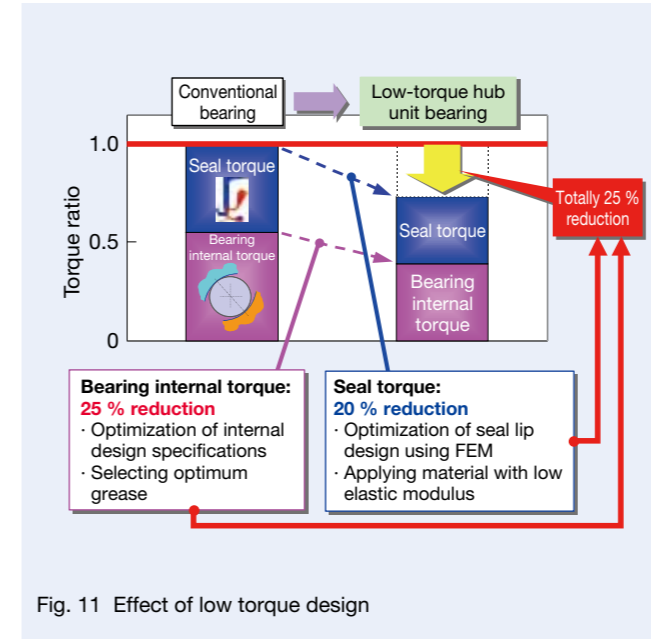


Fig. 11 Effect of low torque design

References

- 1) Masataka Nasada, "Improvement of fuel economy by chassis components," *Automotive Engineering*, 62-3 (2008) 80-81.
- 2) Hiroaki Ishikawa, "Technological trend and tribology for hub unit bearings," *Tribologist*, 54-9 (2009) 580-585.
- 3) Tetsu Takehara, "State-of-the-art technology for hub units," *Design engineering*, 42-8 (2007) 454-455.



Masayoshi Tanahashi

Technological Trends of Bearings for Electric Motors on Board Vehicles

Nobuaki Izawa
Automotive Bearing Technology Center

ABSTRACT

Parts of vehicles are changing both as motor vehicles make the transition from engines solely powered by fossil fuels to hybrids or all-electric power, and as automakers make further improvements to fuel economy. Therefore, demand for electric motors on board vehicles is increasing.

Low torque, low noise, long life under high temperatures, and sealing performance are required of bearings for such electric motors, and different performance criteria are selected to meet the specifications of various applications where motors are used in the vehicle.

In this article, technological trends of electric motors on board vehicles, and bearings for such motors are described.

1. Introduction

In recent years, computerized controls in automobiles have become widely used with increased demand for lower fuel consumption, greater efficiency, and enhanced safety and comfort. Therefore, the number of motors used in automobiles has dramatically increased.

Electronic throttles, variable valve timing systems, exhaust gas recirculation systems (EGR), and dual clutch transmissions for low fuel consumption and high efficiency with precise control of air intake, electric power steering (EPS), electric water pumps, and electric fans for high efficiency, antilock brake systems (ABS), and electronic stability control systems (ESC) such as vehicle stability control (VSC) or vehicle stability assist (VSA) for improved safety, electric powered seats and electric sliding doors for a comfortable ride have been used in recent automobiles. These components are mostly driven and controlled by motors. In addition, fan motors for cooling batteries are equipped in hybrid vehicles (HV), and thus motor demand tends to increase.

Here, recent technological trends of bearings used for on-board motors are described.

2. Principal Features and Technological Trends of Bearings for on-Board Motors

Required performance of bearings for typical on-board motors and features of bearing specifications are described in the following sections.

2.1 Bearings for electric fan motors

Electric fan motor bearings require long-life performance under high operating temperatures, and dimensional stability for fitting in order to respond to positioning by press fitting due to the reduction of the number of components. Therefore, NSK has been adopting long-life

grease for use under high-temperature conditions, bearing rings that have been treated for dimensional stability under high temperatures, and well-sealed, non-contact metal shields. These specifications achieve excellent performance. Principal specifications are as follows:

- (1) Shield: Well-sealed metal shield (ZZ1)
- (2) Cage: Plastic cage
- (3) Grease: EA3 grease (dedicated grease) up to 150 °C
EA6 grease (dedicated grease) up to 160 °C
KF1 grease up to 180 °C
- (4) Specifications for dimensional stability under high temperatures:
Special heat treatment
Improved resistance to indentations can be ensured with this special heat treatment as well as ensuring dimensional stability.

2.2 Bearings for blower motors

Bearings for blower motors are changing from sliding bearings to rolling bearings for the purpose of higher reliability and reducing costs related to motor assembly processing. Quiet-running performance is especially required for blower motors because they are mounted inside the car near the driver. Therefore, it is important that the bearings maintain extremely low-noise performance.

Principal bearing specifications are as follows:

- (1) Seal: Light-contact seal (DDW)
- (2) Cage: Plastic cage
(Specifications with measures to counter cage noise. Refer to Figure 1.)
- (3) Sound grade:
Specifications for ultralow noise (ERU6)
- (4) Grease: NS7 grease that offers superior low-noise performance

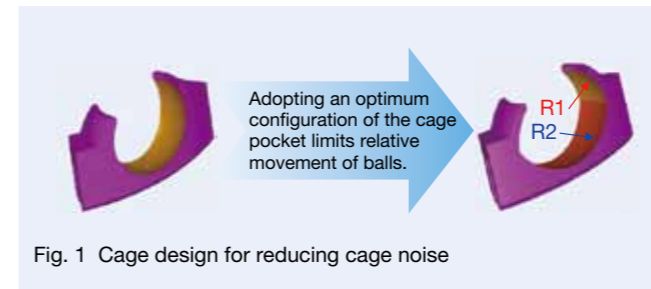


Fig. 1 Cage design for reducing cage noise

- (5) Specifications for resisting indentations due to improper handling:

Special heat treatment
(Dimensional stability under high temperatures is also achieved. Refer to Figure 2 regarding resistance to indentations.)

2.3 Bearings for ABS motors

(1) Bearings serving as eccentric shaft

Anti-lock brake system (ABS) motors have a structure where a plunger moves up and down in line with the outside surface of the bearing mounted to an eccentric shaft, and pressurized hydraulic brake fluid is discharged

by the moving plunger, when the eccentric shaft rotates.

Conventionally, needle roller bearings or standard ball bearings have been mounted to the eccentric shaft, but there is an example of adopting bearings with an inner ring where the bore is positioned off the center axis of the bearing instead of the eccentric shaft and the conventional bearings for the purpose of reducing costs related to eccentric shaft processing (refer to Figure 3).

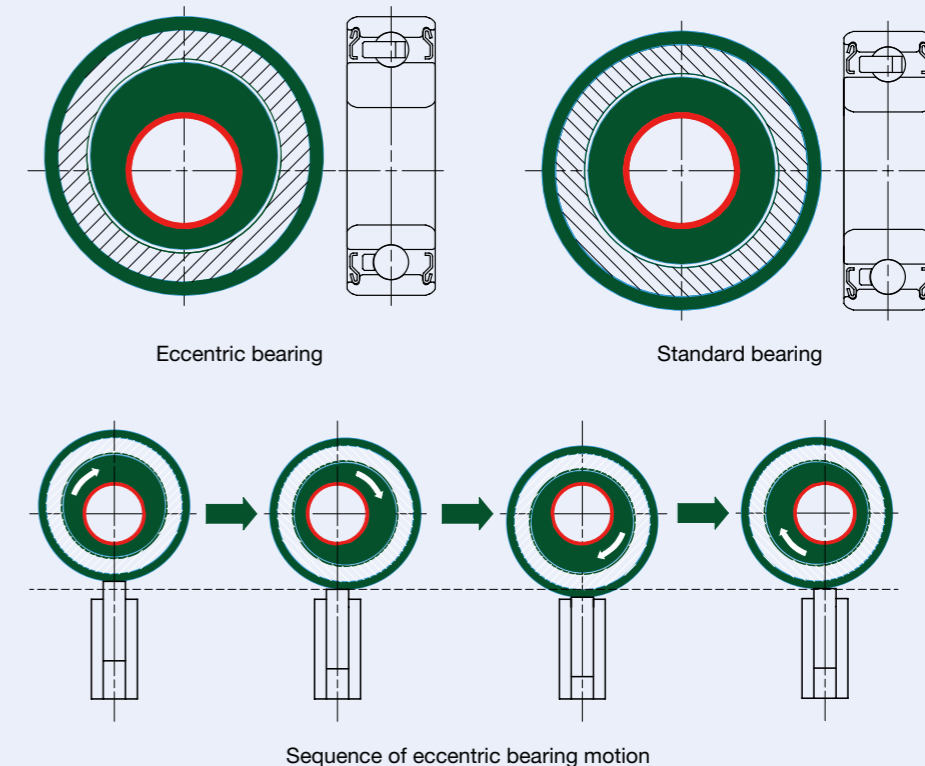


Fig. 3 Comparison of standard and eccentric bearings; and the sequence of eccentric bearing and plunger motion¹⁾

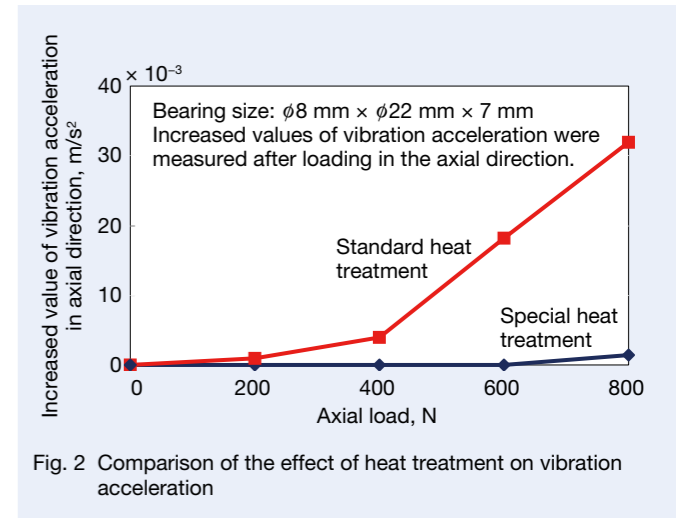


Fig. 2 Comparison of the effect of heat treatment on vibration acceleration

(2) Bearings for front side of motors

ABS motors have a tendency to operate for extended periods of time as a result of developing sophisticated models for active safety, which in turn generates the risk that brake fluid may leak from the plunger piston and outflow to the front side of the motor. If the fluid intrudes into the interior of the front-side bearing, grease in the bearing interior will flow out into the motor and defective rotation of the motor will occur in the worst-case scenario. To prevent such a scenario, bearings with contact seals made of ethylene-propylene-diene ternary copolymer (EPDM) rubber, which is resistant to brake fluid, are used in the front-side bearings. Since there is a tendency for the motor to be operated for extended periods of time due to growing sophistication of active safety systems in recent years, there is increasing demand for bearings with improved seal performance. NSK has developed seals offering highly sealed, low-torque specifications by conducting various analyses and evaluation tests.

2.4 Bearings for throttle support

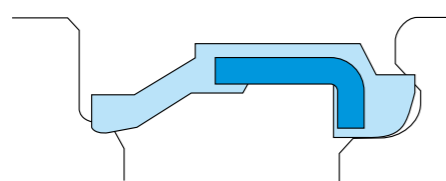
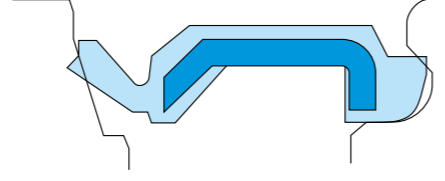
The throttle chamber (including electronically-controlled throttles) is a device that controls the flow rate of air intake into the engine, eliminates the shaft seal, which is conventionally used to maintain an airtight chamber, and tends to fulfill the role of a bearing seal for the purpose of reducing costs. Therefore, throttle support bearing seals have been required to be highly airtight as an alternative to shaft seals. In addition, there is a recent trend of more automobiles using small-sized engines mounted with turbo

chargers, and supercharging pressure from the turbo charger has increased the air pressure. Thus throttle support bearing seals have been required to facilitate even greater airtight sealing performance. NSK developed the airtight DP seal to ensure a sufficient airtight sealing to counter both negative pressure and positive pressure generated in the throttle chamber (refer to Table 1). In addition, NSK has adopted fluorine rubber for the seals, which affords physical stability when resistance to gasoline is required.

2.5 Bearings for motors of precision control system

Bearings of motors for electric control such as controls of electronic throttles (Figure 4), the exhaust gas recirculation (EGR) system (Figure 4) and variable valve-timing systems have been required to provide low torque and long life under high-temperature conditions for the purpose of optimum control in order to achieve lower fuel consumption and higher efficiency. Fluorine grease has been adopted as a lubricant to satisfy these features. In addition, initial break-in running of the motor is sometimes carried out prior to delivery of fully manufactured motors to maintain motor torque stability, and reducing the number of hours needed for initial break-in running is required since the time needed to rotate the motor for breaking it in is directly linked to the cost of the motor. In response, NSK developed low-torque grease that stabilizes torque within a short period of time by introducing nanoparticle technology (refer to Figure 5 and Figure 6).

Table 1 Comparison of conventional and newly developed seals

	Conventional seal (type D)	Newly developed seal (type DP)
Seal configuration		
Features	Standard sealed contact seal The seal lip makes contact with the seal groove of the inner ring in the axial direction.	High pressure resistant seal with low torque Reducing the thickness of the seal lip base portion and improving flexibility of the lip portion improve following capability. The seal lip makes contact with the seal groove of the inner ring in the radial direction, and change of seal torque is controlled by positional changes in the axial direction. The seal lip sliding surface of the inner ring is tapered, and folding over of the lip under positive pressure is prevented.

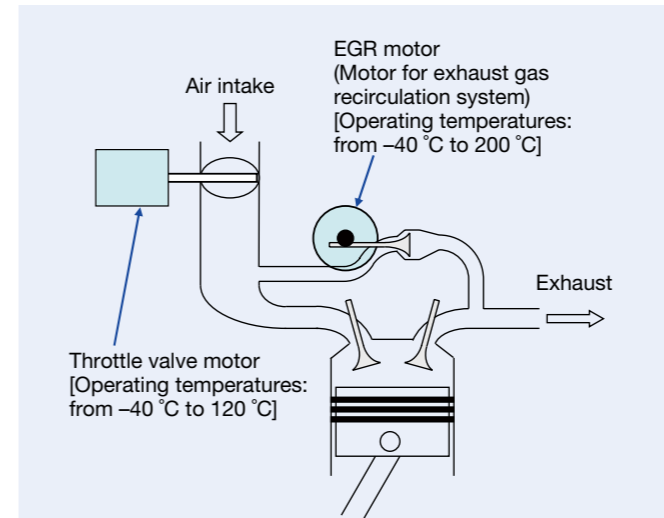


Fig. 4 Positions and ambient operating temperatures of throttle valve motors and EGR motors

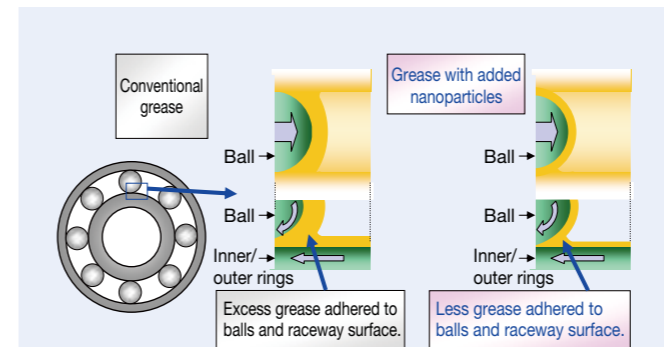


Fig. 5 Mechanism for reducing torque

2.6 Bearings for wiper motors

The shaft of a wiper motor (Figure 7) is a worm gear, and the wiper reciprocates by motor rotation. A combination of a rolling bearing and a sliding bearing is used, and the motor has a structure where a rolling bearing is typically used to sustain the loads. Generally, the generated load is in the axial direction of the motor shaft. If a wiper motor is used to push heavy snow across

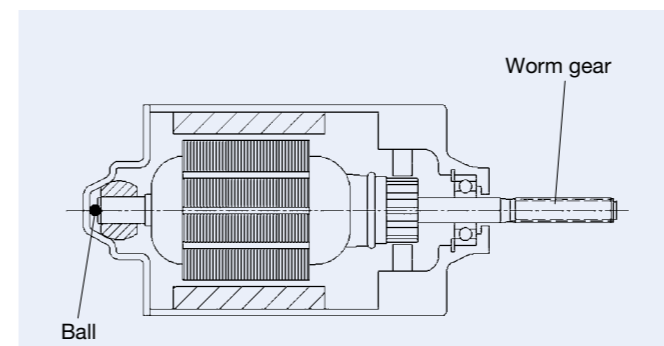


Fig. 7 Cross-sectional view of a wiper motor

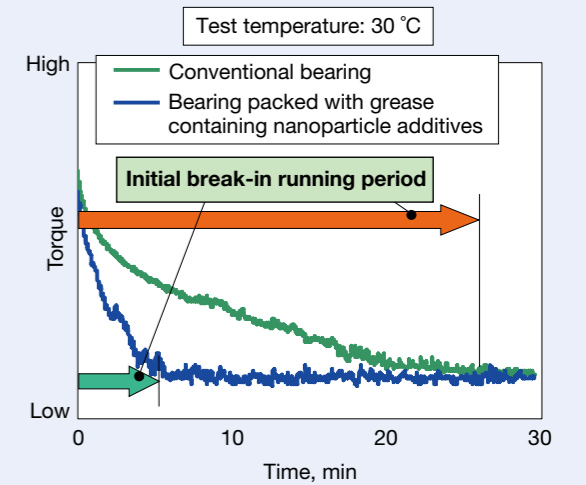


Fig. 6 Comparison of initial break-in running period

the windshield, it is anticipated that large forces will be generated in the axial direction of the motor, and will exceed the permissible axial load of the rolling bearing. Conventionally, a ball has been mounted to the shaft end to support this load, but a recently designed motor eliminates mounting of this ball to simplify the motor production process. For this case, NSK developed a bearing interior design that responds with the required performance of high-load capability to fully support axial loads.

3. Conclusion

This article has introduced trends and technologies of bearings used for recent on-board motors. Other than the motors that have been introduced at this time, such as fan motors for cooling batteries used in hybrid vehicles or electric vehicles, oil-pump motors for transmissions, and dual-clutch motors, the number of these motors using rolling bearings has been increasing. Functions required of bearings are expected to become increasingly diverse. We will further develop highly functional bearings that are able to respond to such applications and operating environments.

Reference

- 1) New Products, "Eccentric Bearings," NSK Technical Journal Motion & Control, 20 (2007) 43-44.



Nobuaki Izawa

Ultrahigh-Speed Ball Bearing for Motors and Power Generators in Next-Generation Hybrid Vehicles

In recent years, the need for greater compactness, lighter weight, and ultrahigh-speed rotational performance to ensure the output power of drive motors and power generators in next-generation hybrid systems in vehicles has been increasing amid efforts to further improve fuel economy.

NSK has developed ultrahigh-speed ball bearings capable of rotational speed in excess of 30 000 rpm, which is 1.5 times that of conventional bearings for use in motors and power generators of next-generation hybrid vehicles (Photo 1).

1. Construction and Specifications

Figure 1 shows a cross-sectional view of the newly developed bearing. By mounting the plate that controls oil flow to the inflow side of the bearing, lubrication properties have been improved by ensuring a steady supply of oil to the inner ring and ball side where lubrication is easily depleted during rotation at ultrahigh-speeds. In addition, a lightweight, plastic cage offering low friction has been adopted, including greater optimization of the bearing internal specifications, to facilitate greater control over friction and heat generation under ultrahigh-speed rotation. Strength of the plastic cage's circular



Photo 1 Ultrahigh-speed ball bearing for motors and power generators in next-generation hybrid vehicles

ring portion is further improved by offsetting a bearing ring groove without extending bearing space to avoid deformation and breakage of the cage resulting from centrifugal forces acting on the cage during ultrahigh-speed rotation.

2. Features

The newly developed bearing has excellent high-speed rotational performance.

High-speed performance exceeding 30 000 rpm has been achieved by optimizing bearing internal specifications, mounting an oil-flow control plate, and by optimum design of the plastic cage (Figure 2).

3. Summary

This newly developed bearing enables ultrahigh speeds for drive motors and power generators and can fully contribute to improved fuel economy for next-generation hybrid vehicles of all sizes from small to large. We will continue to take on the challenge of developing new products with new functions that respond to the needs of a sophisticated market.

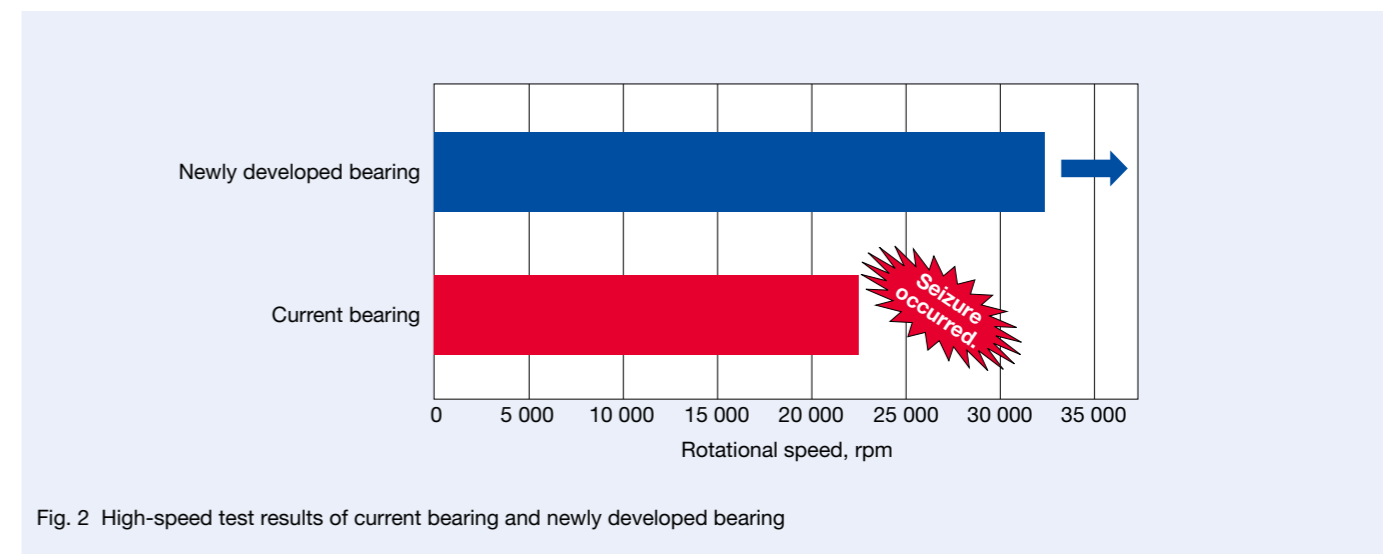


Fig. 2 High-speed test results of current bearing and newly developed bearing

Reducing friction and heat generation

- Reduced friction at inner ring side by mounting an oil-flow control plate
- Reduced friction and heat generation by optimizing bearing specifications

Improving the cage

- Design for withstanding centrifugal forces
- Design for suppressing cage vibration
- Design for a compact size and light weight using offsetting

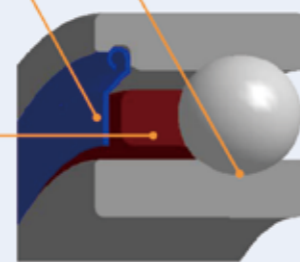


Fig. 1 Cross-sectional view of newly developed bearing

Ultralow-Torque Sealed-Clean Ball Bearings for Transmissions

In recent years, improving the fuel economy of automobiles has been an important issue to address while increasing awareness of environmental issues. Automotive transmissions are required to improve further efficiency, and their bearings are required to offer greater low-torque performance.

NSK has developed new ball bearings with seals resulting in the development of an ultralow-torque sealed-clean ball bearing (Photo 1), whose torque has been successfully reduced by optimum design of the seal lip using FEM analysis.



Photo 1 Ultralow-torque sealed-clean ball bearings for transmissions

1. Features

(1) Seal specifications and torque

Using FEM analysis of the lip configuration, the lips of seals are narrowed by 10 % and lengthened by 70 % compared to lips in current bearings. Lip-following capability has been improved and contact pressure along the lip edge has been equalized using this design.

As a result of this, contact force has been reduced by 50 % that of the current bearing, and the bearing torque has been reduced to half that of current bearings (Figure 1 and Figure 2).

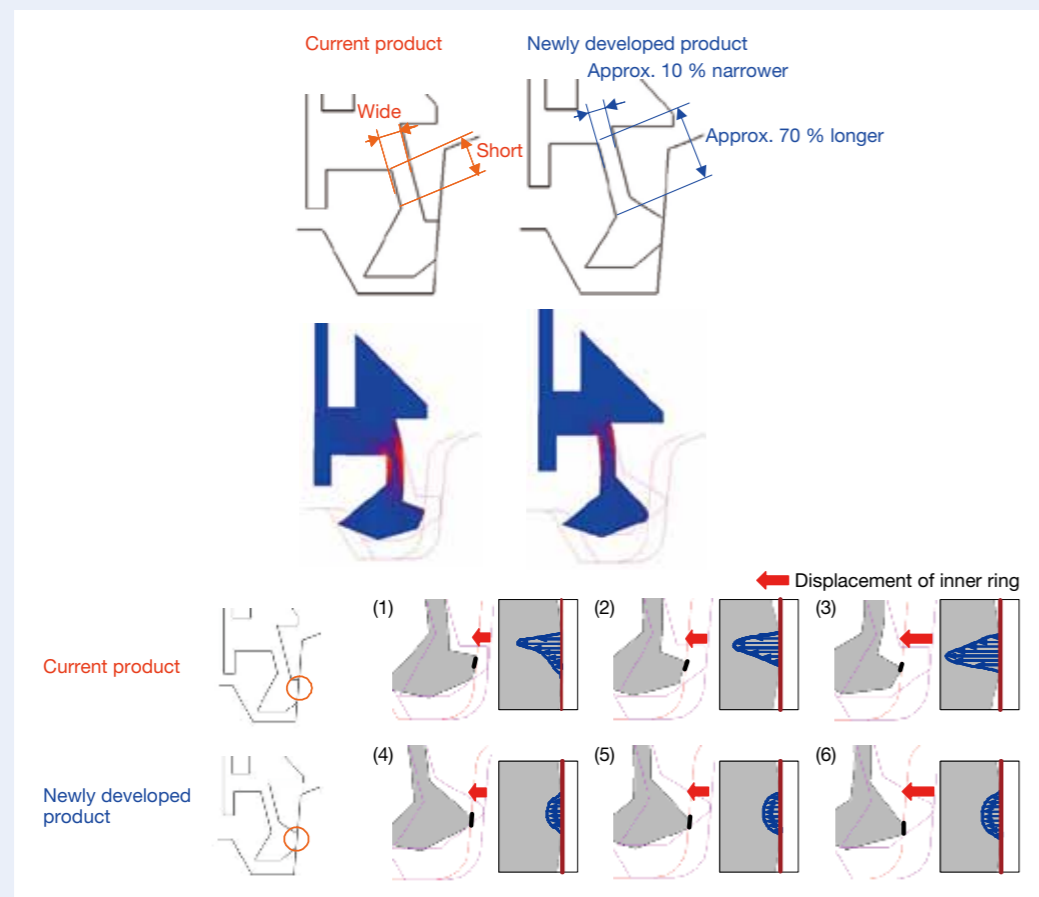


Fig. 1 Comparison of contact conditions of current seal and newly developed seal

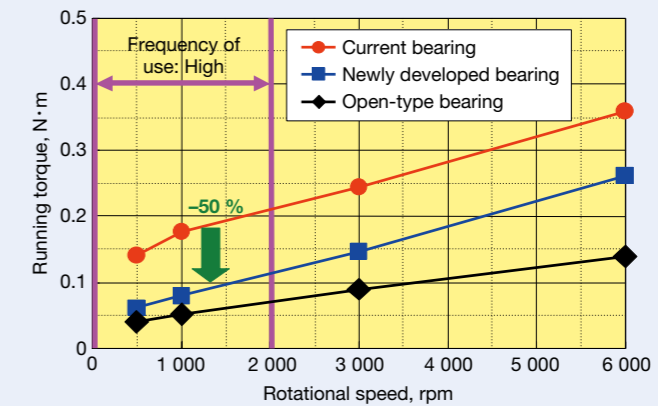


Fig. 2 Running-torque comparison of bearings with current seal and newly developed seal

(2) Bearing life

As a result of the improved lip configuration by FEM analysis, contact surfaces between the inner ring and the seals are ensured even if the inner ring moves in the axial direction.

This prevents foreign particles in the transmission oil from entering into the bearing interior, and this bearing with ultralow-torque seals achieves the same level of endurance as the current bearing (Figure 3).

2. Summary

This ultralow-torque sealed-clean ball bearing is capable of responding to customers' demands at many NSK manufacturing sites of ball bearings around the world. Thus, this product can be delivered in a timely manner from various NSK sites around the world to customers on a global scale.

Test bearing	φ35 mm × φ78 mm × 16 mm
Radial load	4 193 N
Axial loads	+ 7 561 N (60 s) - 1 890 N (2 s)
Rotational speed	7 000 rpm
Oil amount	Shaft center
Oil temperature	120 °C ± 3 °C
Foreign particles	0.2 g / L
Misalignment	2 / 1 000

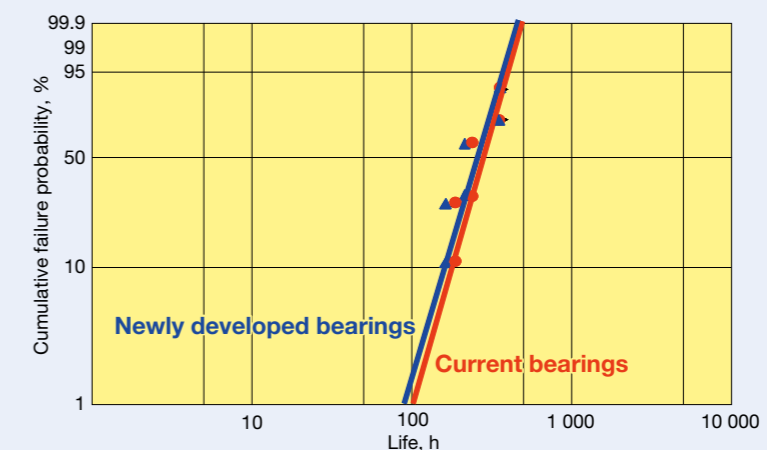


Fig. 3 Endurance test results of current sealed bearings and newly developed sealed bearings

High-Speed-Type Miniature Roller & Cage Assembly for Planetary Gears

In recent years, demand for reducing CO₂ emissions and improving the fuel economy of automobiles has been increasing, and applications for automotive transmissions that are compact, lightweight, and highly efficient have been expanding. Many planetary gears are mounted to automatic transmissions, push-belt continuous variable transmissions, and transmissions for hybrid vehicles in order to advance more compact designs. Needle roller bearings are used to support the pinion gears of such planetary gears.

NSK has developed the world's smallest class of high-speed-type miniature roller and cage assemblies (Photo 1) for planetary gears, which facilitate the compact size, lightweight design, and high efficiency of planetary gears operated at much higher-speed rotation.

1. Specifications

Cages of bearings for planetary gears are required to have high strength and high durability under conditions of increasingly high rotational and revolving speeds of planetary pinions.



Smallest size of previous mass-produced product for high-speed use
Roller diameter: ϕ 2.5 mm
Bore diameter: ϕ 11 mm
(Pinion shaft diameter)

Newly developed miniature product for high-speed use
Roller diameter: ϕ 1.5 mm
Bore diameter: ϕ 7 mm
(Pinion shaft diameter)

Photo 1 The newly developed high-speed-type roller and cage assembly (right) and the previous smallest product (left) for planetary gears

NSK has already marketed a high-speed-type roller and cage assembly with an M-shape cage (M cage) that has been improved in terms of strength and durability by adopting chromium molybdenum steel for the cage material, and by manufacturing an M-shape cross-section for the cage configuration for use in planetary gears operated at much higher-speed rotation.

The high-speed-type roller and cage assembly with an M cage with a shaft diameter of 11 mm and roller diameter of 2.5 mm used to be the minimum size in high-speed-type roller and cage assemblies that NSK had mass-produced for planetary gears in the past.

Optimum design using computer analysis, durability testing, and various processing experiments were conducted resulting in NSK achieving the world's smallest class of high-speed-type miniature roller and cage assemblies with a newly developed M cage with a shaft diameter of 7 mm and roller diameter of 1.5 mm for use in planetary gears.

2. Features

Previously, miniature needle roller bearings whose shaft diameter was less than 10 mm used either full-complement type assemblies or roller and cage assemblies with a cage that is manufactured to have a wave-shape cross section for the cage configuration (previous cage) depending on the specific planetary gear application (Photo 2). However, such assemblies were not suitable for high-speed use.

The following items describe features of this newly developed high-speed-type product in comparison with conventional technologies.

- (1) Improved seizure resistance (in comparison with the full-complement type)
- (2) Reduced torque loss (in comparison with the full-complement type)
- (3) Improved cage strength and cage durability (in comparison with the previous cage)



Photo 2 Flow of development of miniature needle roller bearings for planetary gears

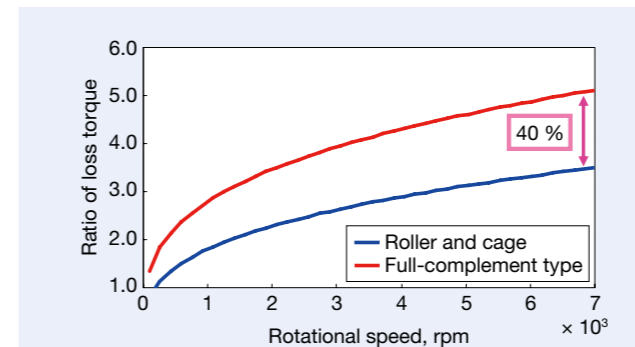


Fig. 1 Comparison of loss torque between roller and cage assembly and full-complement-type assembly

(4) Improved rolling durability life (in comparison to the bearing with the previous cage)

Full-complement-type bearings are not suitable for high-speed rotation over 10 000 rpm and require a lubrication oil supply exceeding 0.3 L/min because they have no cage and their rollers make direct contact with each other with a sliding motion resulting in heat generation. In addition, their torque loss is larger than other types of bearings due to roller sliding contact.

The newly developed high-speed-type miniature roller and cage assembly is improved in terms of seizure resistance even under severe lubrication conditions, enables high-speed rotation exceeding 20 000 rpm, and reduces torque loss by approximately 40 % (Figure 1) because roller sliding contacts are eliminated by adopting a roller and cage assembly.

Table 1 provides a comparison of specifications between the newly developed M cage and the previous cage for roller and cage assemblies. As rotational speeds of the planetary gear carrier (pinion revolution) increase, high stress acts on the fillet portion of the cage pocket corner due to centrifugal forces and occasionally leads to fatigue failure of the cage. Cage strength and durability of the newly developed bearing has been improved, and cage durability tests confirmed an increased rotational limitation speed (pinion revolution) exceeding 1.5 times that of the previous bearing (Figure 2). In addition, rolling durability life is improved by approximately 14 % (Figure 3) by lengthening the rollers an additional 0.5 mm while maintaining the same outer dimensions of the

Table 1 Specifications of newly developed M cage and previous cage

Part	Item	Previous cage	Newly developed M cage	Target
Cage	Shape	Wave shape	M shape	Forming M shape (flanged type at both ends) → Improving cage rigidity
	Material	Low carbon steel (carbonitriding)	Chromium molybdenum steel (carbonitriding)	Adoption of high-strength case-hardening steel → Improving cage strength
Roller	Roller size	Roller diameter: ϕ 1.5 mm	Roller diameter: ϕ 1.5 mm	Optimum simultaneous pursuit of M shape and thinner plate for cage → reducing bearing weight Increased roller length by extending space in the axial direction → Improving rolling durability life
		Roller length: 11.3 mm	Roller length: 11.8 mm	

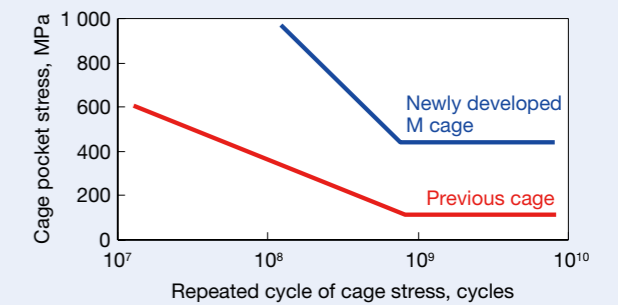


Fig. 2 Comparison of stress between previous cage and newly developed M cage

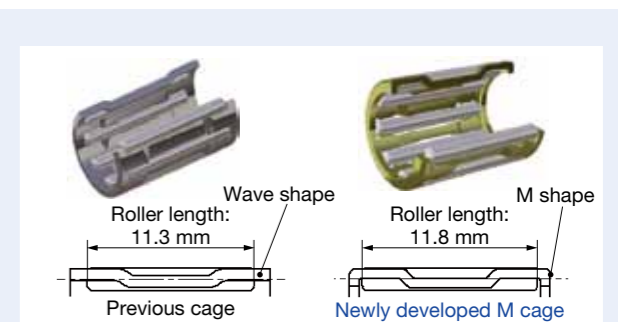


Fig. 3 Cross-sectional view of previous cage and newly developed M cage

bearing since it became possible to lengthen the cage pockets by improving the cage-flange rigidity.

In addition, cage weight is successfully reduced by approximately 20 % using a thinner plate for the cage, which results in an approximate 5 % reduction in weight for the whole bearing.

3. Summary

The newly developed high-speed-type miniature roller and cage assembly for planetary gears is effective for compact and lightweight planetary gears for use in various types of transmissions. We anticipate that this new product will further contribute to improving fuel economy in automobiles and reducing CO₂ emissions.

Long-Life Thrust Needle Roller Bearings Using Alternative Material to SK85

In recent years, the number of automatic transmissions (ATs) with high transmission-efficiency of engine power and with multi-speed gears has been increasing in order to improve fuel economy and to reduce shift shock. In addition, the transmission bearings for hybrid vehicles are required to be compact and lightweight to further improve fuel economy. In many cases, the transmission oil with low viscosity is used in the ATs with multi-speed gears for improving transmission efficiency. In these ATs, thrust needle roller bearings are used in excess of seven locations where they are subjected to severe lubrication conditions. In some cases, the oil pump is not operating during EV mode where the vehicle is being run only by a motor, and then, under these conditions, there are cases where the thrust needle roller bearings for transmissions are subjected to severe scarce-lubricant conditions.

Therefore, NSK developed and commercialized a thrust needle roller bearing that offers long service life performance even under such severe conditions (Photo 1).



Photo 1 Long-life thrust needle roller bearing with lipped washer

1. Specifications

1.1 PCR5 material (NSK proprietary steel)

NSK has adopted a proprietary PCR5 steel material that offers improved toughness in comparison to our current JIS SK85 steel, which was achieved by reducing the amount of carbon and silicon, and by increasing the amount of chromium in the new steel. Adopting PCR5 steel offers improved press workability of the products, and enables the possibility to produce a new bearing with a washer thickness of 2.5 mm.

1.2 Carbonitriding

NSK's proprietary PCR5 steel is treated with special carbonitriding resulting in a material that simultaneously offers enhanced toughness, surface hardness, and fatigue strength. This material has been adopted for this thrust bearing washer.

2. Features

- (1) The quality of carbonitriding heat-treated PCR5 steel achieves sufficient stability on a par with bearing steel (AISI 52100, JIS SUJ2) even though the same process applied to SK85 steel has less stability (Figure 1).
- (2) PCR5 steel is available for the lipped washer of thrust bearings since PCR5 steel features press workability, whereas bearing steel is more difficult to press.
- (3) The product using PCR5 steel achieved over 3 times longer service life under severe lubrication conditions compared with the current product using SK85 steel, which was normally quenched and tempered (Figure 2).

3. Summary

Responding to the demand for improved fuel economy of automobiles, oil viscosity will continue to be lower than ever to improve AT efficiency, in addition to improved AT efficiency as a result of further advances made in the compact and lightweight designs of transmissions. Under these conditions, the operating environment of bearings will become increasingly severe. We anticipate that longer service life of bearings under such severe conditions will be further needed, which is especially true at a rapid pace for bearings used in hybrid vehicles. This newly developed bearing is expected to meet such demand.

NSK will continue to promote the development of products that can meet the future needs of the market.

	SK85 steel (current material)	PCR5 steel
Quenching and tempering		
Carbonitriding		

Fig. 1 Quality of SK85 steel and PCR5 steel of heat treatment

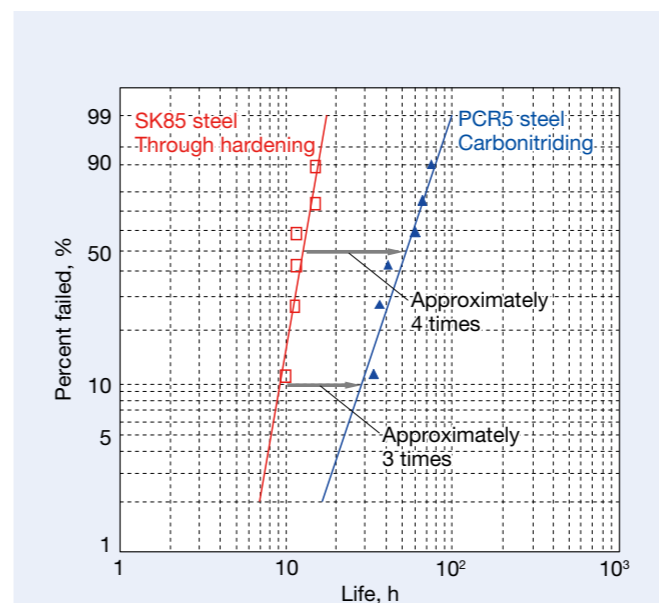


Fig. 2 Results of bearing life test comparing the materials of SK85 steel and PCR5 steel

High-Strength, Pressed-Steel Pulley

Idler pulleys used in the front end accessory drive system (FEAD system) are sometimes used under high-tension conditions. Machined-steel pulleys are used when the pressed-steel pulleys are insufficient in terms of strength performance, but using machined-steel pulleys sometimes presents the challenges of weight and cost. NSK has commercialized a new high-strength, pressed-steel pulley (Photo 1) that offers improved load capability in order to solve this problem.



Photo 1 High-strength, pressed-steel pulley

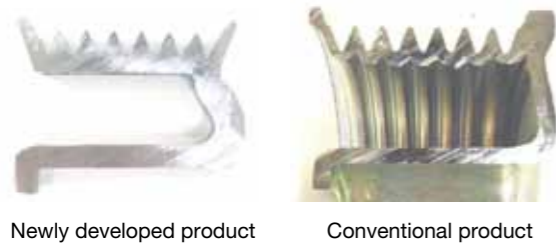


Photo 2 Comparison of newly developed product with conventional product

1. Construction and Specifications

Improving the manufacturing technology used in the press process in addition to designing an optimum configuration enabled NSK to process a high-strength, pressed-steel pulley. This achievement offers improved load capability of the pressed-steel pulley.

2. Features

The high-strength, pressed-steel pulley is pressed into shape from a thick base material without reducing thickness at bent positions where high stress is applied, as shown in Photo 2. As a result, any stress acting on the high-strength, pressed-steel pulley when a belt load is applied can be mitigated, as shown in Figure 1, and it becomes possible to use the high-strength, pressed-steel pulley under a range of high-load conditions where conventional pressed-steel pulleys cannot be used.

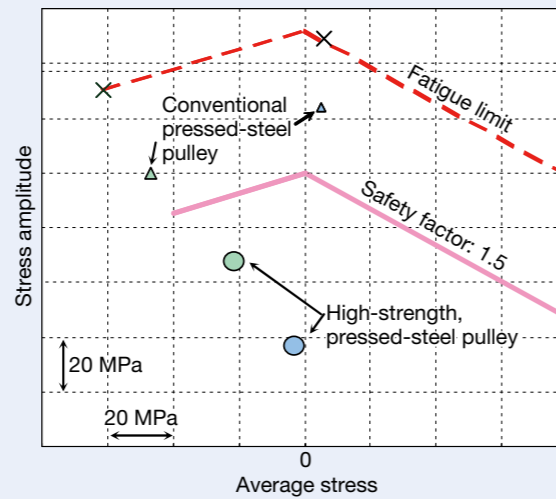


Fig. 1 Reduced stress acting on the high-strength, pressed-steel pulley

3. Applications

This product contributes to noticeable weight reductions for pulley units used for idler pulleys or belt-tensioner pulleys in the FEAD system mounted to automotive engines. The applicable range of the pressed-steel pulley has been extended, as shown in Figure 2, and the high-strength, pressed-steel pulley can also be used in a wide range of applications where a machined-steel pulley is conventionally applied in order to ensure sufficient high-load capability.

4. Summary

The high-strength, pressed-steel pulley can be used as a replacement for machined-steel pulleys that are used under high-load conditions. The high-strength, pressed-steel pulley contributes to weight savings and cost reductions as it is possible to use under a range of high-load conditions where conventional machined-steel pulleys are used.

NSK will continue to take on the challenge of developing a thicker pressed-steel pulley in the future.

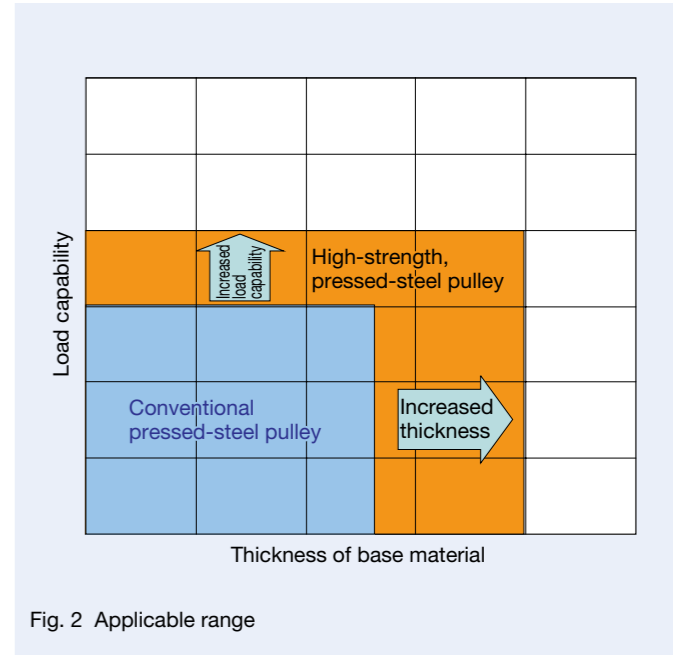


Fig. 2 Applicable range

Newly Developed, Highly Durable Clutch Pulley Unit

NSK has been mass-producing clutch pulley units for alternators since 2001 in order to prevent belt slip noise, which occurs because of fluctuations in engine speed. In recent years, the fluctuation of engine rotational speeds has been increasing with the introduction of technologies for improving fuel economy. Accordingly, the alternator has become larger to meet the requirements for increased amounts of electric power generation. Against the backdrop of these trends, clutch pulley units have been required to further improve durability performance. NSK has conducted various technical investigations and improved the performance of clutch pulley units in order to respond to these needs, and has developed a new clutch pulley unit (Photo 1).



Photo 1 Cutaway view of the newly developed, highly durable clutch pulley unit

1. Construction and Operation

The basic elements of this newly developed clutch pulley unit are its roller-type one-way clutch and ball bearings that are mounted at both ends of the one-way clutch to support loads acting on this unit (Figure 1). This clutch pulley unit is lubricated by grease. Though rotational engine speeds fluctuate minutely (Figure 2), fluctuations in the rotational speed of the alternator shaft and the attendant fluctuations in belt tension are reduced by unlocking alternator inertia during rotational speed deceleration against the fluctuation transmitted to the pulley using an integrated one-way clutch. As a result, belt slip noise is significantly prevented.

2. Design

We acquired a clearer understanding of the states and behaviors of the roller clutch during operation using the following methods, and applied this knowledge to optimizing the roller clutch specifications, which resulted in achieving significantly improved performance.

- (1) Understanding the behavior of an actual engine using a test engine (Photo 2).
- (2) Understanding the behavior of internal parts of the roller clutch using analysis based on waveforms of engine behavior by means of originally developed numerical analysis software (Figure 3).
- (3) Understanding the actual condition of each part used in the roller clutch during operation by analyzing stress and deformation caused by loads being applied to the clutch (Figure 4).

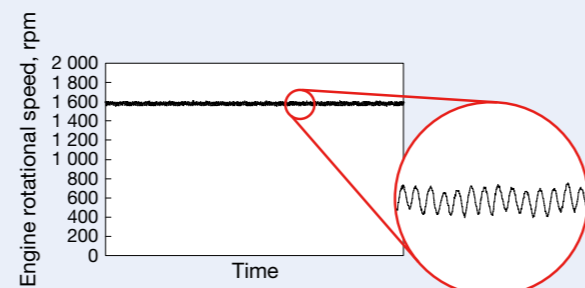


Fig. 2 Fluctuation of engine rotational speed with magnified view



Photo 2 Measuring engine behavior with a clutch pulley mounted to an actual engine

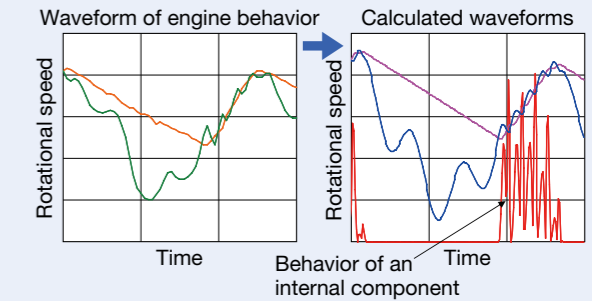


Fig. 3 Numerical analysis based on waveforms of engine behavior

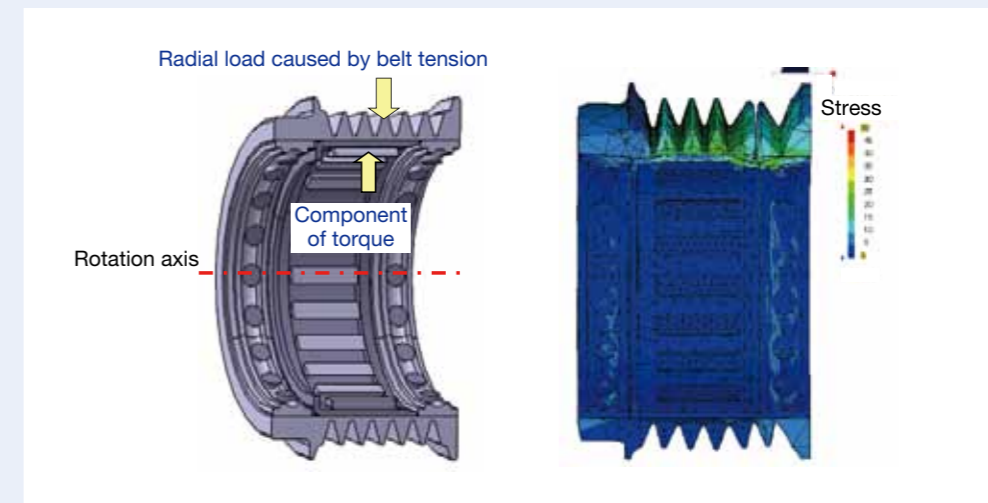


Fig. 4 Analysis of part deformation caused by external and internal forces

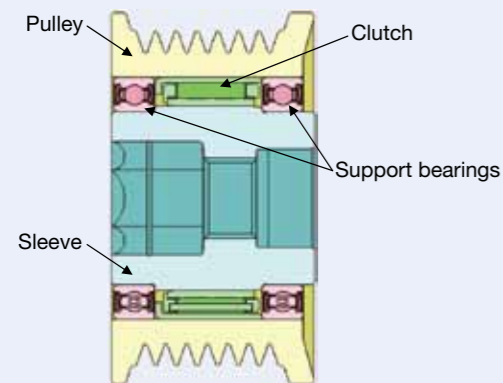


Fig. 1 Cross-sectional view of clutch pulley unit

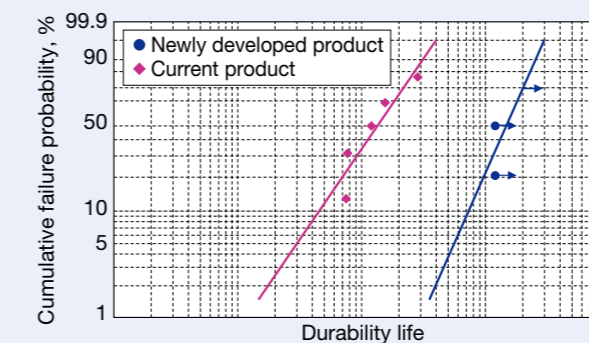


Fig. 5 Comparison of accelerated durability test results for current and newly developed clutch pulley units

3. Features

Service life of the newly developed, highly durable, clutch pulley unit, which was designed using the above-mentioned advances, is confirmed to have been significantly improved in terms of durability compared with current products, based on accelerated durability testing using a motor (Figure 5).

4. Applications

The newly developed, highly durable, clutch pulley unit is mainly used as an alternator pulley for engines of passenger cars.

Electric Power Steering System for Excellent On-Center Steering Feel

A vehicle mostly travels under conditions of straight-running on public roads during its lifetime. NSK's newly developed "Electric Power Steering System (EPS) for Excellent On-Center Steering Feel" is a newly developed product resulting from applying electronic control technology to the EPS that reduces steering effort. This newly developed EPS includes new functionality that detects the reaction forces due to the crowned road, tilting of the vehicle caused by uneven load, uneven wear of tires, etc., under straight-running conditions, and utilizes this information to automatically make adjustments using electronic control technology for improving on-center steering feel.

This new functionality will reduce the burden on the driver and help with long-distance driving.



Photo 1 Electric power steering system for excellent on-center steering feel

1. Features

(1) Reduce the burden on the driver and improved on-center steering feel

This EPS calculates the reaction force that is generated at the tires utilizing signals from sensors that have already been equipped for the original assisting functionality of this EPS. Using the calculated results, this newly developed EPS infers the vehicle's straight-running conditions and makes adjustments to the steering system to ensure straight-running driving. As a result, this EPS improves on-center steering feel in addition to reducing the burden on the driver by decreasing steering effort required to keep straight-running driving. This product further enhances the comfort and safety of driving on highways and other major roads where automobiles are mostly driven under straight-running conditions.

(2) Inhibition of large increase of cost

This new electric power steering system for excellent on-center steering feel was developed with a focus on the software for electronic control technology and utilizing current hardware components that are already used for the EPS. As a result, driving performance is improved with a simple architecture that is the same as that for conventional EPS systems. In addition, the cost is suppressed compared to conventional driving control systems with expensive sensors mounted on the vehicle.

2. Applications

This new product is available for use in a wide range of automobiles from compact cars to large passenger vehicles. It is especially suitable for automobiles driven in areas where there are many long straight roads, such as in North America.

3. Summary

NSK's newly developed electric power steering system for excellent on-center steering feel will reduce the burden on the driver and will contribute to improved comfort and safe driving.

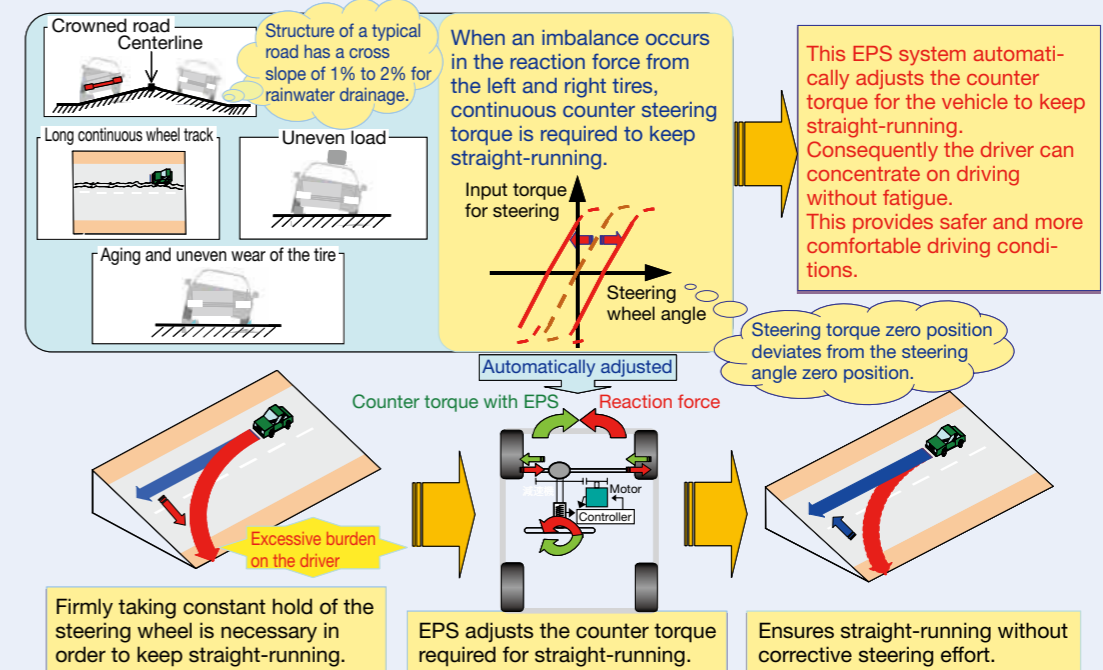


Fig. 1 Factors that interfere with straight-running of the vehicle

EPS system calculates the reaction force (SAT=self-aligning torque) of the tire that is generated during straight-running. It then detects degradation of straight-running performance of the vehicle using the calculated reaction force and compensates accordingly.

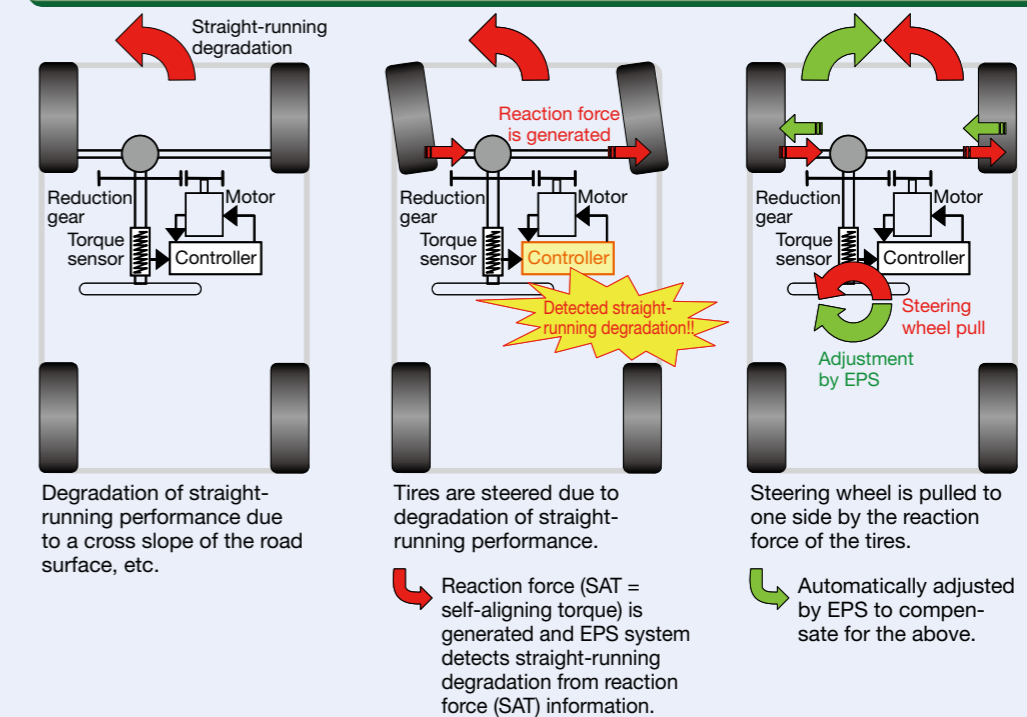


Fig. 2 Principle of detecting a situation in which straight-running feel (on-center steering feel) is degraded, and compensation control for the reaction force (SAT)

Ball Screw for Motorcycle Brake Systems

In recent years, large super-sport motorcycles have widely adopted devices that finely control braking by applying electrical control to both interlock brake systems for the front and rear wheels and antilock brake systems (ABS) in order to make difficult braking easier for skilled riders and enable average riders to perform such braking with ease of mind. These are brake-by-wire systems that control braking as follows; the electronic control unit (ECU) detects the rider applying the brakes, the ECU calculates optimum braking force, and the rotation of motors located in each brake unit of each front and rear wheel generates hydraulic pressure.

A newly developed ball screw for motorcycle brake systems is used for the power unit of this brake-by-wire system to generate hydraulic pressure by changing motor rotation to linear motion and pushing a piston with a ball screw shaft (Figure 1).

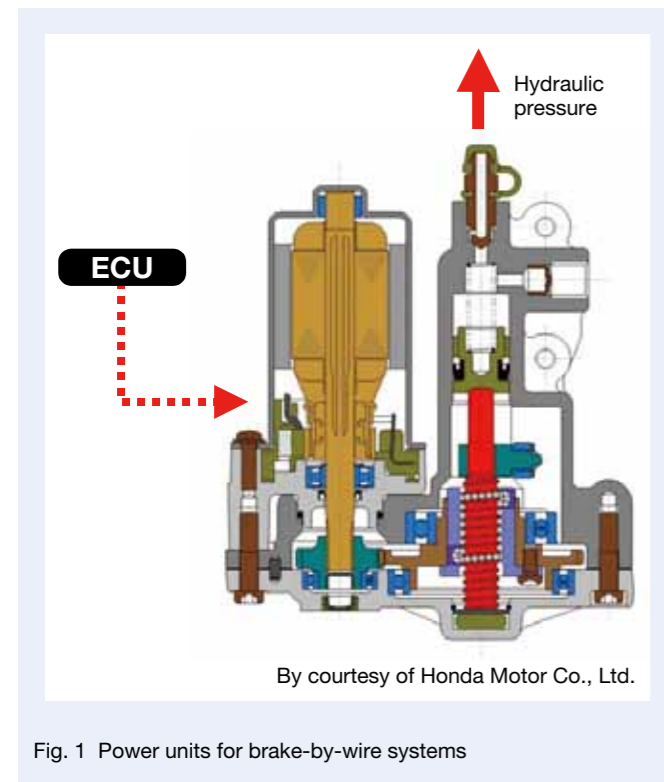


Fig. 1 Power units for brake-by-wire systems

1. Construction and Specifications

The newly developed ball screw adopts a deflector-type ball screw (screw shaft diameter: $\phi 10$ mm, lead: 2.5 mm) that makes it possible to reduce the size. Moreover, the part used for securing the deflector has been removed, and we developed a new structure in which the screw shaft pushes the piston directly, which reduces the product weight (Photo 1).



Photo 1 Ball screw for motorcycle brake systems

2. Features

(1) Design of ball screw without a ball at the outside of the ball passage circuit

We developed a new structure of ball screw in order to prevent operating failure of the braking system caused by a locked-up ball screw due to a ball entering into the grooves that are outside of the ball passage circuit. In the new structure, the nut grooves that are outside of the ball passage circuit are processed to be shallow grooves (Figure 2 and Figure 3).

(2) Adopting a metal deflector

Highly reliable metal is used as the deflector material in place of conventional plastic. Numerous simulations and durability tests verified the high reliability of the metal deflector for practical use (Photo 2).

(3) Reducing diameter

Swaging to secure the deflector is adopted as the new securing method (Photo 3). As a result, a weight reduction of 11 % and an inertia reduction of 15 % have been achieved compared with the conventional securing method.

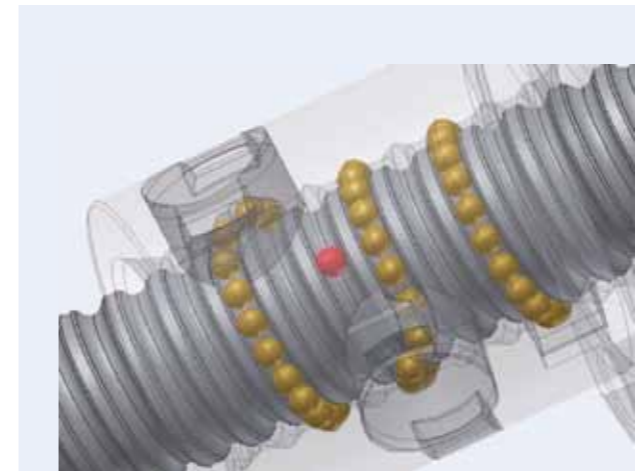


Fig. 2 A ball (red ball) at the outside of the ball passage circuit of a ball screw



Photo 2 Metal deflector

(4) Integrating a shaft and push rod

We have adopted a new structure in which the screw shaft directly pushes the piston, and as a result, the push rod that conventionally pushed the piston is removed.

Through these improvements, the newly developed ball screw achieves reductions in size and weight that are required of brake systems for super-sport motorcycle models, and achieves a weight reduction of approximately 70 % compared with ball screws, such as those used for CVTs of motorcycles.

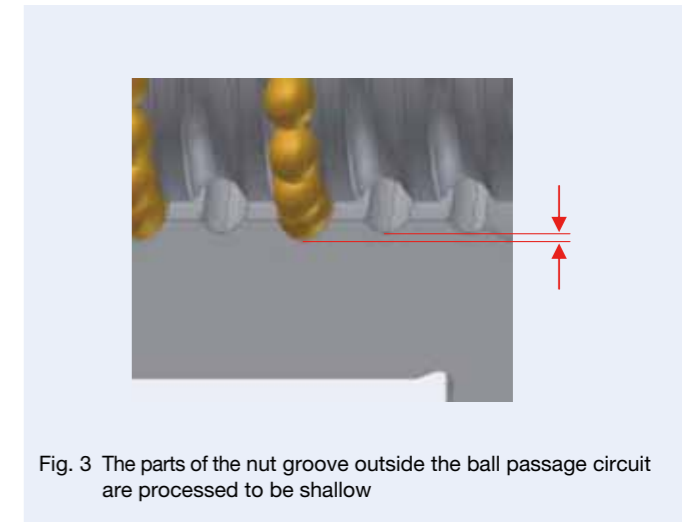


Fig. 3 The parts of the nut groove outside the ball passage circuit are processed to be shallow

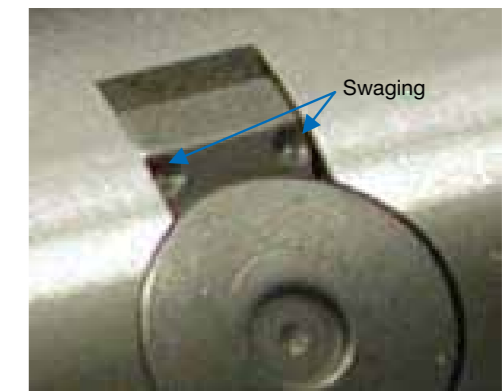


Photo 3 Swaging method for securing the deflector

3. Summary

The electrification of operation and reductions in size and weight will continue to advance in order to improve the safety, comfort, and environmental friendliness of motorcycles and automobiles. We will continue to promote the development of ball screws for brakes in the future, responding to both the need for reducing size and weight and for the electrification of operation.

Mechanism of Dent Initiated Flaking and Bearing Life Enhancement Technology under Contaminated Lubrication Condition

Part I: Effect of Tangential Force on Dent Initiated Flaking

T. Ueda and N. Mitamura
Corporate Research & Development Center

ABSTRACT

In this paper, we have clarified experimentally the mechanism of dent initiated flaking as observed in rolling element bearings operating under contaminated lubrication conditions. A characteristic of dent initiated flaking is the initiation of cracks on the trailing edge of dents relative to the rolling direction. Based on the results of twin-disk testing and ball-on-rod rolling contact fatigue (RCF) testing conducted, we have confirmed that the crack initiation at the edge of a dent is strongly influenced by the tangential force. The tangential force leads to the generation of a large tensile stress at the trailing edge of dents, which in turn leads to crack initiation.

Reprinted from Tribology International, 41, T. Ueda, N. Mitamura, Mechanism of dent initiated flaking and bearing life enhancement technology under contaminated lubrication condition Part I: Effect of tangential force on dent initiated flaking, 965-974, Copyright (2008), with permission from Elsevier.

1. Introduction

The flaking of rolling element bearings due to rolling contact fatigue (RCF) is generally classified into either subsurface or surface originated flaking, depending on the origin of the flaking. Typically, subsurface originated flaking occurs under ideal lubricating conditions, whilst surface originated flaking occurs under poor lubrication condition, i.e. insufficient oil film thickness or contaminated lubrication [1-4]. In the case of subsurface originated flaking, the crack normally originates from a non-metallic inclusion in the material. Therefore, improving the cleanliness of the material is an effective countermeasure to subsurface originated flaking.

In recent years, the cleanliness of bearing steel has improved significantly due to advancements in steel making technology. As a result, the occurrence of subsurface originated flaking due to non-metallic inclusions has decreased. Today, it is normal for a bearing operating under good lubrication conditions to achieve an actual life of more than 10 times the life calculated using Lundberg-Palmgren's theory [5, 6]. Conversely, in the case of surface originated flaking initiated at a dent in the raceway surface caused by contamination of the lubricant with debris, the life of the bearing is significantly reduced. In some cases, the life of the bearing is actually less than the life calculated using Lundberg-Palmgren's theory. This presents a major problem when trying to determine the life of bearings used in applications where the lubrication is prone to contamination resulting in denting of the raceways. To try and address this problem, a significant amount of research has been conducted in to surface flaking resulting from dents in the bearing raceway. The

research has included a study of the mechanism of dent initiated flaking [7-9], influence of debris and dents on RCF life [10-15] and also how to produce dents [16-18].

One characteristic of dent initiated flaking studied by many researchers [19-25] is the initial crack that leads to flaking, which overwhelmingly occurs on the trailing edge of the dent with respect to the rolling direction. In order to clarify the mechanism of this flaking, it is important to clarify the reason why such flaking tends to occur on the trailing edge.

Lubrecht et al. [19] calculated that the contact pressure was higher at the trailing edge of dents due to the "squeeze effect." Wedeven [20] dynamically measured the oil film thickness around the dents and discovered that the local film thickness at the trailing edge was greater than the leading edge. As a result, the local EHD pressure at the trailing edge was higher and the stress concentration effect correspondingly larger.

Lubrecht et al. [19] pointed out that there was a relationship between the direction of load movement (rolling direction) and the position of the dent edge where flaking occurs. Nèlias and Ville [21], Ai and Cheng [22, 23] and Xu [24] have offered a relationship between the direction of sliding and the position of a dent where flaking occurs. Nèlias and Ville [21], Ai and Cheng [22, 23] and Xu [24] conducted an EHL analysis that took sliding in to consideration and determined that there was a relationship between the direction of sliding and the position of a dent edge where excessive pressure is generated. They reported that the flaking was generated as a consequence of the stress concentration caused by the excessive pressure. Shimizu et al. [25] reported that the tangential force was

the cause of the crack initiation at the trailing edge of the dents with respect to the rolling direction. They used X-ray diffraction to verify that tensile stress remained behind the trailing edge of a dent and that compressive stress remained behind at the leading edge.

Although many studies on dent initiated flaking have been carried out over the years, including those mentioned above, researchers have yet to clarify the actual mechanism of dent initiated flaking and why flaking tends to occur at the trailing edge of dents. It is extremely important to clarify the mechanism of dent initiated flaking in order to establish a life theory for bearings operating under conditions of contaminated lubrication and also to help develop a long-life bearing. In this study, we clarify the mechanism of dent initiated flaking by determining the cause of flaking that tends to occur at the trailing edge of a dent with respect to the rolling direction and identify the factors that lead to dent initiated flaking.

2. Test Method

Reports discussing the phenomenon of flaking that tends to occur on only one side of a dent take in to consideration either (a) rolling direction (direction of load movement), or (b) direction of tangential force (direction of sliding). In order to determine whether the rolling direction or direction of tangential force was involved, we conducted RCF testing using a twin-disk test machine with dents introduced in to the disk surface. In the twin-disk test, the rolling direction and direction of tangential force are clearly defined; however, the relationship between the rolling direction and the direction of tangential force is different for the two contacting disks. In addition, RCF testing was carried out using a ball-on-rod tester. The ball-on-rod RCF tester more closely simulates a bearing structurally, and because sliding that is generated at the contact surface between the ball and rod is only differential slip, it becomes easier to understand the direction of sliding in the contact area.

2.1 Twin-disk test

Fig. 1 shows a schematic of the twin-disk machine. The driving disk (with higher peripheral speed) was directly connected to a motor. The driven disk (lower peripheral speed) rotated at a reduced speed to create sliding using gears. Two types of disk were used as test pieces for the testing carried out (Fig. 2). Both types were made in bearing steel (JIS SUJ2), which had been heat treated (through-hardened and tempered) to produce a surface hardness of 60 to 64 HRC.

Following heat treatment, one type of disk was ground to produce a crowned radius on the outer circumference and a surface roughness (R_a) of 0.09 μm (Fig. 2 (a)). The other type was ground to produce a straight profile and a surface roughness (R_a) of 0.05 μm (Fig. 2 (b)). After grinding, eight evenly spaced dents were introduced axially in to the center of the outer circumference of the

disks with a straight profile and surface roughness (R_a) of 0.05 μm (Fig. 2 (b)). The dents were formed with a diameter of 150 μm and a depth of approximately 10 μm using a Rockwell C indenter.

Table 1 lists the three different sets of test conditions used for the twin-disk tests conducted. Each test was carried out using one disk test piece of each type (Fig. 2). All of the tests were conducted using the same maximum contact pressure of $P_{\text{max}} = 3.2 \text{ GPa}$ and ISO-VG68 drip-feed lubrication conditions. The first set of test conditions involved using the disk test pieces with no indents (Fig. 2 (a)) as the driving disk and the disk test piece with indents (Fig. 2 (b)) as the driven disk. The speed of the driving disc was maintained at a constant speed (500 rpm), whilst the speed of the driven disk was adjusted to give a slip ratio of 5%. The second set of test conditions used were the same as the first, but the configuration of the disk test pieces was reversed, i.e. the one with no indents was used as the driven disk and the one without indents as the driving disk. The third set of test conditions was the same as the first, but the speed of the driven disk equaled the speed of the driving disk, i.e. zero slip.

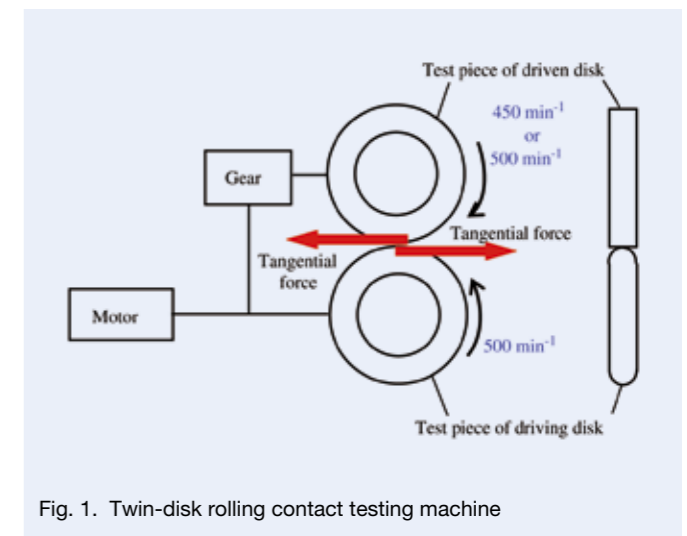


Fig. 1. Twin-disk rolling contact testing machine

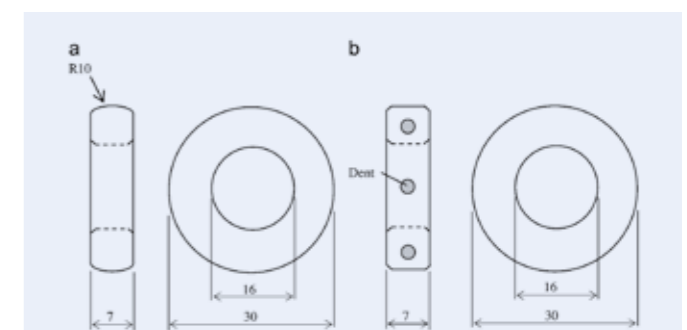


Fig. 2. Driving and driven disks of the twin-disk test machine (mm): (a) Test piece (outside diameter contact surface with rounded shape and no dents). (b) Test piece with dents.

Table 1 Twin-disk test conditions

	Contact pressure P_{max} (GPa)	Rotating speed of driving member (rpm)	Slip ratio (%)	Lubrication oil	Test piece in driving member	Test piece in driven member
I	3.2	500	5	Drip-feed lubrication of VG68 oil	Fig. 2 (a)	Fig. 2 (b)
II					Fig. 2 (b)	Fig. 2 (a)
III					[Fig. 2 (a)]	[Fig. 2 (b)]

2.2 Ball-on-rod rolling contact fatigue (RCF) test

Fig. 3 shows a schematic of the ball-on-rod RCF tester. The ball-on-rod RCF test is a rolling element test that is similar in structure to the actual bearings. It is composed of two outer rings with a tapered bore, a 12.6 mm diameter rod that acts like the inner ring of a bearing, and three 27/32 in diameter balls. The rod was made in bearing steel (JIS SUJ2), which had been heat treated (through-hardened and tempered) to produce a surface hardness of 60 to 64 HRC. Following heat treatment, the surface of the rod was ground circumferentially to produce the required surface finish (R_a) of less than 0.10 μm .

The test conditions consisted of a maximum contact pressure between the rod and balls of $P_{max} = 4.8$ GPa, a rod rotating speed of 8 000 rpm, and ISO-VG68 oil bath lubrication. Testing was conducted for one hour on each test piece to produce a faint running band. The test was then stopped and eight equally spaced dents were then made in the surface of each test piece (rod). Half of the test pieces had the dents made at the center of the running band and the other half had dents made at the edge of the running band.

The dents were made in the surface of the test pieces using a Rockwell C indenter varied in size. The dents made in the test pieces at the center of the running band had a diameter of 150 μm and a depth of approximately 10 μm . The dents made in the test pieces at the edge of the running band had a diameter of 300 μm and a depth of approximately 35 μm . The dents along the edge of the

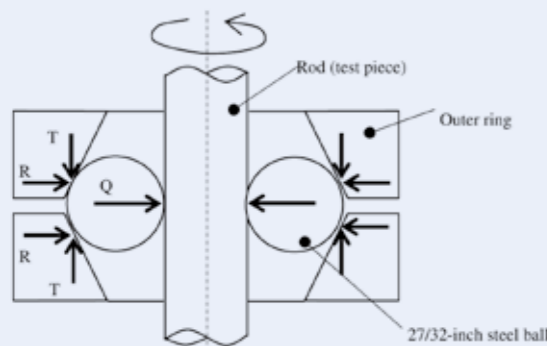


Fig. 3. Ball-on-rod rolling contact fatigue tester.

running band were made larger because flaking will not originate from the smaller dents due to the low contact pressure in this area. In the case of small dents at the edge of the running band, the tendency is for the test piece to fail by flaking due to subsurface originate fatigue at the center of the running band, where the contact pressure is high.

3. Test Results

3.1 Twin-disk test

Fig. 4 shows the condition of the edge of a dent after 50 hours of testing. In Fig. 4, all of the photographs are displayed in the same orientation, i.e. the rolling direction (direction of load movement) is in the same direction. Fig. 4 (a) shows the results for a driven disk test piece with dents (test condition I in Table 1) and Fig. 4 (b) shows the results for a driving disk test piece with dents (test condition II in Table 1). The driven disk in Fig. 4 (a) was subjected to a tangential force in the same direction as the rolling direction, whilst the driving disk in Fig. 4 (b) was subjected to a tangential force in the opposite direction to the rolling direction. When Fig. 4 (a) and 4 (b) are compared with each other, Fig. 4 (a) reveals that cracking had initiated from the trailing edge of the dent with respect to the rolling direction. Fig. 4 (b) reveals that cracking had initiated from the leading edge of the dent with respect to the rolling direction. In fact, cracking initiated from the trailing edge of all eight dents in the driven disk, similar to that shown in Fig. 4 (a). Conversely, cracks initiated at the leading edge of only two of the eight dents in the driving disk, similar to that shown in Fig. 4 (b). Additionally, Fig. 4 (c) shows that no cracks initiated at the edge of dents under conditions of zero tangential force (i.e. no slip), even after 50 hours of testing.

Twin-disk test results with artificial dents introduced in to the disk surface revealed: (1) tangential force (sliding) accelerates crack initiation at the edge of a dent, (2) the position of a crack initiated at the edge of a dent is affected by the direction of the tangential force (sliding direction), rather than the rolling direction (direction of load movement), and (3) cracks initiate more easily at the edge of a dent in the driven disk compared to the driving disk.

3.2 Ball-on-rod rolling contact fatigue (RCF) test

Fig. 5 shows the condition of adjacent dents after ball-on-rod RCF testing. Given the slip speed distribution

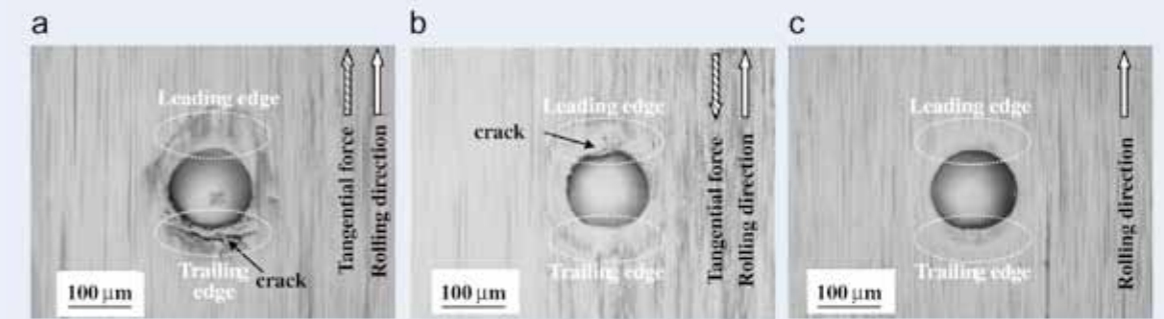


Fig. 4. Cracks initiated from edge of dent in twin-disk test: (a) Slip ratio of 5 % driven member. (b) Slip ratio of 5 % driven member. (c) Slip ratio of 0 %. Test conditions: $P_{max} = 3.2$ GPa; rotating speed of driving member $n = 500$ min^{-1} . Lubrication oil: ISO-VG68; drip-feed lubrication; test time: 50 h.

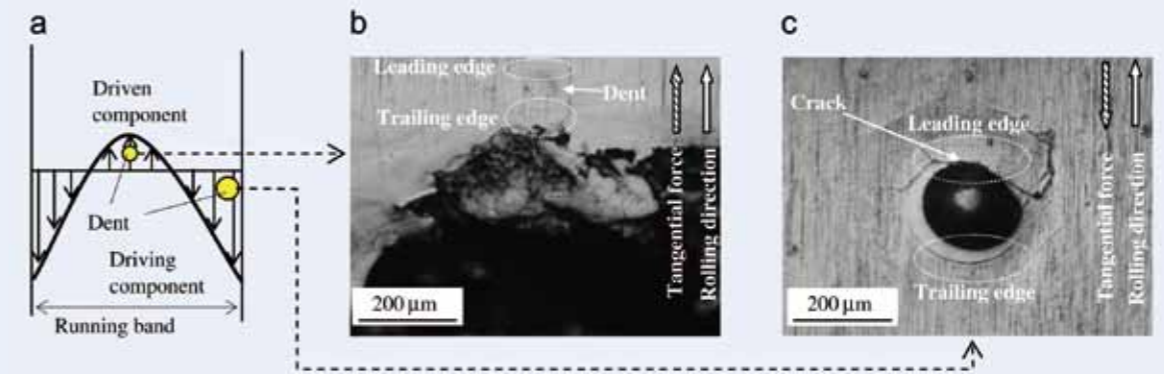


Fig. 5. Flaking and crack generated from edge of dent in ball-on-rod RCF test (a) Slip speed distribution. (b) Center of the running band, 22 h. (c) Edge of the running band, 50 h. Test conditions: $P_{max} = 4.8$ GPa; $n = 8\ 000$ min^{-1} ; lubrication oil: ISO-VG68; oil-bath lubrication.

shown in Fig. 5 (a), Fig. 5 (b) shows that dent initiated cracking and subsequent flaking occurred in the center of the running band, where the rod acts as the driven component and tangential force is generated in the rolling direction. Fig. 5 (c) shows a crack caused by a dent located on the edge of the running band, where the rod acts as the driving component and tangential force is in the opposite direction to the rolling direction. We observed that in Fig. 5 (b), the flaking occurred at the trailing edge of the dent with respect to the rolling direction. Fig. 5 (c) shows that the crack initiated at the leading edge of the dent with respect to the rolling direction. Fig. 5 (c) also illustrates that there were many cases where a crack initiated at the edge of a dent, where the rod acted as a driving component, but did not propagate and cause flaking.

From the results of the ball-on-rod RCF test, and also the twin-disk test, it appears that there is a correlation between the position of crack initiation at the edge of a dent and the direction of the tangential force. Furthermore, cracks initiated at the trailing edge of a

dent, when the tangential force is in the same direction as the rolling direction, propagate more easily than cracks initiated at the leading edge of dents when the tangential force is in the opposite direction to the rolling direction.

4. Discussion

4.1 Reason why tangential force involves dent initiated flaking

The results of the twin-disk testing and ball-on-rod RCF testing described in Section 3 clearly show that the tangential force plays a significant role in crack initiation at the edge of a dent. In the following sections, the reason why the direction of tangential force determines the position of crack initiation at the edge of a dent, as shown by the test results, will be discussed.

Fig. 6 shows a dent in the outer raceway of a thrust ball bearing before and after fatigue testing. The dent was

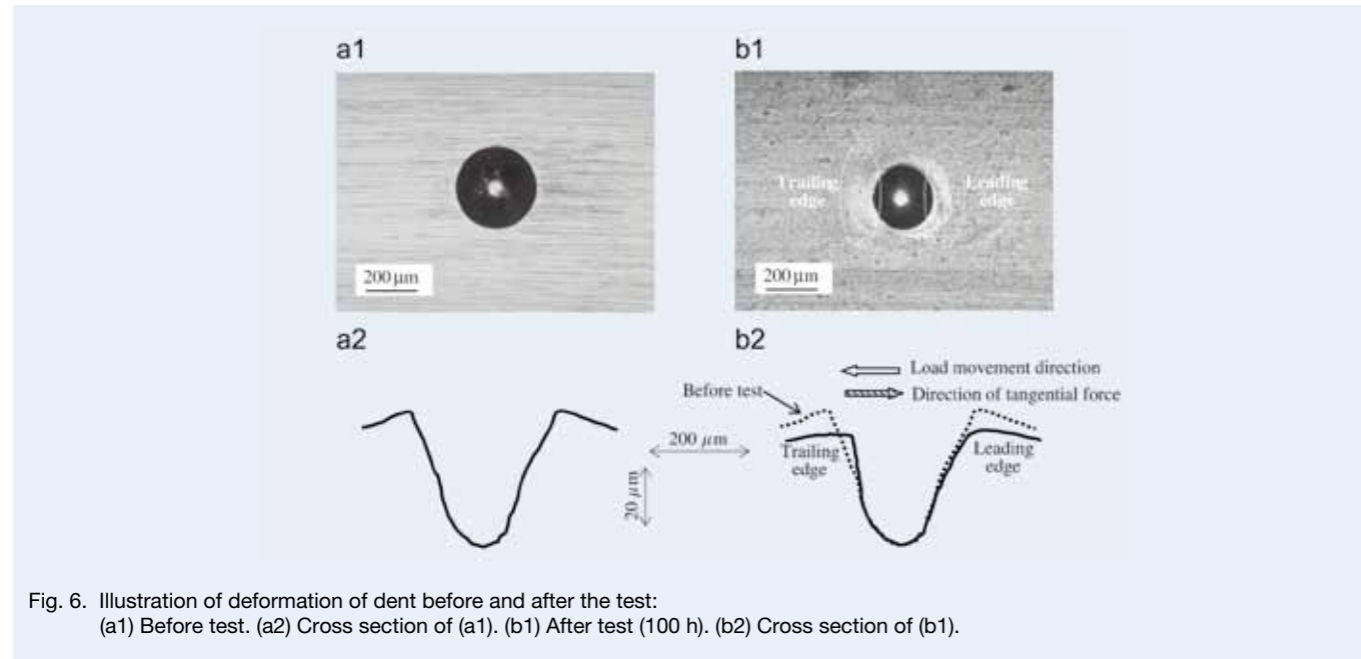


Fig. 6. Illustration of deformation of dent before and after the test: (a1) Before test. (a2) Cross section of (a1). (b1) After test (100 h). (b2) Cross section of (b1).

introduced in to the outer raceway of the bearing (bearing no. 51305) in the center of the running band prior to testing. The dent, with an approximate diameter of 280 μm and an approximate depth of 40 μm, was made using a Rockwell C indenter. During testing the thrust bearing outer raceway with the indents remains stationary. The fatigue test conditions used were; contact pressure, $P_{max} = 3.4 \text{ GPa}$, speed, $n = 1000 \text{ min}^{-1}$, number of cycles = 1.8×10^7 , and oil-bath lubricating using ISO-VG68 oil. Fig. 6 (a1) and (b1) show the appearance of dents before and after testing. Fig. 6 (a2) and (b2) shows the cross section of the dents before and after testing. The cross section of the dents was measured by optical interferometry.

In the cross sectional view of the dent shown in Fig. 6 (b2), the tangential force is generated from left to right as indicated. As shown in Fig. 6 (b2), the material at the left edge of a dent deforms and fills in the dent, whilst the material at the right edge of the dent deforms to broaden the dent. In other words, a large tensile stress is generated at the left edge of the dent and a large compressive stress generated at the right edge.

Fig. 7 illustrates the mechanism where flaking tends to occur on one edge of a dent and is based on the results shown in Fig. 6. Fig. 7 assumes a model where a dent exits on the raceway and a rolling element (ball) rolls over the dent. As the ball, and consequently the load, passes over the dent with a degree of slip, a large tangential force is generated at the edge of the dent due to the bulge of material in this area (Fig. 7 P2). The large tangential force generated then causes plastic flow of the material around the dent. Furthermore, if the tangential force is generated from left to right, a large tensile stress is generated at the left edge of the dent and a large compressive stress is generated at the right edge (Fig. 7 P2). In the event that a dent does not exist, the magnitude of the tensile

and compressive stress generated in the contact area due to the tangential force is the same at each contact point due to a constant tangential force. However, in the event that a dent exists, tensile stress generates at the entrance of the contact area (Fig. 7 P2) becomes larger than the compressive stress generates at the exit of the contact area at the left edge of the dent (Fig. 7 P3). This is because the tangential force becomes large at the edge of dent. However, at the right edge of the dent, compressive stress generated at the exit of the contact area (Fig. 7 P2) becomes larger than the tensile stress generates at the entrance of contact area (Fig. 7 P1).

The graphs shown in Fig. 7 illustrate the cyclic tension-compression stress pattern in the tangential direction that is generated at both edges of the dent at the load passes over. At the left edge of the dent the stress ratio of the cyclic stress, $R (= \sigma_{min} / \sigma_{max})$ is < -1 , and at the right edge of the dent $R > -1$. Even for the same stress amplitude, the fatigue life associated with a stress ratio, $R > -1$ is shorter than for a stress ratio, $R < -1$. Hence, a crack initiates at the left edge of the dent and easily propagates to cause flaking.

4.2 Reason why flaking tends to occur at the trailing edge of dents with respect to rolling direction

The model in Fig. 7, which was discussed in the earlier section, relates to dents that exist in the driven disk test piece and the direction of tangential force generated at the edge of a dent is the same as the rolling direction. In the case of Fig. 7, a large tensile stress is generated at the trailing edge of the dent with respect to the rolling direction and hence a crack initiates at the trailing edge of the dent. Conversely, Fig. 8 shows a dent that exists

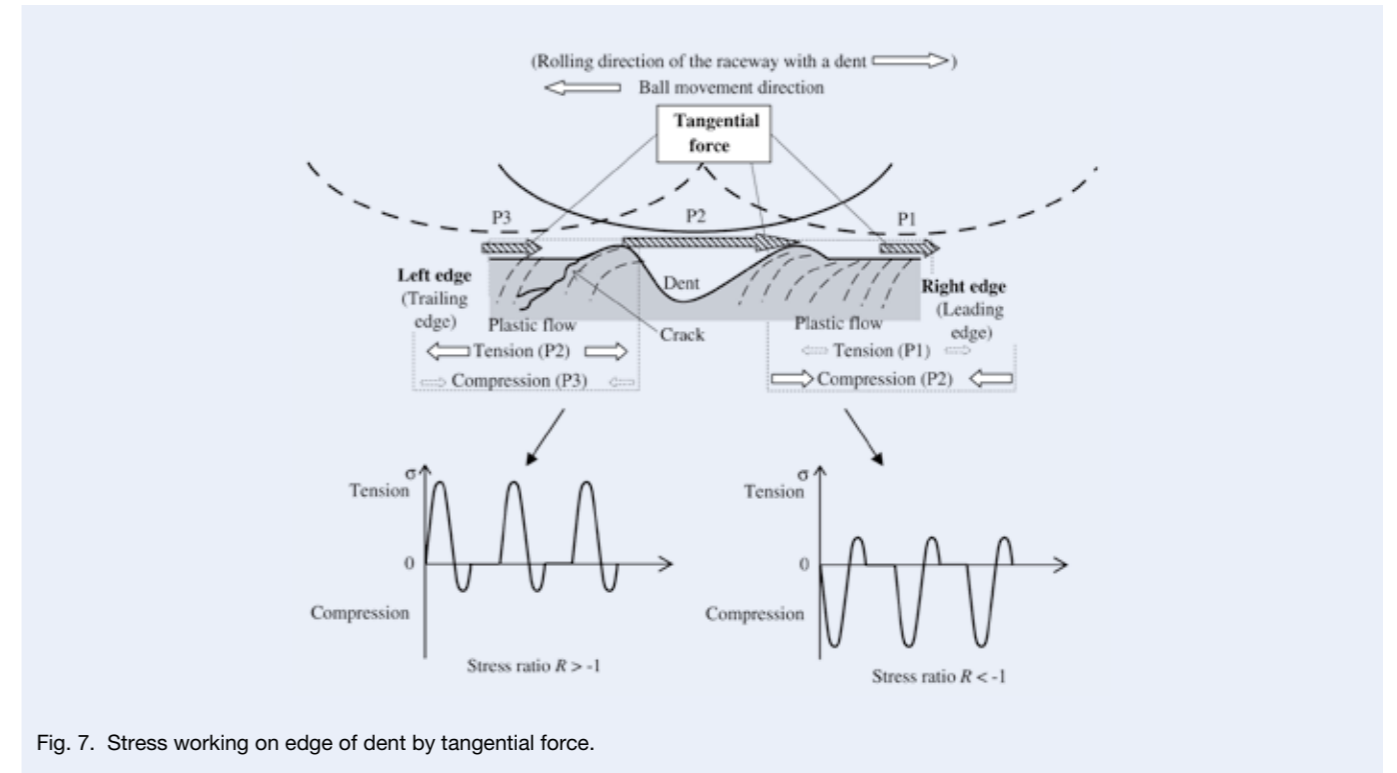


Fig. 7. Stress working on edge of dent by tangential force.

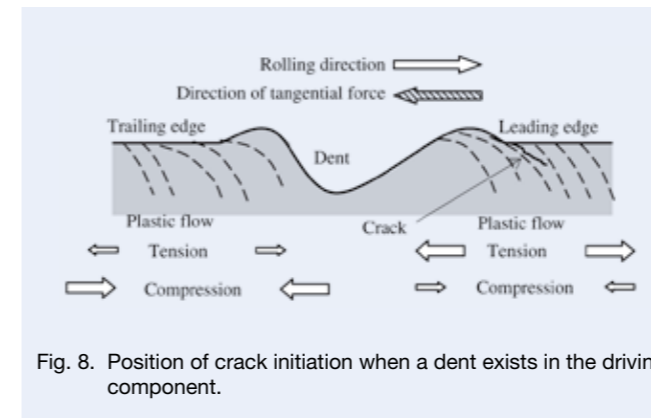


Fig. 8. Position of crack initiation when a dent exists in the driving component.

in the driving disk test piece. In the case of Fig. 8, the direction of tangential force generated at the edge of the dent is in the opposite direction to the direction of rolling. Additionally, a large tensile stress is generated at the leading edge of the dent with respect to the rolling direction, and hence a crack is initiated.

In the case of an actual rolling element bearing, flaking could occur at the leading or trailing edge of a dent with respect to the rolling direction. It depends on whether the dent is in a bearing component that is driving or being driven. However, as described previously, flaking occurs mainly at the trailing edge of the dent with respect to the rolling direction. The reason for this is that, based on the twin-disk testing and ball-on-rod RCF testing discussed earlier in Section 3, cracks initiate and propagate easily in the driven component, where the trailing edge of a dent

with respect to the rolling direction becomes the edge that has the largest tensile stress due to the influence of the tangential force.

This phenomenon, where flaking occurs more readily in the driven component compared to the driving component, is common for surface originated RCF [26-29], but not for dent initiated flaking. Flaking occurring more easily in the driven component is explained by the theory that a tensile stress is generated in the driven component as opposed to a compressive stress in the driving component just before the rolling element enters the contact area [26]. Using fracture mechanics, Murakami et al. [28, 29] proved that in the driven component, a crack grows by tensile mode due to the hydraulic effect of the oil, which has penetrated in to the crack, acting on the crack faces [30]. Since dent initiated flaking also occurs easily in the driven component for similar reasons, flaking occurs at the trailing edge of a dent with respect to the rolling direction.

4.3 Life test where direction of tangential force was changed

According to Nakajima et al. [31] and Lee et al. [32], pitting life can be extended by reversing the direction of tangential force if a dent does not exist in a contact surface. Nakajima et al. [31] have reported that reversing the tangential force extends the life because a crack will not easily grow if plastic flow intersects the direction of crack growth, and a crack grows more easily if the plastic flow exists along the crack. Lee et al. [32] have reported that under conditions where the tangential force is small, there is little change in life if the rolling direction

(the direction of tangential force) is reversed; but if the tangential force is large, life is enhanced by the repeat of normal and reverse rotation. Consequently, in order to verify the influence of tangential force on dent initiated flaking, we conducted a fatigue test where the direction of the tangential force acting in a bearing with artificial dents was reversed by changing the direction of rotation.

Life tests were conducted using a thrust ball bearings (bearing no. 51305), which each had eight artificial dents introduced in to the outer raceway, which remains stationary during testing. The dents, with an approximate diameter of 280 μm and an approximate depth of 40 μm , were made using a Rockwell C indenter. Fig. 9 shows a schematic of the fatigue test machine used. Three sets of test were conducted. Table 2 shows the preliminary test conditions before fatigue test. The first set involved rotating the test bearings in the normal direction for the full duration of the test. In the second and third, the test bearings were first rotated in the reverse direction (reverse rotation) for 10 hours and 20 hours, respectively. The test bearings were then rotated in the normal direction for the remaining duration of the test. All of the tests were conducted under the same conditions; 3 balls, maximum contact pressure, $P_{\text{max}} = 3.4 \text{ GPa}$, speed, $n = 1\,000 \text{ min}^{-1}$, and oil bath lubrication using ISO-VG68 oil.

Fig. 10 shows the Weibull distribution of the test results. The life (horizontal axis) did not include the 10 or 20 hours of reverse rotation. The results in Fig. 10 show that the bearing life is extended by the reverse rotation. Even though it is small, the longer the reverse rotation, the longer the bearing life is extended. Based on the results

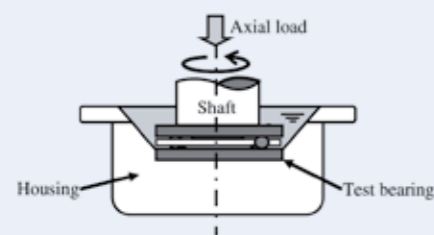


Fig. 9. Fatigue test machine for thrust ball bearings.

Table 2 Preliminary test conditions before fatigue test

	Preliminary test conditions	Symbol plotted in Fig. 10
Condition 1	Introduction of dent into the raceway	●
Condition 2	Operated for 10 hours in reverse rotation of fatigue test after introducing a dent	△
Condition 3	Operated for 20 hours in reverse rotation of fatigue test after introducing a dent	○

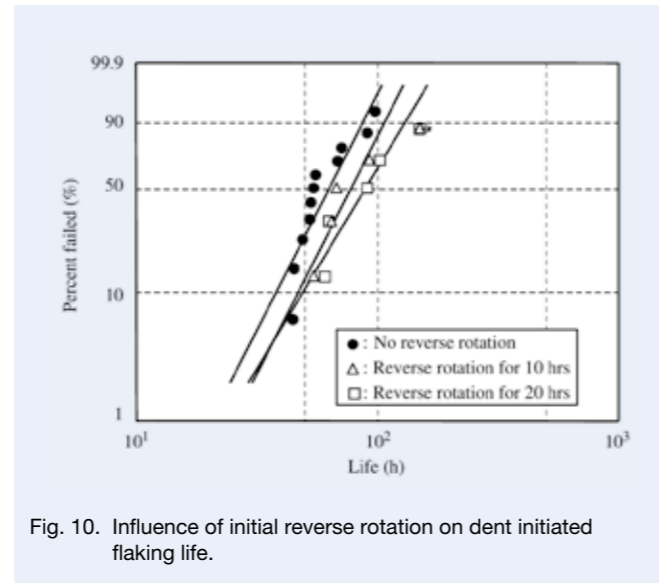


Fig. 10. Influence of initial reverse rotation on dent initiated flaking life.

shown in Fig. 10 and data reported by Nakjima et al. and Lee et al., we believe that during reverse rotation a tangential force is generated in the opposite direction to the tangential force generated during testing in the normal direction. This process creates plastic flow, which then intersects the direction of crack growth during the fatigue test, thus inhibiting the crack growth. We believe that during reverse rotation, a large compressive stress is generated at the edge of a dent (see right edge, Fig. 7) where a large tensile stress is generated and crack initiation takes place under normal rotation (see left edge, Fig. 7). This large compressive generated during reverse rotation persists during testing of the bearing rotating in the normal direction. [25].

Therefore, we are able to determine that the life enhancing effect, shown in Fig. 10, is influenced by the plastic flow intersecting the direction of crack growth, and residual compressive stress. In other words, the results of Fig. 10 indirectly suggest that the direction of tangential force (direction of plastic flow), which is changed by the direction of rotation, influences flaking life.

4.4 Influence of traction oil on dent initiated flaking

To further verify the influence of tangential force on dent initiated flaking, a fatigue test was conducted using traction oil, which has a high tangential force coefficient (traction coefficient), and a general industrial multi-purpose lubrication oil. In order to prevent differences in dent formation caused by the type of lubrication oil, the bearings with dents formed by the common condition listed in Table 3 were washed thoroughly and tested with each type of lubrication oil mentioned earlier. Fig. 11 shows the test machine used to form dents and conduct fatigue testing. This cantilevered-type test machine is such that radial load is applied directly to the test bearing. Fatigue

Table 3 Test conditions for developing a dent

Radial load (kN)		6.2
Rotating speed (rpm)		3 000
Test time (h)		1.0
Lubrication oil	Type	ISO-VG68
	Quantity (L)	1.2
Contaminant	Size (μm)	74 to 147
	Quantity (g)	0.05
	HV (kgf/mm^2)	520

testing was conducted with a deep groove ball bearing (bearing no. 6206) under radial loading of 6.2 kN at a rotating speed of 3 000 min^{-1} .

It is well known that in a clean lubrication environment, there is a relationship between RCF life and the lubricant film parameter ($\lambda = h_{\text{min}} / \sigma$, where h_{min} is the minimum lubricant film thickness, and σ the R_q roughness of the contacting surfaces) [33-35]. The major lubrication factor affecting lubricant film thickness is kinematic viscosity. Therefore, we used a traction oil and a multi-purpose lubrication oil of nearly the same kinematic viscosity (ISO-VG32 equivalent) in this test in order to eliminate the difference of life caused by the difference of oil film thickness.

Table 4 lists the traction oil and multi-purpose lubrication oil properties and lubricant film parameters that were used for life testing. The Dowson-Higginson equation [36] was used to calculate lubricant film parameters. The lubricant film parameters were almost equal for both the traction oil and the multi-purpose lubrication oil as shown in Table 4. Table 4 also shows the friction coefficients of each lubrication oil. Friction coefficients were measured using a ball-on-disk test with only a few drops of each lubrication oil, contact pressure of $P_{\text{max}} = 0.8 \text{ GPa}$, slip velocity of $V = 0.79 \text{ m/s}$, an ambient temperature of 20 $^{\circ}\text{C}$. The ball and disk were made in hardened and tempered JIS SUJ2, and had a surface roughness of 0.005 μm R_a (ball and disk). Under these conditions, the friction coefficient of traction oil was about 1.7 times that of the friction coefficient of the multi-purpose lubrication oil.

Fig. 12 shows the result of fatigue test. Fig. 12 shows that even if the values of lubricant film parameter are almost equal, life for dent initiated flaking becomes shorter under traction oil lubricated conditions. Although

Table 4 Property of multi-purpose lubrication oil and traction oil

Type of lubrication oil	Density @ 15 $^{\circ}\text{C}$ (g/cm^3)	Kinematic viscosity @ 40 $^{\circ}\text{C}$ (mm^2/s)	Pressure-viscosity coefficient (GPa^{-1})	λ of test conditions in Fig. 12	Friction coefficient (measured by ball on disk testing)
Multi-purpose lubrication oil	0.87	32.1	13.9	1.4	0.09
Traction oil	0.96	31.9	18.5	1.6	0.15

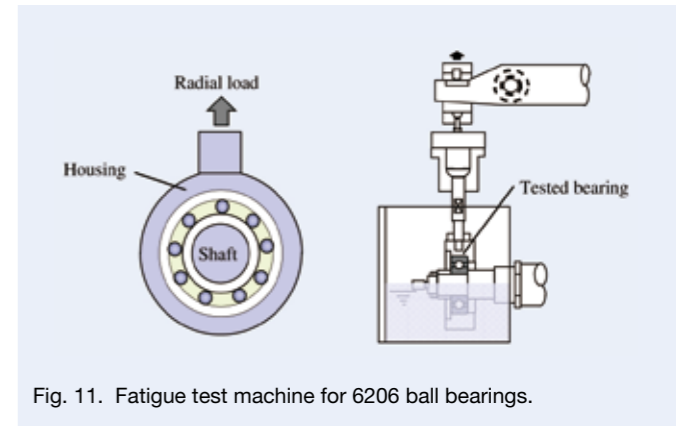


Fig. 11. Fatigue test machine for 6206 ball bearings.

it is necessary to investigate the influence of additives besides traction coefficient, based on the results shown in Fig. 12 under the condition of lubrication oil with a high traction coefficient, cracks at the edge of a dent initiate and propagate easily because tangential force generated at the edge of a dent increases. Therefore, tangential force plays a role in dent initiated flaking.

4.5 Mechanism of dent initiated flaking

In general, slip generated between the contact surfaces of a rolling element and the raceway of a bearing is small, and the influence of tangential force on RCF life is negligible. Therefore, the influence of tangential force in previous research on the RCF life of bearings was not considered in depth. In fact, the macroscopic value of the tangential force between the rolling element and the raceway was small. Therefore, if the stress was calculated in consideration of the macroscopic tangential force value, any clear difference from the stress value in the case of pure rolling was not obtained.

However, we think that the local tangential force generated between projections of roughness or generated in the bulge at the edge of a dent is large. As described above, there is a relation between the position where a crack initiates from the edge of a dent and the direction of tangential force. By reversing the direction of tangential force, dent initiated flaking life is extended. When high-traction coefficient lubrication oil is used, life under conditions of contaminated lubrication becomes short. We can thus determine that the influence of tangential force on dent initiated flaking life is large. Based on the above results, dent initiated flaking is generated by the following process:

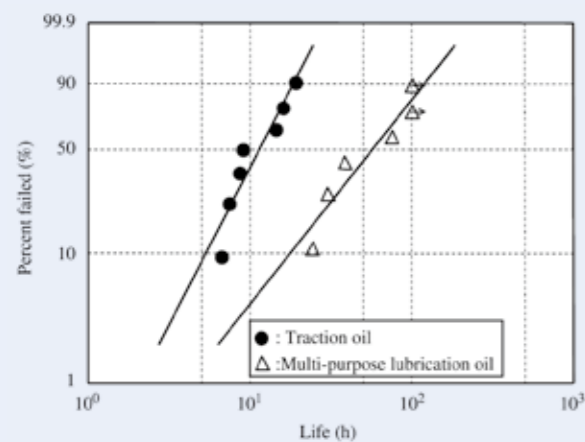


Fig. 12. Influence of traction oil on dent initiated flaking life.

- (1) Since a bulge exists on at the edge of a dent, a large tangential force is generated at the edge of a dent, and large plastic flow occurs at the edge of the dent.
- (2) Due to the influence of tangential force, fatigue cracks initiate from the edge of the dent where a large tensile stress is generated.
- (3) Fatigue cracks propagate by the shear stress and tensile stress due to a hydraulic effect of the oil as it penetrates in to the crack, and flaking occurs.

However, quantitative measurements and analyses to determining the magnitude of local tangential force working at the edge of a dent and also the stress distribution around the dent has still to be carried out. In the future, we will quantitatively evaluate the influence of contact pressure, slip rate, size of dents, and height of the bulge at the edge of a dent on the magnitude of tangential force generated at the edge of a dent, and the stress distribution around a dent. Hopefully, this will enable us to predict dent initiated flaking life and enhance life of rolling element bearings life.

5. Conclusion

Research was been conducted to try and clarify experimentally the mechanism of dent initiated flaking as observed in rolling element bearings operating under conditions of contaminated lubrication. The knowledge obtained from the research is summarized as below:

1. The results of a twin-disk test and ball-on-rod RCF test show the following: (1) Tangential force accelerates the crack initiation at the edge of a dent. (2) The position of crack initiation at the edge of a dent is determined by the direction of tangential force rather than the rolling direction. (3) Compared to the driving component, fatigue crack initiates and propagates much more easily at the edge of a dent in the driven component.
2. Based on measurements taken of changes in dent

configuration before and after fatigue test, we have verified that a large tensile stress due to the tangential force is generated on the trailing edge of a dent in the direction of the tangential force. Also, that a large compressive stress due to tangential force is generated on the leading edge of the dent. Since a fatigue crack easily initiates from the edge of the dent, where there is a large tensile stress caused by the influence of tangential force and flaking easily occurs, we determined that the direction of tangential force influences the position of crack initiation at the edge of a dent.

3. The reason why flaking occurs mainly at the trailing edge of the dent with respect to the rolling direction, is that cracks initiate and propagate easily in the driven component, where the trailing edge of a dent with respect to the rolling direction becomes the edge that has the largest tensile stress due to the influence of the tangential force.
4. Dent initiated flaking life is extended by repeatedly reversing the tangential force in the test bearing. The enhancement in life is the result of a plastic flow that intersects the direction of crack growth and also compressive residual stress at the edge of a dent where a large tensile stress is generated and cracks initiate during fatigue testing.
5. Lubrication oils with a high traction coefficient can significantly reduce the dent initiated flaking life of rolling element bearings.
6. Based on the results described above, tangential forces generated between the raceway and rolling elements significantly influence dent initiated flaking life.

Acknowledgments

The authors thank Dr. Andrew Dodd of NSK EUROPE for checking this paper.

References

- [1] Littmann WE, Widner RL, Wolfe JO, Stover JD. The role of lubrication in propagation of contact fatigue cracks. *Trans ASME F* 1968; 90: 89–100.
- [2] Furumura K, Shirota S, Hirakawa K. The surface-initiated and subsurface-initiated rolling contact fatigue. *NSK Bearing J* 1977; 636: 1–10.
- [3] Ichimaru K. Studies on rolling contact fatigue from the standpoints of contact mechanics and fracture mechanics. *J Jpn Soc Tribology* 1994; 39 (8): 660–7.
- [4] Furumura K, Murakami Y, Abe T. The development of bearing steels for long life rolling bearings under clean lubrication and contaminated lubrication. *Creative Use of Bearing Steels, ASTM STP 1195*, 1993. p. 199–210.
- [5] Lundberg G., Palmgren A. Dynamic capacity of rolling bearings. *Acta Polytechnica Mech Eng* 1947; 1 (3).
- [6] Lundberg G., Palmgren A. Dynamic capacity of roller bearings. *Acta Polytechnica Mech Eng* 1952; 2 (4).
- [7] Bastias PC, Hahn G T, Rubin CA., Gupta V, Leng X.

Analysis of rolling contact spall life in 440C bearing steel. *Wear* 1994; 171: 169–178.

- [8] Toda K, Mikami T, Hoshino T. Effect of dent on rolling fatigue life. *Jour Jpn Soc Trib* 1993; 38 (6): 526–532.
- [9] Chiu Y P, Liu J Y. An analytical study of the stress concentration around a furrow shaped surface defect in rolling Contact. *Trans ASME F* 1970; 92: 258–263.
- [10] Takata H. Study on the possibility of newly developed fatigue life calculating method for rolling element bearings. *Jour Jpn Soc Trib* 1994; 39 (6): 526–532.
- [11] Murakami Y, Takemura H, Fujii, A, Furumura K. Rolling contact fatigue life under contaminated lubrication with several foreign particles. *NSK Technical Journal* 1993; 655: 17–24.
- [12] Sada T, Mikami T. Effect of lubricant film thickness on ball bearing life under contaminated lubrication (Part 1) —Life tests for ball bearings in contaminated oil—. *Jour Jpn Soc Trib* 2004; 49 (12): 948–953.
- [13] Toda K, Mikami T, Shibata M, Hoshino T. Effect of debris on life of tapered roller bearing in contaminated Lubricant. *Jour Jpn Soc Trib* 1996; 41 (3): 232–239.
- [14] Lorösch H. Research on longer life for rolling-element bearings. *Lubrication Engineering* 1985; 41 (1): 37–43.
- [15] Sayles R S, Ioannides E. Debris damage in rolling bearings and its effects on fatigue life. *Trans ASME F* 1988; 110: 26–31.
- [16] Sada T, Mikami T. Effect of lubricant film thickness on ball bearing life under contaminated lubrication (Part 2) —Relation between film thickness and dents formation—. *Jour Jpn Soc Trib* 2005; 50 (1): 62–67.
- [17] Ville F, Nélias D. An experimental study on the concentration and shape of dents caused by spherical metallic particles in EHL contacts. *Tribology Transactions* 1999; 42 (1): 231–240.
- [18] Kang YS, Sadeghi F, Ai X. Debris effects on EHL contact. *Trans ASME F* 2000; 122: 711–720.
- [19] Lubrecht AA, Venner CH, Lane S, Jacobson B, Ioannides E. Surface damage-comparison of theoretical and experimental endurance lives of rolling bearings. *Proc of the Japan International Tribology Conference Nagoya* 1990; 185–190.
- [20] Wedeven LD. Influence of debris dent on EHD lubrication. *ASLE Transaction* 1978; 21 (1): 41–52.
- [21] Nélias D, Ville F. Detrimental effects of debris dents on rolling contact fatigue. *Trans ASME F* 2000; 122: 55–64.
- [22] Ai X, Cheng HS. The influence of moving dent on point EHL contacts. *Tribology Transactions*, 1994; 37 (2): 323–335.
- [23] Ai X, Lee, SC. Effect of slide-to-roll ratio on interior stresses around a dent in EHL contacts. *Tribology Transactions*, 1996; 39 (4): 881–889.
- [24] Xu G., Sadeghi F, Hoepflich MR. Dent initiated spall formation in EHL rolling / sliding contact. *Trans ASME F* 1998; 120: 453–462.
- [25] Shimizu K, Hirota T, Nagata H, Ishihara T, Imajou Y. Effects of indentation on bearing surface fatigue based on an X-RAY analysis of residual stress. *Fujikoshi Engineering Review*. 1993; 49 (2): 29–48.
- [26] Soda N, Yamashita M, Osora K. Effect of tangential force on rolling fatigue. *Jour JSLE* 1971; 16 (8): 573–584.
- [27] Soda N, Yamamoto T. Effect of tangential traction and roughness on crack initiation / propagation during rolling contact. *ASLE Trans* 1982; 25 (2): 198–206.
- [28] Murakami Y, Kaneta M, Yatsuzuka H. Analysis of surface crack propagation in lubricated rolling contact. *ASLE Trans* 1985; 28 (1): 60–68.
- [29] Murakami Y, Sakae C, Ichimaru K. Three-dimensional fracture mechanics analysis of pit formation mechanism under lubricated rolling-sliding contact loading. *Tribology Trans* 1994; 37 (3): 445–454.
- [30] Way S. Pitting due to rolling contact. *J. Appl Mech* 1935; 2 (2): A49–A58.
- [31] Nakajima A, Ichimaru K, Hirano F, Nishimura M. Effects of combination of rolling direction and sliding direction on pitting of rollers. *Jour JSLE Int Ed* 4 1983; 93–98.
- [32] Lee HY, Sakamoto N, Kawamoto M, Okabayashi K. A study on rolling fatigue of steel by X-ray diffraction (Part 2) —Effects of alternation of rolling direction and contact pressure—. *Jour Jpn Soc Trib* 1989; 34 (1): 51–57.
- [33] Skurka JC. Elastohydrodynamic lubrication of roller bearings. *Trans ASME F* 1970; 92: 281–291.
- [34] Tallian TE. On competing failure modes in rolling contact. *ASLE Trans* 1967; 10: 418–439.
- [35] Takata H, Aihara S. Effect of oil film thickness upon rolling fatigue life. *NSK bearing Journal* 1977; 636: 11–16.

Mechanism of Dent Initiated Flaking and Bearing Life Enhancement Technology under Contaminated Lubrication Condition

Part II: Effect of Rolling Element Surface Roughness on Flaking Resulting from Dents, and Life Enhancement Technology of Rolling Bearings under Contaminated Lubrication Condition

T. Ueda and N. Mitamura
Corporate Research & Development Center

ABSTRACT

The dent initiated flaking life of a bearing is sometimes shorter than the calculated life. Therefore, it is important to develop an enhanced-life bearing for contaminated lubrication conditions. In this paper, the authors indicated that the dent initiated flaking life of a raceway is significantly reduced in bearings where the general surface roughness of the rolling elements is increased by dent generation due to operating in contaminated lubrication. Additionally, we confirmed that the bearings with rolling elements made of material with fine silicon and manganese nitride precipitates, for the purpose of reducing the degradation of surface roughness, are effective in enhancing bearing life.

Reprinted from Tribology International, 42, T. Ueda, N. Mitamura, Mechanism of dent initiated flaking and bearing life enhancement technology under contaminated lubrication condition. Part II: Effect of rolling element surface roughness on flaking resulting from dents, and life enhancement technology of rolling bearings under contaminated lubrication condition, 1832-1837, Copyright (2009), with permission from Elsevier.

1. Introduction

As concern over climate change and other environmental issues continues to grow, manufacturers are marketing machinery and equipment that are more compact, lightweight, consume less energy, and help to improve fuel economy for a given application. Such a trend is placing a greater demand on the operational requirements of the rolling bearings used in these machinery and equipment. Rolling bearings used in automotive transmissions and differential gears are subjected to wear debris that gets crushed between the rolling elements and raceway. The debris forms dents on the raceway surface, which eventually leads to flaking. Bearing life, as it relates to surface dent originated flaking, is sometimes shorter than the calculated life depending on certain conditions. But overall, so-called dent initiated flaking life hampers the ability to further develop a more compact bearing. Therefore, clarifying the mechanism of dent initiated flaking, determining the life reduction and developing an enhanced-life bearing for contaminated lubrication conditions are desired. Set against a backdrop of global climate change and taking into account the implications it will have upon society, research for clarifying the mechanism of dent formation [1-3], calculating the stress at the edge of dent [4-6] and development on enhancing bearing life to counter dent initiated flaking has been

conducted [7-11].

Webster et al. [4] conducted the contact analysis for a debris dent and calculated the state of stress within the bearing raceway. Furthermore, they predicted the reduction in fatigue life due to debris dents by using the stress data calculated in conjunction with their developed fatigue model. Ai and Nixon [5] analyzed stress concentration due to debris denting in EHL contacts and proposed a fatigue life reduction model. Their study shows that life reduction is affected by dent slope, indentation area-density and contact load. Chiu and Liu [6] clarified that stress concentrations at the dent edge determine flaking life. Their work suggests that the larger the r/c value, where r is the radius of the dent shoulder and c is the half value of dent width, the smaller the stress concentration at the dent edge.

Furumura et al. [7, 8] applied the theory of Chiu and Liu and focused on retained austenite as a means to maximize the r/c value and to reduce stress concentrations. In order to achieve a higher r/c for dents formed in the raceway, Furumura et al. increased the amount of retained austenite in the raceway surface. Thus, they were able to develop a long-life bearing that restricts the generation of dent initiated flaking. After Furumura et al. published the results of their research, Toda et al. [9, 10], Maeda et al. [11] also applied the theory, which clarified the mechanism of dent initiated flaking as being caused by

stress concentrations at the edge of a dent, and developed long-life bearings with higher amounts of retained austenite.

According to the Chiu and Liu [6] theoretical model, stress concentrations in the rolling direction of the leading edge and the trailing edge of a dent are of equal value. Therefore, the rates of flaking that occur at both the leading and trailing edges are also the same. However, the Chiu and Liu [6] model fails to explain why in actual services conditions the dent initiated flaking tends to occur on the trailing edge in the rolling direction more often than the leading edge.

Therefore, the authors conducted both a twin-disk test and a ball-on-rod rolling contact fatigue (RCF) test with dents introduced into the specimen surface to clarify the cause of flaking that occurs on the trailing edge of a dent in the rolling direction, as reported in our last paper [12]. Results from both tests and other researcher's reports [13-16] confirmed that there is a relation between where a crack initiates and the direction of tangential force. Test results further revealed that cracks initiate at the edge of a dent where it is subjected to large tensile stresses due to the influence of tangential forces. Additionally, test results proved that lubricating oil with a high traction coefficient shortened dent initiated flaking life and that reversing the direction of tangential force enhanced dent initiated flaking life. Therefore, it was proven that tangential force influenced dent initiated flaking. Consequently, it is important to reduce the tangential force acting on the edge of a dent for the enhancement of dent initiated flaking life.

Surface roughness of the two contacting surfaces is known to be one of the factors affecting the tangential force [17]. Therefore, we will show in this paper that the surface roughness of a rolling element affects flaking life, and will propose a method for enhancing dent initiated flaking life by means of reducing the degradation in the surface roughness of the rolling element, which occurs under conditions of contaminated lubrication, and by minimizing tangential force acting on the edge of a raceway dent.

2. Effect of Rolling Element Surface Roughness on the Dent Initiated Flaking of a Raceway

2.1 Test method

Life testing was conducted on three types of bearing, each having rolling elements with varying degrees of surface roughness. We then investigated the influence of said surface roughness on dent initiated flaking life. For this, testing was conducted using 6206 deep groove ball bearings with a 30 mm bore diameter and a 62 mm outside diameter. The inner and outer rings of the bearings were made of through-hardened, tempered, SAE52100 steel; and the rolling elements were made of carbonitrided, quenched, tempered SAE52100 steel. The rolling elements

were carbonitrided to produce a material strength that was higher than that of the raceways, which facilitated flaking on the raceways instead of the rolling elements for investigating the influence of surface roughness of a rolling element on dent initiated flaking life of the bearing raceways.

Under actual service conditions involving contaminated lubricant, dents that are generated by foreign matter not only cause flaking but also cause the deterioration of surface roughness of the rolling elements and raceways. Therefore, in order to conduct testing that most closely resembled actual service conditions, we altered the surface roughness of the rolling elements by adding dents using foreign matter. The test was conducted using three sets of bearings; A, B, and C. The bearings from set A had rolling elements with dents. The bearings from set B also had rolling elements with dents, but these were different from the dents in the rolling elements of set A. The bearings from set C had new (standard) rolling elements that were free of any dents. Fig. 1 shows the test rig used to generate the dents in the bearings. The design of the cantilever test rig is such that a radial load is applied directly to the test bearing.

Table 1 lists the test conditions used to generate dents

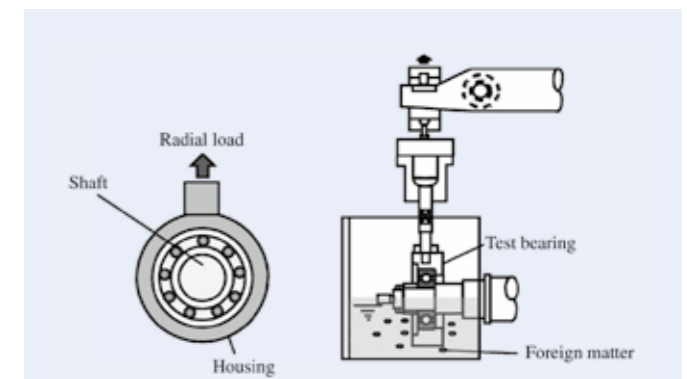


Fig. 1. Layout of dent-generating test rig.

Table 1 Dent-generating test conditions

Part	Rolling element		Raceway
	Bearings A	Bearings B	Common
Bearing			
Radial load (kN)	6.2		
Rotating speed (min ⁻¹)	3 000		
Time (h)	1.0		
Lubrication oil	Type	ISO-VG68	
	Quantity (L)	1.2	
Foreign matter	Size (μm)	74-147	
	Quantity (g)	0.05	
	Hardness HV	870	520
	Material	Cementite	Stainless-steel

on the rolling elements and raceways of each bearing. Dents were generated by operating the bearings for one hour using lubricant that was contaminated with foreign matter. The hardness of foreign matter used for generating dents was *HV* 870 for the rolling elements of the bearings from set A, and *HV* 520 for the rolling elements of the bearing from set B. The conditions for generating the dents were the same for the rolling elements of the bearings from sets A and B, except for the material and hardness of the foreign matter. Conditions for generating dents on the raceways of the bearings from sets A, B, and C were the same as the conditions used for generating dents on the rolling elements of the bearings from set B. In other words, the surface roughness of the raceways of the bearings from sets A, B and C was the same. Table 2 lists the conditions of the raceway and rolling element surfaces before testing.

The dented surface roughness maximum height, R_z , of the rolling elements of the bearings from set A, after dent generation with foreign matter of hardness *HV* 870, was 0.53 μm . Similarly, the R_z value of the rolling elements of the bearings from set B, after dent generation with foreign matter of hardness *HV* 520, was 0.28 μm . The R_z value of the new rolling elements of the bearings from set C was 0.11 μm . After dents were generated, the rolling elements and the raceways were thoroughly cleaned. Life testing was conducted under clean lubrication conditions, a radial load of 6.2 kN, a rotating speed of 3 900 rpm, and forced-circulation oil lubrication (ISO-VG68). Although the test rig used for this clean life test was basically the same as that for generating dents (see Fig. 1), a different lubricating method was used. Oil bath lubrication was used when generating dents, and forced-circulation oil lubrication with 10 and 3 μm filtering was used during clean life testing.

2.2. Test results

Fig. 2 shows the results of the life test in the form of a Weibull plot. In this figure, the single-line arrow denotes a bearing without flaking, and the double-line arrow denotes




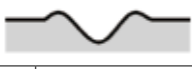
a bearing with flaking on the rolling element. Among the bearings with flaking, only one of the bearings from set C had flaking on the rolling elements; all the others had flaking on the raceways. Fig. 3 shows an example of dent initiated flaking. All of the flaking that occurred on the raceway was dent initiated flaking as shown in Fig. 3. Fig. 2 confirmed that the dent initiated flaking life of a raceway was significantly reduced in those bearings with rolling elements that had an increased surface roughness caused by dents generated whilst operating with lubricant contaminated with hard foreign matter.

2.3 Discussion

It is generally known that the greater the surface roughness of two contacting surfaces, the greater the tangential force—a condition that promotes a greater reduction in the rolling contact fatigue life [17]. In this test, since the surface roughness of the rolling elements in the bearings from sets A and B was higher than that of the bearings from set C, the tangential force acting between the rolling elements and raceway was larger in the bearings from sets A and B in comparison with bearings from set C. Also, as described above, the authors clarified experimentally in a previous paper [12] that there is a correlation between the position where crack initiates at the edge of a dent and the direction of tangential force [13-16]. It was proved that tangential force acting on the edge of a dent affects dent initiated flaking life. On the basis of previously published papers [12, 17], the life test results shown in Fig. 2 revealed that when the surface roughness of the rolling elements was increased, and consequently the amount of tangential force acting on the edge of dent, then the dent initiated flaking life was reduced.

Conversely, under conditions of clean lubrication that is free of foreign matter, it is well known that the rolling contact fatigue life correlates with the lubricant film parameter $\lambda = h_{\text{min}} / \sigma$; where h_{min} represents minimum lubricant film thickness and σ is the composite surface roughness of two contacting surfaces [18-20]. Skurka

Table 2 Surface conditions of bearing component used for life testing

	Bearings A	Bearings B	Bearings C
Rolling element	Dents were generated with foreign matter of <i>HV</i> 870  $R_a = 0.024 (\mu\text{m})$ $R_z = 0.53 (\mu\text{m})$	Dents were generated with foreign matter of <i>HV</i> 520  $R_a = 0.022 (\mu\text{m})$ $R_z = 0.28 (\mu\text{m})$	New ball  $R_a = 0.007 (\mu\text{m})$ $R_z = 0.11 (\mu\text{m})$
Raceway	Dents were generated with foreign matter of <i>HV</i> 520  $R_a = 0.039 (\mu\text{m})$		
λ of life test	2.0	2.7	3.0
Symbol in Fig. 2	▲	■	○

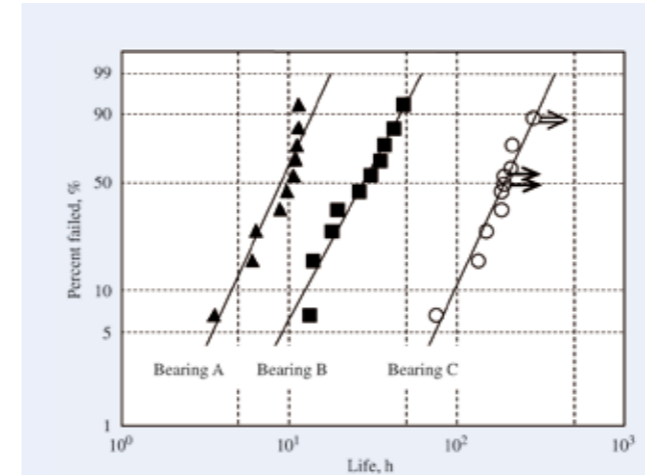


Fig. 2. Influence of surface roughness of rolling element on dent initiated flaking. Test bearing 6206, $F_r = 6.2$ (kN); $n = 3$ 900 (rpm); lubrication: ISO-VG68 forced circulation.

[18] and Takata and Aihara [20] have reported that in a region where λ is 3 or less, the smaller the value of λ , the shorter the rolling contact fatigue life. The life test illustrated in Fig.2 and listed in Table 1 had a λ value of 3 or less depending on the surface roughness of the rolling elements. As the surface roughness of the rolling elements increased, λ decreased and the dent initiated flaking life became shorter. When λ is smaller, metal-to-metal contact increases, and the friction coefficient increases with an increase in the tangential force as well. Therefore, it is difficult to examine λ and tangential force separately. However, as reported in the previous paper [12], bearings that underwent life testing with traction oil with a high friction coefficient (tangential force coefficient) had an overwhelmingly shorter dent initiated flaking life, even under conditions where the value of λ was almost the same (slightly higher). As for the dent initiated flaking life of the bearings, the tangential force had a greater influence than that of λ . More specifically, test results confirm that increasing the surface roughness of rolling elements (see Fig. 2) shortens dent initiated flaking life, which further increases the surface roughness that is generated, and increases the amount of tangential force generated.

In the past, research and development for enhancing the dent initiated flaking life of a bearing focused on enhancing material strength or on reducing stress concentrations in the area where flaking occurred [7-11]. However, the results in Fig. 2 clearly indicate that the raceway dent initiated flaking life is related to the rolling element surface roughness, as they are the mating parts in a rolling bearing. (Naturally, the dent initiated flaking life is affected by the slip, contact pressure, lubrication condition, etc., together with the surface roughness.) Under conditions of contaminated lubrication, foreign matter is crushed between the raceway and the rolling

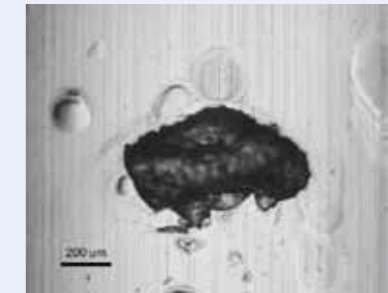


Fig. 3. Dent initiated flaking. Bearing A, $L = 11$ (h), Inner ring flaking.

elements generating dents on the raceway and the surface of the rolling elements, thus degrading surface roughness. The degradation in surface roughness gives rise to large tangential force acting on the edge of the dents, which in turn reduces the dent initiated flaking life. Therefore, a new approach is considered to enhance the service life of bearings operating under conditions of contaminated lubricant, such as developing a method that improves dent resistance of the mating parts for reducing the tangential force acting on dent edge.

3. Improving Dent Resistance of Rolling Elements

As discussed in the previous section, it is important to improve the dent resistance of the part contacting with the part that is susceptible to flaking in order to enhance dent initiated flaking life. One method for improving the dent resistance of bearing material is explained below.

The material factor most affecting dent resistance is hardness. Naturally, the harder the material, the higher the dent resistance. The hardness of martensite, which is the main phase of general bearing steel, is roughly determined by the carbon content, and is hardly affected by alloying elements. As the carbon content of bearing steel is already high, there is little scope to increase the material hardness by increasing the hardness of the martensite.

Producing finely dispersed precipitates within the martensite can increase the hardness of the material. Typically, in bearing steel, cementite is precipitated throughout the material. If the amount of cementite is significantly increased, for instance by carburizing, then it may precipitate at the grain boundaries to form a grain boundary network, which may sometimes become the fracture origin. This can be avoided by using alloying elements such as tungsten (W) or titanium (Ti), which form carbides that precipitate independently of the cementite. However, these alloying elements are very expensive.

An inexpensive alloying element such as silicon (Si)

can be used, although it is less effective in forming carbides. Silicon is used in various structural steels, and forms a very hard nitride during the nitriding process. Also, silicon does not concentrate in the cementite and is mostly soluble in the matrix. Therefore, for high carbon martensite steel such as bearing steel, where cementite is finely dispersed, silicon is a suitable element for promoting additional finely dispersed precipitates separate to the cementite. Consequently, nitriding material containing high quantities of silicon for precipitating silicon nitride improves dent resistance of the material.

Dent testing of material containing fine silicon nitride precipitates was conducted to demonstrate the above assumptions. Testing was conducted using through-hardened and tempered SAE52100 bearing steel (hereinafter SAE52100) and carbonitrided material containing higher quantities of silicon in comparison with SAE52100 for precipitating silicon nitride (hereinafter called nitride precipitated material). The dent testing method used is shown in Fig. 4. Testing was conducted by applying a contact force between a 2 mm diameter SAE52100 hardened steel ball and a 60 mm diameter and 6 mm thick disc made of the material described above. The disk finish had a surface roughness of approximately $R_a = 0.005 \mu\text{m}$. Test conditions included a loading speed of 0.5 mm/sec, and the application of the load for 10 seconds. Dent resistance was evaluated by measuring the depth of the dents produced in the disk using an optical interferometer.

Table 3 lists the surface hardness the disks of SAE52100

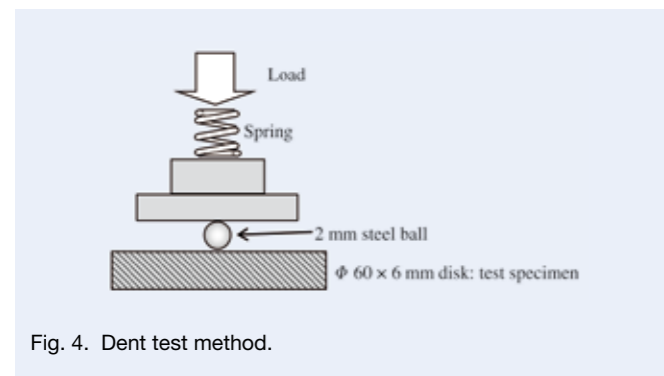
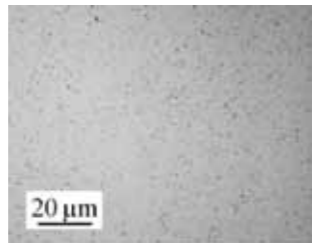
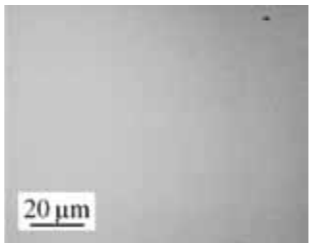


Fig. 4. Dent test method.

Table 3 Surface conditions of bearing component used for life testing

	Nitride precipitated material	SAE52100
Surface hardness	HV 861	HV 776
Metallurgical micrograph of disk surface		

and nitride precipitated material and includes an optical micrograph showing the surface of each disk. The nitride precipitated material disk surface shows fine precipitates (black spots) that cannot be observed on the SAE52100 disk surface. The fine precipitates were analyzed using an energy dispersive X-ray (EDX) analyzer, which revealed Si, nitrogen (N) and manganese (Mn), which is an alloying element in steel. Therefore, it is considered that these fine precipitates are Si-Mn nitride. Due to the high hardness of the silicon and manganese nitrides, the surface hardness of the nitride precipitated material disk was harder than that of the SAE52100 disk by approximately HV 100.

Fig. 5 illustrates the relation between maximum contact pressure and depth of dent on the disk surface produced by the steel ball. The depth of the dent in the longitudinal axis is shown in the drawing of the dent (see Fig. 5), and does not include the height of the shoulder at the edge of the dent. As shown in Fig. 5, for a given contact pressure, the depth of the dent on the surface of the nitride precipitated material disk is smaller than the dent on the surface of the SAE52100 disk. This confirms that the resistance to denting of the nitride precipitated material is superior to that of the SAE52100.

4. Effectiveness of Extending Life by Improving Rolling Element Dent Resistance

As reported in the previous paper, dent initiated flaking tends to occur on the surface of the driven component, where its circumferential speed is slower than that of the driving component [12]. In ball bearings, the raceway is the driven component at the center of the contact area with high Hertz contact pressure in the loaded zone, which is where dent initiated flaking easily occurs. As described above, it is important to improve the dent resistance of the part contacting with the part that is susceptible to flaking in order to enhance dent initiated flaking life. Therefore, one solution to enhance the service life of a ball bearing operating under conditions of contaminated lubricant would be to improve the dent resistance of the rolling elements. Accordingly, we assembled some test bearings using rolling elements made from nitride precipitated

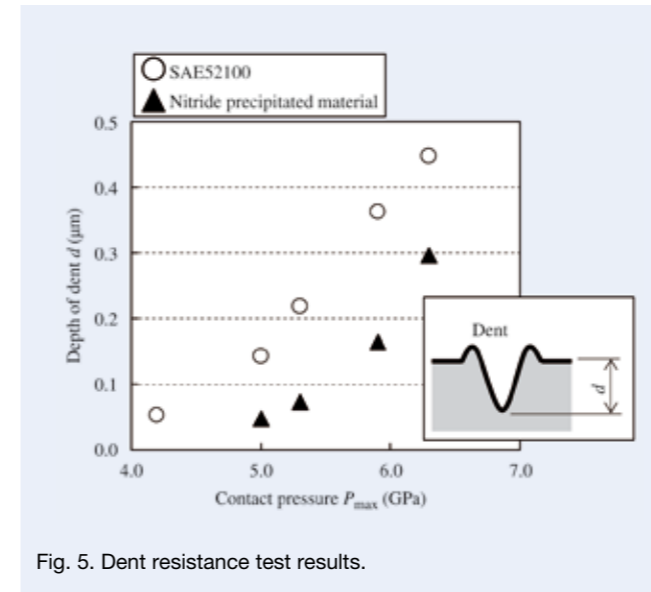


Fig. 5. Dent resistance test results.

material, in which dent resistance was improved. Life testing was then conducted using these bearings under the conditions of contaminated lubricant.

The test rig used for this life test was of the same design as the rig illustrated in Fig. 1. Test conditions were the same as those listed in Table 1 for bearings from set A. Test conditions included a 6206 bearing; a radial load of $F_r = 6.2 \text{ kN}$; a rotating speed of $n = 3\,000 \text{ rpm}$; and oil-bath lubrication (ISO-VG68 lubricant). Foreign matter used for contamination included: a hardness of HV 870; particle sizes ranging from $74 \mu\text{m}$ to $147 \mu\text{m}$; and a quantity of 0.05 g per 1.2 liters of lubrication oil. The raceway material was standard, through-hardened, tempered SAE52100 steel and the rolling elements were nitride precipitated material. For comparison purposes, testing

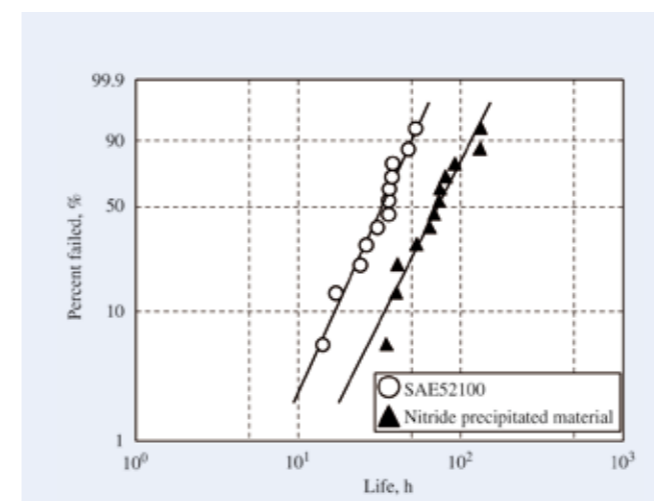


Fig. 6. Enhance life of rolling elements made from material containing fine nitride precipitates. Test bearing 6206, $F_r = 6.2 \text{ (kN)}$; $n = 3\,000 \text{ (rpm)}$; lubrication: ISO-VG68 oil bath; contaminants: hardness HV 870; size $74 \mu\text{m}$ to $147 \mu\text{m}$; quantity: 0.05 g.

was also conducted using a bearing with standard SAE52100 rolling elements.

Fig. 6 shows the life test results. Flaking occurred only on the raceways of the two types of bearing tested and the dent initiated flaking life of the bearings with dent-resistant rolling elements made from nitride precipitated material was nearly doubled that of the bearings with SAE52100 rolling elements.

Life testing was interrupted for one hour to check for dents generated on the rolling elements in order to verify that life enhancement was achieved only through the dent resistance of the rolling elements. After one hour life testing, the dented surface roughness maximum height R_z , of the rolling element made from nitride precipitated material was $0.23 \mu\text{m}$ and R_z , of SAE52100 rolling element was $0.42 \mu\text{m}$. Fig. 7 illustrates the relation between the number and depth of the dents, which were measured using a roundness-measuring instrument. The number of dents and the depth of each dent were measured along an arbitrarily selected circumference of all nine balls in each bearing. Measured results (see Fig. 7) show that rolling elements made of material with nitride precipitated material had fewer and shallower dents in comparison with rolling elements that were made of SAE52100 material.

The results shown in Fig. 7 and previous reporting [12], confirm that life enhancement was achieved through the use of rolling elements made from nitride precipitated material, which provided improved dent resistance, less degradation of surface roughness, and reduced tangential force acting on the dent edges on the raceway.

Bearing materials that were developed to provide greater life enhancement in the past used expensive alloying elements in the raw material, and required complicated

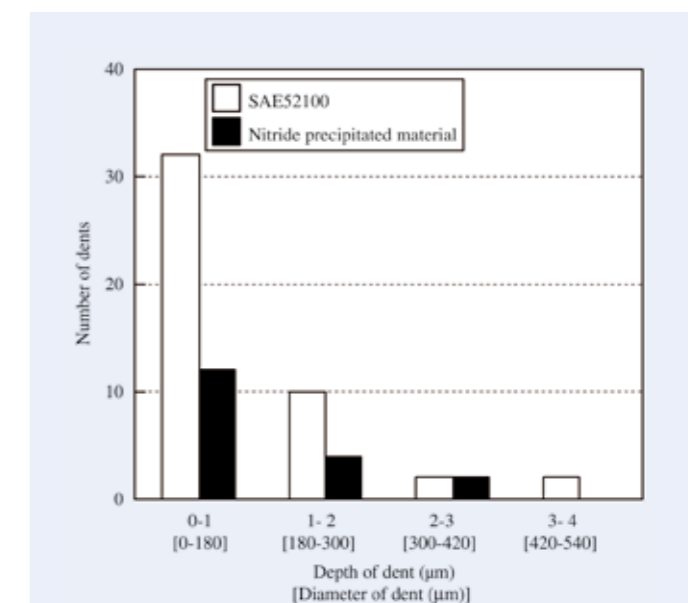


Fig. 7. Dent generation on rolling elements during life testing. Nitride precipitated material: $R_a = 0.017 \text{ (}\mu\text{m)}$, $R_z = 0.23 \text{ (}\mu\text{m)}$. SAE52100: $R_a = 0.023 \text{ (}\mu\text{m)}$, $R_z = 0.42 \text{ (}\mu\text{m)}$.

heat treatment processes. The impact on the environment from manufacturing such bearings and their recycling efficiency has been less than favorable. Consequently, such bearings fail to meet the current environmental demands. However, the technology discussed in this work can be used to manufacture fully functional bearings only by making changes to the material used for the rolling elements, which is one of the components of rolling bearing. Furthermore, this technology is versatile, increase productivity and can be used to develop more compact, lightweight bearings that are highly functional. Therefore, this technology contributes to society in terms of greater environmental sensitivity.

5. Conclusion

In the previous paper, the authors clarified that tangential forces acting on the edge of a dent had a negative impact on dent initiated flaking life. In this paper, we investigated the influence of rolling element surface roughness on dent initiated flaking life of the raceway. Additionally, we confirmed changes made in the material of a rolling element for the purpose of reducing the degradation of surface roughness, which occurs during bearing operation, are effective in enhancing bearing life. Changes in rolling element material were also shown to minimize tangential forces acting on the edge of dents on the bearing raceway. Conclusions are as follows:

1. In tests where the test conditions for generating dents on the raceway were the same for each tested bearing, the greater the surface roughness of the rolling elements, the shorter the dent initiated flaking life of the raceway.
2. In comparison to bearing components made from standard bearing material, components made from material with a high degree of hardness due to fine silicon and manganese nitride precipitates had superior dent resistance, and provided greater resistance to surface roughness degradation of the rolling elements, which occurs under conditions of contaminated lubricant.
3. In comparison to bearings with rolling elements made of standard bearing steel, life test results of bearings with rolling elements made of material with fine silicon and manganese nitride precipitates operated under conditions of contaminated lubricant showed that the raceways had a dent initiated flaking life that was twice as long. Thus, we believe that rolling element material with fine silicon and manganese nitride precipitates can extend bearing life by providing greater resistance to dent generation, by preserving the surface roughness of rolling elements, and by reducing the amount of tangential force acting on the edge of raceway dents.

Acknowledgments

The authors thank Dr. Andrew Dodd of NSK EUROPE for checking this paper.

References

- [1] Sayles, R. S. and Ioannides, E. Debris Damage in Rolling Bearings and Its Effects on Fatigue Life. *Trans ASME F* 1988; 110: 26–31.
- [2] Dwyer-Joyce, R. S., Hamer, J. C., Sayles, R. S. and Ioannides, E. Lubricant Screening for Debris Effects to Improve Fatigue and Wear Life. *Proceedings of the 18th Leeds-Lyon Symposium on Tribology*, D. Dowson et al. Editors, Amsterdam, Elsevier, 1992; 57–63.
- [3] Ville, F. and Nélias, D. An Experimental Study on the Concentration and Shape of Dents Caused by Spherical Metallic Particles in EHL Contacts. *Tribology Transactions*, 1999; 42 (1): 231–240.
- [4] Webster, M. N., Ioannides, E. and Sayles, R. S. The effect of topographical defects on the contact stress and fatigue life in rolling element bearings. *Proceedings of the 12th Leeds-Lyon Symposium on Tribology*, Lyon, Butterworths, 1985; 207–221.
- [5] Ai, X. and Nixon, H. P. Fatigue Life Reduction of Roller Bearings Due to Debris Denting: Part I—Theoretical Modeling. *Tribology Transactions*, 2000; 43 (2): 197–204.
- [6] Chiu Y P, Liu J Y. An analytical study of the stress concentration around a furrow shaped surface defect in rolling Contact. *Trans ASME F* 1970; 92: 258–263.
- [7] Murakami, Y., Matumoto, Y., Furumura, K. Long Life TF Bearings under Debris Contaminated Lubrication. *NSK Technical Journal* 1989; 650: 1–11.
- [8] Frumura, K., Murakami, Y., Abe, T. The Development of Bearing Steels for Long Life Rolling Bearings Under Clean Lubrication and Contaminated Lubrication. *Creative Use of Bearing Steels ASTM STP 1195* 1993; 199–210.
- [9] Toda, K., Mikami, T., Johns, T. M. Development of Long Life Bearing in Contaminated Lubrication. *SAE Tech Pap* 921721; 1992.
- [10] Toda, K., Mikami, T., Hoshino, T. Effect of Ridge around Dent and Retained Austenite on Rolling Fatigue Life. *J. Japan Inst Metals* 1994; 58: 1473–1478.
- [11] Maeda, K., Nakashima, H., Kashimura, H. Development of Long Life TAB and ETA Bearings and Their Automotive Applications. *NTN TECHNICAL REVIEW* 1996; 65: 17–22.
- [12] Ueda, T., Mitamura, N. Mechanism of dent initiated flaking and bearing life enhancement technology under contaminated lubrication Part I: Effect of tangential force on dent initiated flaking. *Tribology International* 2008; 41: 965–974.
- [13] Nélias D, Ville F. Detrimental effects of debris dents on rolling contact fatigue. *Trans ASME F* 2000; 122: 55–64.
- [14] Ai X, Cheng HS. The influence of moving dent on point EHL contacts. *Tribology Transactions*, 1994; 37 (2): 323–335.
- [15] Ai X, Lee, SC. Effect of slide-to-roll ratio on interior stresses around a dent in EHL contacts. *Tribology Transactions*, 1996; 39 (4): 881–889.
- [16] Xu G., Sadeghi F, Hoepflich MR. Dent initiated spall formation in EHL rolling / sliding contact. *Trans ASME F* 1998; 120: 453–462.
- [17] Soda, N., Yamamoto, T. The Role of Surface Traction for the Pitting on Gear Teeth. *J. JSLE* 1975; 20: 268–275.
- [18] Skurka, J. C. Elastohydrodynamic Lubrication of Roller Bearings. *Trans. ASME, F* 1970; 92: 281–291.
- [19] Tallian, T. E. On Competing Failure Modes in Rolling Contact. *ASLE Trans.* 1967; 10: 418–439.
- [20] Takata H, Aihara S. Effect of oil film thickness upon rolling fatigue life. *NSK bearing Journal* 1977; 636: 11–16.

Oil Film Behavior under Minute Vibrating Conditions in EHL Point Contacts

Taisuke Maruyama and Tsuyoshi Saitoh
Corporate Research & Development Center

ABSTRACT

The oil film thickness was measured under conditions of minute vibrations using an elastohydrodynamic lubrication (EHL) ball-on-disk test rig. Poly-alpha-olefin (PAO) oil was used as the lubricant under conditions of pure sliding where only the ball specimen was minutely vibrated. It was found that an oil film formed when the amplitude ratio was more than 1.6. Moreover, when conditions were changed to the maximum vibrating speed, oil viscosity, and maximum contact pressure, the critical amplitude ratio at which the oil film began to form remained at 1.6. Consequently, calculated results showed that the oil film was formed when the amplitude ratio was $\pi/2$ (nearly equal to 1.6), which closely agreed with our test results.

Reprinted from Tribology International, 43, Taisuke Maruyama, Tsuyoshi Saitoh, Oil film behavior under minute vibrating conditions in EHL point contacts, 1279-1286, Copyright (2009), with permission from Elsevier.

1. Introduction

Rolling bearings used in various machines may suffer from fretting wear (false brinelling) that is generated on almost all of the bearing raceways as a result of being forcibly subjected to minute vibrating movements. Such fretting wear can result in poor bearing performance, such as bearings that are excessively noisy, have higher bearing torque, or generate wear-induced flaking, etc. References [1], [2], [3], and [4] mentioned that a decrease in amplitude influences oil film collapse, which leads to wear. They also mentioned the fact that at certain amplitude, the oil film failed to form.

Here, the parameter of the amplitude ratio is explained. In this research, the level of amplitude is expressed as a parameter, which is referred to as the amplitude ratio. The amplitude ratio is expressed as A/D where A is amplitude, which represents moving distance of the contact area, and D represents the diameter of the Hertz contact area (see Fig. 1), which expresses the degree of vibration.

In a high surface-pressure environment, such as that which is found under EHL conditions, oil is introduced to the contact area at the average speed of the two sliding surfaces (rotational speed of the rollers). Under pure rolling line contacts, the critical amplitude ratio at which oil is introduced to whole contact area is 1.0. Under conditions of pure sliding line contacts, however, that ratio becomes 2.0.

Ichimaru [1] simulated the oil film thickness in EHL point contacts in order to determine how the oil film begins to form from a stationary or static condition, and found that oil was introduced into the contact area at a speed equivalent to that of the rolling speed.

Ikeuchi et al. [2] analyzed the process and mechanism of fluid film formation, and had already investigated and determined that the length of minimum sliding distance

for non-contact conditions was twice length of the initial contact width under sliding line contacts. In other words, oil film formation was possible when the amplitude ratio was greater than 2.0 under pure sliding line contacts.

Mitjan et al. conducted fretting wear testing under pure sliding point contacts, and investigated the fretting resistance of a diamond-like carbon (DLC) film [3]. Test results shows that when the amplitude ratio was less than 2.0, the DLC coated specimen showed improved wear resistance over that of the uncoated specimen. However, when the amplitude ratio was more than 2.0, they noted that there was no significant difference, and that the oil film had readily formed.

Kaneta et al. [4] determined that the existence of a limited amplitude that is always forming an oil film during reciprocating motion in a reciprocating seal.

Moreover, there have been numerous studies regarding the behavior of EHL systems under non-steady state conditions [5]-[11].

Sugimura et al. [5] showed that an oil film thickness that was subjected to constant acceleration could be approximated with a simple model based on the continuity of flow.

Glovnea et al. [6, 7] measured oil film thickness under rapid deceleration with the use of a high-speed video

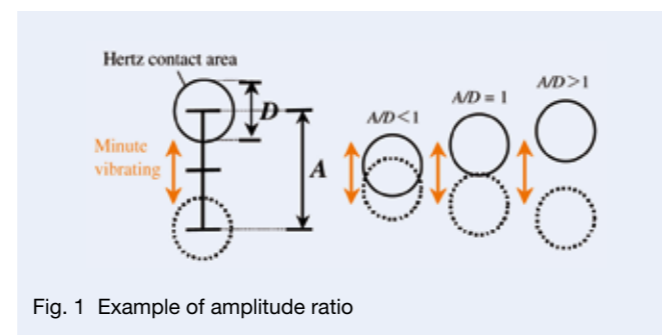


Fig. 1 Example of amplitude ratio

camera, and also analyzed theoretically about the behavior of the oil film thickness.

Wang et al. [8] conducted research on oil film thickness under short stroke reciprocating motions under pure rolling EHL point contacts. They also compared the experimental results with numerical results of EHL theory, which took into account conditions of oil starvation. Their research showed that experimental and theoretical results agreed well with each other.

Jang et al. [9] applied a multigrid multi-level method to calculate a transient EHL film thickness in sliding and rolling line contacts. Results showed that the minimum oil film thickness was dependent on entraining velocity, whereas the minimum oil film thickness, which included the squeeze film effect, was dependent on the amount of load being applied.

Messé et al. [10] calculated the profile of an oil film thickness under non-steady state conditions. Using numerical simulation, they predicted that the evolution of an oil film thickness profile is a function of varying velocity, geometry, and load.

Izumi et al. [11] found the numerical simulation to represent oil film formation in point contacts under reciprocating rolling conditions, which showed that oil film thickness decreased with cycle repetition under fully flooded conditions; that the oil film almost always recovered when the contact area returned to the stroke center; and that nearly the same oil film thickness trajectory was traced along with changes in entrainment velocity.

However, no investigation has been published in regards to the existence of the amplitude limit where an oil film is always formed during the reciprocating motion in the point contact. Consequently, this research discusses the investigation into critical amplitude ratio when an oil film

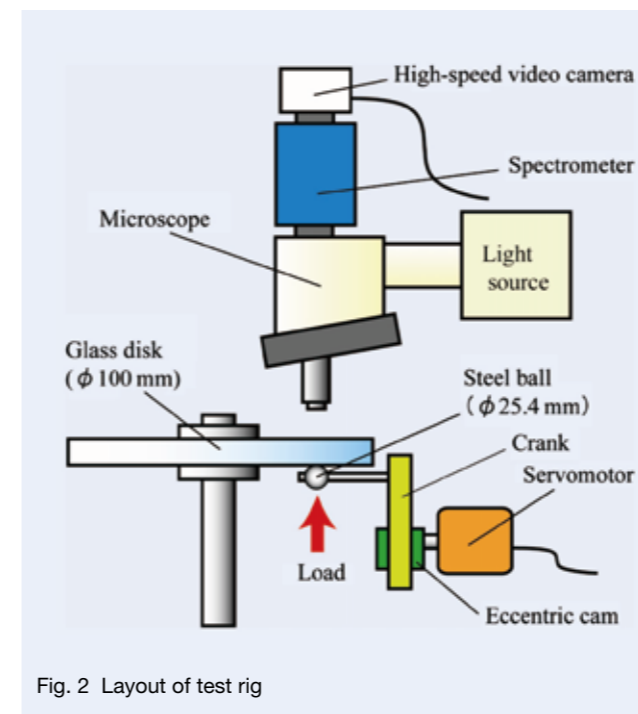


Fig. 2 Layout of test rig

begins to form. Also, the influences of maximum vibrating speed, lubrication oil viscosity, and maximum contact pressure on oil film behavior are investigated.

2. Testing Method

Fig. 2 shows a layout of the ball-on-disk test rig used to measure EHL oil film thickness under sliding point contacts in this research. An eccentric cam and crank mechanism was used to minutely vibrate the ball specimen against a stationary glass disk. Table 1 lists the ball specimen and glass disk specifications used in the test rig. In this research, the maximum vibration speed (V_{max} as shown in Fig. 3) remained constant even if the amplitude ratio was changed.

Thickness of the oil film was measured using the space layer method [12]. Fig. 4 shows a close-up view of the glass disk and ball specimen. One side of the glass disk was treated with a semi-reflective film of chromium.

Table 1 Specimen specifications

	Ball specimen	Disk specimen
Diameter	25.4 mm	100 mm
Material	SUJ2	BK7 (Glass)
Young's modulus	210 GPa	73.1 GPa
Poisson's ratio	0.3	0.23
Surface roughness	0.0081 $\mu\text{m Ra}$	0.0023 $\mu\text{m Ra}$

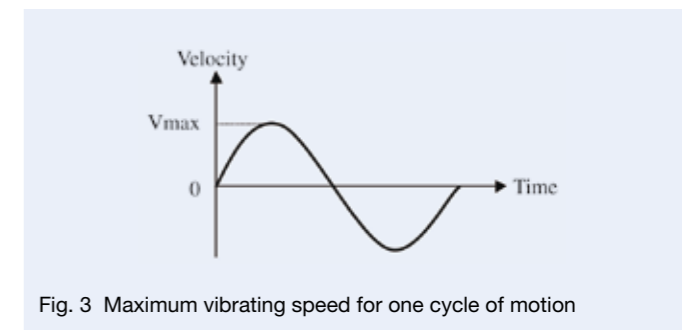


Fig. 3 Maximum vibrating speed for one cycle of motion

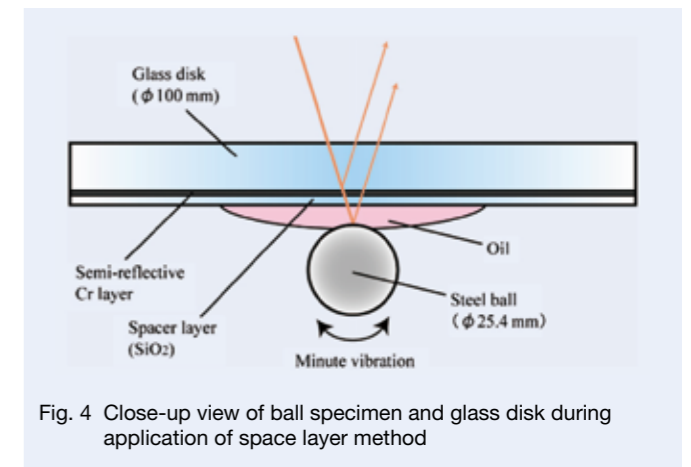


Fig. 4 Close-up view of ball specimen and glass disk during application of space layer method

Then, a spacer layer of SiO₂ was deposited on the Cr coating. Spacer film thickness was about 800 nm. The ball specimen was pressed up against the underside of the glass disk. A white light was shone on the contact area while the interference fringes were observed. The interfering light was directed to a spectrometer where it was dispersed into its component wavelengths. A high-speed video camera recorded the images from the spectrometer. Camera specifications are shown in Table 2. These images were analyzed to measure the optical path difference. Whereas the spacer layer thickness was already known, it was possible to measure the oil film thickness.

Fig. 5 shows a picture of the interference fringe. In

Table 2 Camera specifications

Image pickup device	CMOS Monochrome picture
Number of pixels	512 × 512 pixels
Frame rate	500 frames/s
Measuring time	0.3 s

this paper, the oil film thickness was measured at the centerline of the contact area as shown in Fig. 5. This centerline and the direction of vibration were parallel. Before testing, both the ball and the disk were cleaned by ultrasonic washing for 5 minutes in petroleum benzene and cleaned for 5 minutes in acetone.

Fig. 6 shows the behavior of oil film profiles in the

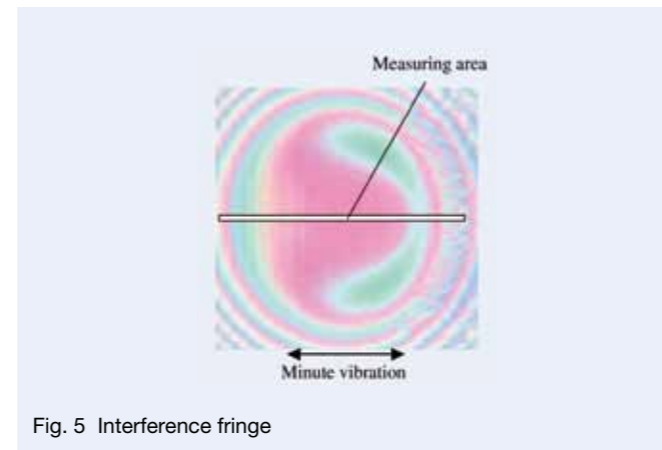


Fig. 5 Interference fringe

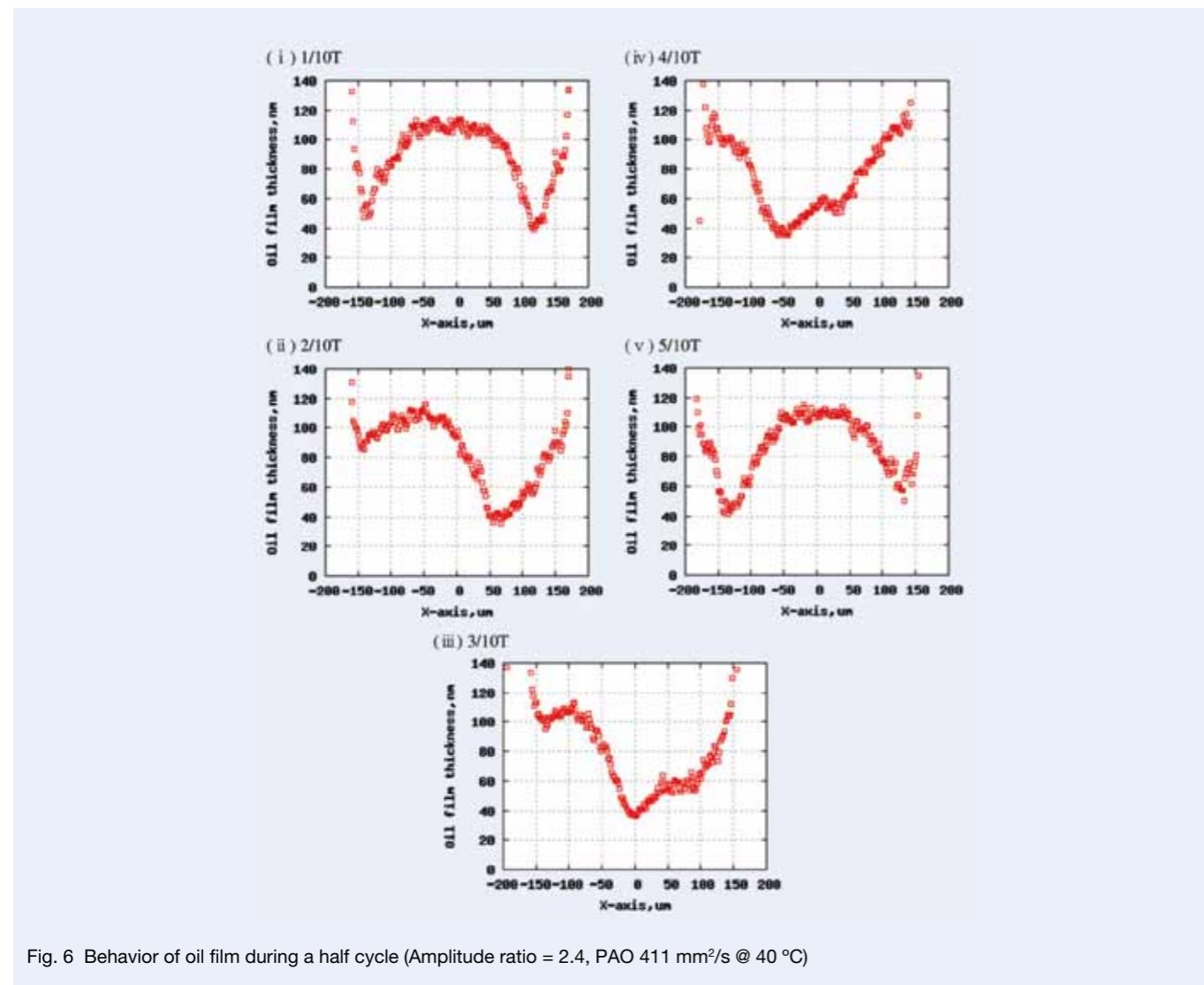


Fig. 6 Behavior of oil film during a half cycle (Amplitude ratio = 2.4, PAO 411 mm²/s @ 40 °C)

centerline of the contact area during a half cycle (= 1/2T) when the amplitude ratio was 2.4. The x-axis in each graph indicates the vibrating direction. In this paper, the minimum oil film thickness is defined as the minimum value of oil film thickness during one cycle of motion.

3. Test Results

3.1 Relationship between amplitude ratio and minimum oil film thickness

Table 3 lists the test conditions, and Fig. 7 illustrates the oil film profiles for a given amplitude ratio using highly viscous lubricating oil (411 mm²/s @ 40 °C) when the maximum vibration speed was 20 mm/s. Fig. 7 shows that the amplitude ratio had a direct effect on the minimum oil film thickness. Notably, when the amplitude ratio was more than 1.6, an oil film had formed even when the ball specimen was positioned at the end of a cycle of vibrating movement (halting motion) where sliding speed was 0 mm/s. The presence of this oil film is a result of the squeeze film effect. Fig. 8 illustrates the relationship between minimum oil film thickness and the amplitude ratio, where an oil film fails to form when the amplitude ratio is less than 1.6. However, when the amplitude ratio was between 1.6 and 2.9, oil film thickness varied depending on the amplitude ratio, and once the amplitude ratio began exceeding 2.9, it no longer influenced the minimum oil film thickness.

3.2 Influence of maximum vibrating speed

Subsequently, oil film behavior was investigated after changing the maximum vibrating speed (V_{max}) from 2 mm/s to 30 mm/s. Table 4 lists the test conditions. Fig. 9 illustrates three oil film profiles for the amplitude ratio of 1.5 under maximum vibrating speeds (V_{max}) of 10, 20, and 30 mm/s. Within the contact area, the thick section of the oil film became thicker with increase in speed, but the minimum oil film thickness remained at 0 nm. This means that the oil did not satisfy the whole contact area

Table 3 Test conditions

Temperature	25 ± 0.5 °C
Oil	Poly-alpha-olefin oil (PAO)
Viscosity	411 mm ² /s @ 40 °C
Maximum contact pressure	0.37 GPa
Amplitude ratio	0.6–4.3
Maximum vibrating speed	20 mm/s
Slide-to-roll ratio Σ ^a	200 %
Speed of disk specimen V _D	0 mm/s

$$^a \Sigma = \frac{V_B - V_D}{V_B + V_D} \times 100$$

V_B: speed of ball specimen;
V_D: speed of disk specimen.

when the amplitude ratio was less than 1.6. In Fig. 10, the relationship between minimum oil film thickness and amplitude ratio is shown. Furthermore, this figure shows that the faster the maximum vibrating speed, the thicker the minimum oil film thickness when the amplitude ratio is more than 2.9. Also, when the amplitude ratio was less

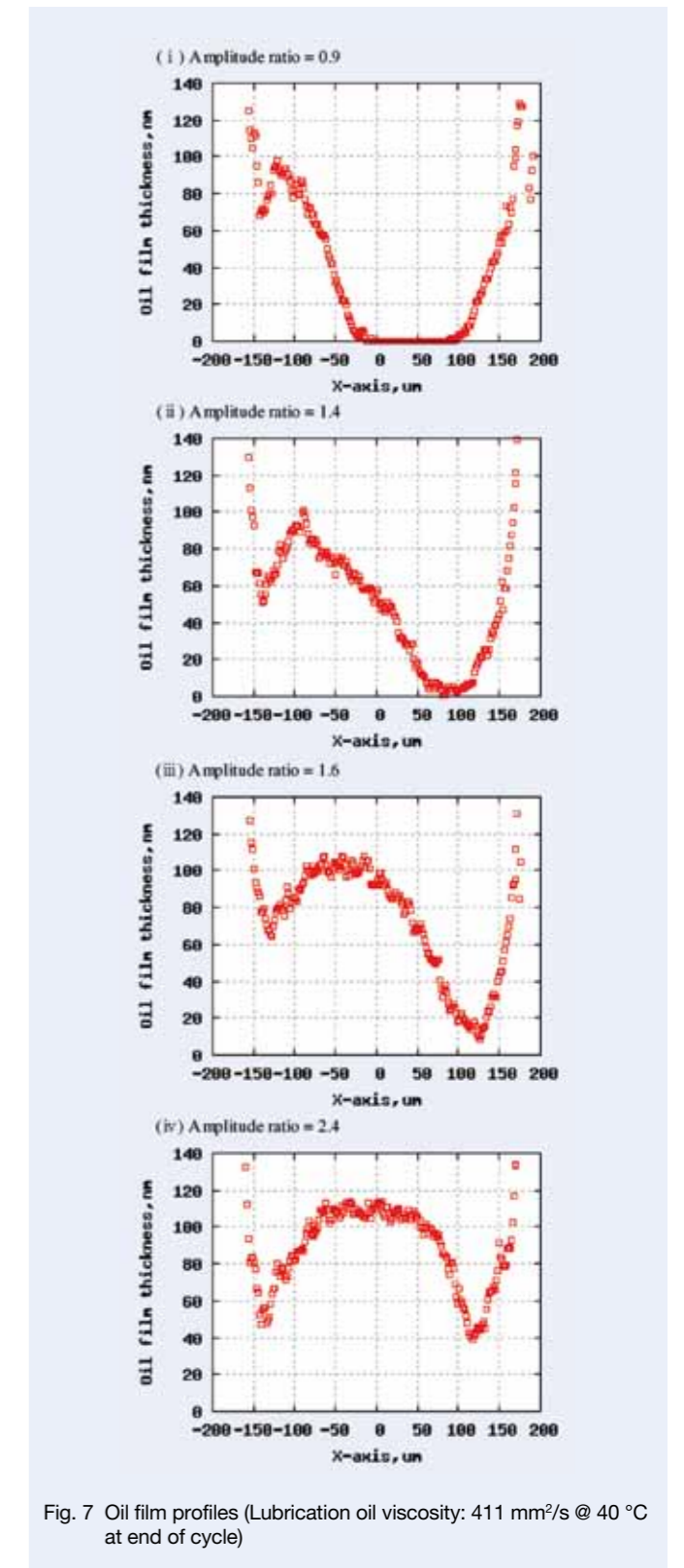


Fig. 7 Oil film profiles (Lubrication oil viscosity: 411 mm²/s @ 40 °C at end of cycle)

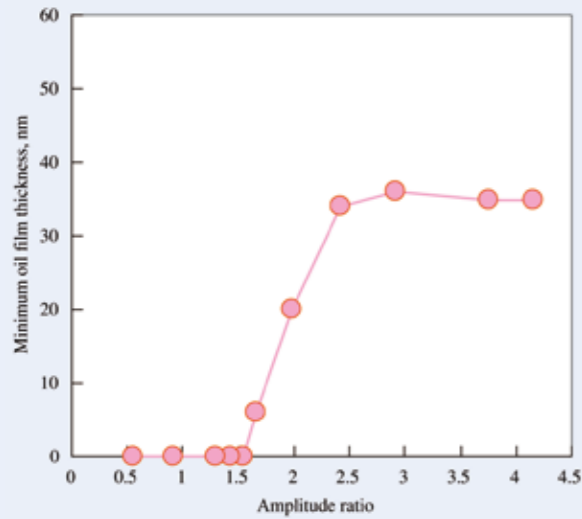


Fig. 8 Relationship between minimum oil film thickness and amplitude ratio at 0.37 GPa

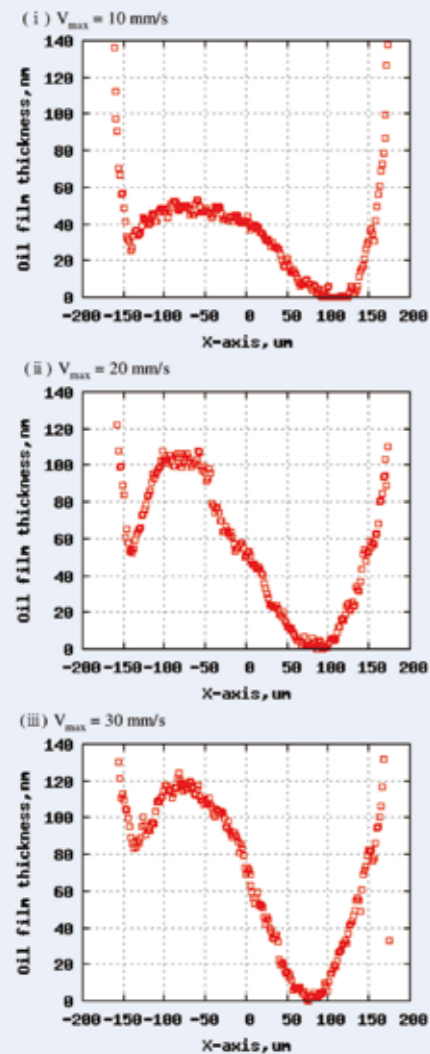


Fig. 9 Oil film profiles (Amplitude ratio = 1.5 at end of cycle)

Table 4 Test conditions

Temperature	25 ± 0.5 °C
Oil	Poly-alpha-olefin oil (PAO)
Viscosity	411 mm ² /s @ 40 °C
Maximum contact pressure	0.37 GPa
Amplitude ratio	0.6–4.3
Maximum vibrating speed	2 to 30 mm/s
Slide-to-roll ratio Σ ^a	200 %
Speed of disk specimen V _D	0 mm/s

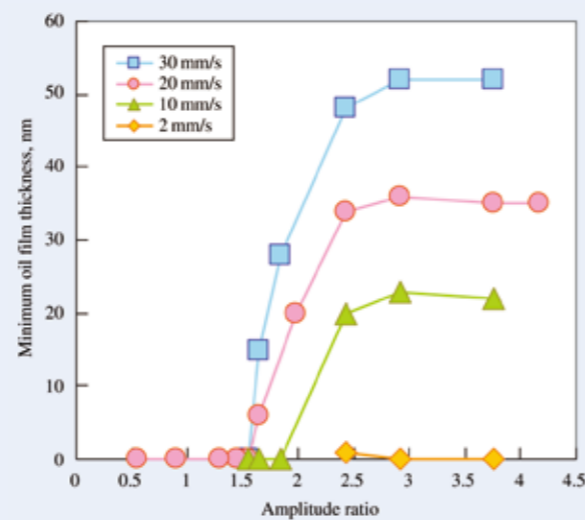


Fig. 10 Relationship between minimum oil film thickness and amplitude ratio for varying vibration speeds

than 1.6, the oil film fails to form and remains unaffected by vibrating speed. In fact, the critical amplitude ratio is constant even if the maximum vibrating speed is increased.

3.3 Influence of lubrication oil viscosity

In this section, the relationship between minimum oil film thickness and amplitude ratio under conditions of differing oil viscosities was investigated. Test conditions are shown in Table 5. The test results in Fig. 11 show that when the amplitude ratio was more than 1.6, an oil film formed, and that the higher oil viscosity, the thicker the oil film became. However, when the amplitude ratio was less than 1.6, the oil film failed to form, and the critical amplitude remained the same even if oil with a higher viscosity was used. These results coincided with the results shown in Fig. 10 where the maximum vibrating speed was changed.

Table 5 Test conditions

Temperature	25 ± 0.5 °C
Oil	Poly-alpha-olefin oil (PAO)
Viscosity	30 mm ² /s @ 40 °C 411 mm ² /s @ 40 °C
Maximum contact pressure	0.37 GPa
Amplitude ratio	0.6–4.3
Maximum vibrating speed	20 mm/s
Slide-to-roll ratio Σ ^a	200 %
Speed of disk specimen V _D	0 mm/s

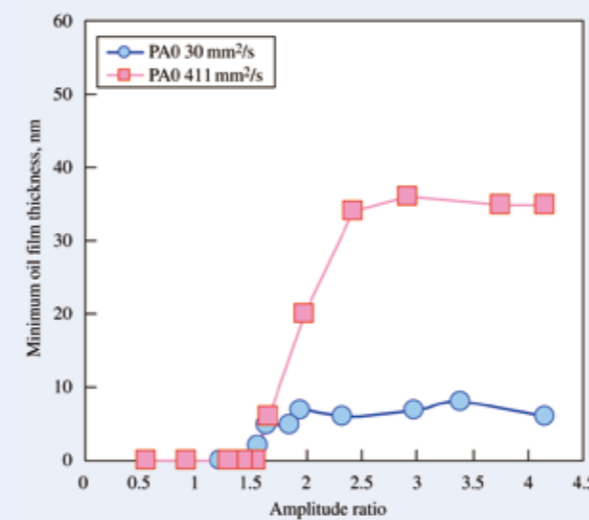


Fig. 11 Relationship between minimum oil film thickness and amplitude ratio for varying viscosities

3.4 Influence of maximum contact pressure

Next, the relationship between minimum oil film thickness and the amplitude ratio when the maximum contact pressure was changed from 0.29 GPa to 0.54 GPa was investigated. The test conditions are shown in Table 6. The test results illustrated in Fig. 12 show that the oil film was unable to appear when the amplitude ratio was less than 1.6. This means that the critical amplitude ratio was constant even if the diameter of the contact area changed. Further, Fig. 12 also shows that the minimum oil film thickness was almost the same even after changing the contact pressure. Generally, the influence of pressure on oil film thickness is much smaller than that of velocity and viscosity, and these results are also similar to it.

4. Discussion

The experimental results presented in this paper were

Table 6 Test conditions

Temperature	25 ± 0.5 °C
Oil	Poly-alpha-olefin oil (PAO)
Viscosity	411 mm ² /s @ 40 °C
Maximum contact pressure	0.29 to 0.54 GPa
Amplitude ratio	0.6–4.3
Maximum vibrating speed	20 mm/s
Slide-to-roll ratio Σ ^a	200 %
Speed of disk specimen V _D	0 mm/s

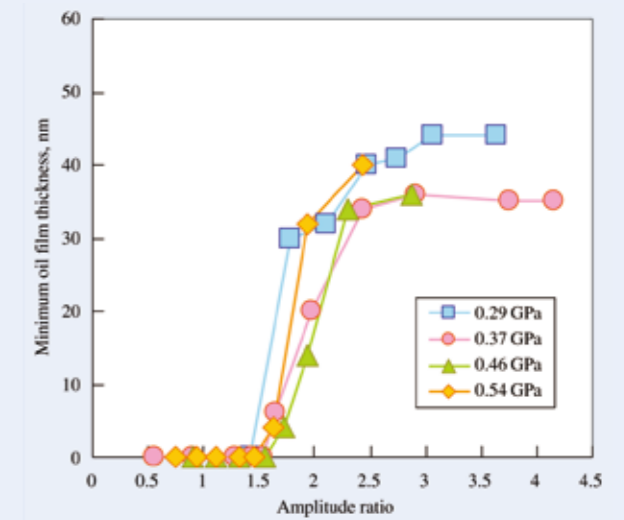


Fig. 12 Relationship between minimum oil film thickness and amplitude ratio for varying contact pressures

used to determine the minimum oil film thickness under pure sliding EHL point contacts after changing the amplitude ratio. The test results presented in Fig. 8 show that the oil film was unable to form when the amplitude ratio was small. However, after increasing the amplitude ratio to more than 1.6, the oil film began forming. Test results presented in Figs. 10–12, also show that the critical amplitude ratio was 1.6, even after vibrating speed, lubricating oil viscosity, or contact pressure were changed. Why the oil film was unable to form when the amplitude ratio was less than 1.6 is discussed below.

An EHL theory based on Reynolds equation was applied, which asserts that there is no fluid-slip at the wall (see below):

$$\frac{\partial}{\partial x} \left(\frac{\rho h}{12\eta} \frac{\partial p}{\partial x} \right) + \frac{\partial}{\partial y} \left(\frac{\rho h}{12\eta} \frac{\partial p}{\partial y} \right) = \frac{V_B + V_D}{2} \frac{\partial(\rho h)}{\partial x} + \frac{\partial(\rho h)}{\partial t}$$

where x, y is the Cartesian coordinates fixed in the Hertz contact area, ρ the density of lubrication oil, η the viscosity

of lubrication oil, p the pressure, h the oil film thickness, t the time, V_B the velocity of fluid on ball specimen surface, and V_D the velocity of fluid on disk specimen surface.

Here, the left side of above equation is negligible in an EHL contact area; thus the above equation becomes the equation below.

$$\frac{V_B + V_D}{2} \frac{\partial(\rho h)}{\partial x} + \frac{\partial(\rho h)}{\partial t} \approx 0$$

The solution to the above partial differential equation has the following form:

$$h(x, y, t) \approx h\left(x - \frac{V_B + V_D}{2} t, y\right)$$

Here, $V_D = 0$ mm/s in this paper. Therefore, in a high surface-pressure environment, such as that which is found under EHL, lubrication oil is introduced into the contact area at the average speed of the two sliding surfaces. In other words, the lubrication oil must be introduced to the whole contact area initially when the amplitude ratio is more than 2.0. Ikeuchi et al. had already determined that the length of minimum sliding distance for non-contact conditions was twice the length of initial contact width [2]. However, this condition applies only to a line contact. Fig. 13 illustrates the point contact area of a ball specimen. Compared to the contact length D of line segment a-a' near the center of the contact area, contact length D' of line segment b-b', which is the perimeter of line segment a-a', is shorter. Therefore, for example, even though the amplitude ratio at line segment a-a' is less than 2.0, the amplitude ratio of line segment b-b' likely becomes more than 2.0.

Fig. 14 shows the oil film profile of line segments a-a' and b-b' when amplitude ratio was 1.4. Line segment b-b' is positioned apart from line segment a-a' by 100 μm . This figure indicates that even though the oil film does not form at line segment a-a', an oil film forms sufficiently at line segment b-b'. In a point contact, the oil film can be formed even if the amplitude ratio is less than 2.0 because the oil film can appear at line segment b-b' and support the load.

The critical amplitude ratio at which an oil film begins to form was roughly estimated by calculating the average

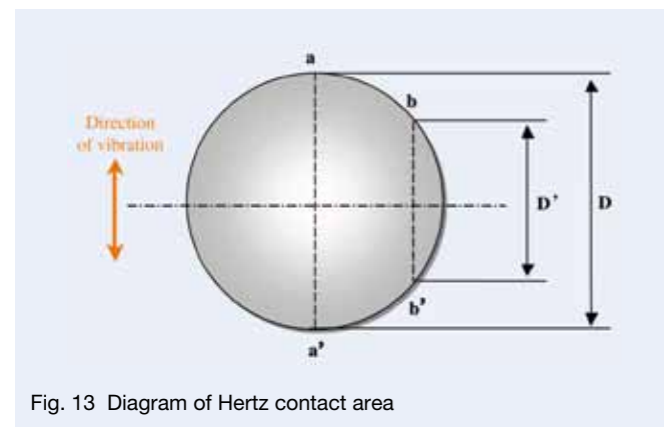


Fig. 13 Diagram of Hertz contact area

contact length of D_A because the contact length differs depending on the position like the differences of line segments a-a' and b-b' as shown in Fig. 13. In other words, a point contact was regarded as a line contact. Contact length $2y$ (Fig. 15) at each x -coordinate can be indicated as follows:

$$2y = 2\sqrt{\left(\frac{D}{2}\right)^2 - x^2}$$

Accordingly, the average contact length of D_A is indicated as follows:

$$D_A = \frac{2}{D} \int_0^{D/2} 2y dx = \frac{4}{D} \int_0^{D/2} \sqrt{\left(\frac{D}{2}\right)^2 - x^2} dx = \frac{\pi D}{4}$$

Here, the oil film begins to form when the amplitude ratio is more than 2.0 under a line contact.

$$\frac{A}{D_A} = \frac{4A}{\pi D} \geq 2.0$$

$$\therefore \frac{A}{D} \geq \frac{\pi}{2} \approx 1.6$$

Therefore, an oil film can appear under pure sliding EHL point contacts when the amplitude ratio is more than $\pi/2$ (nearly equal to 1.6), which closely coincides with our test results. In addition, this calculation result shows that the critical amplitude ratio is not affected by the speed maximum vibrating speed, the lubricating oil viscosity, or the maximum contact pressure.

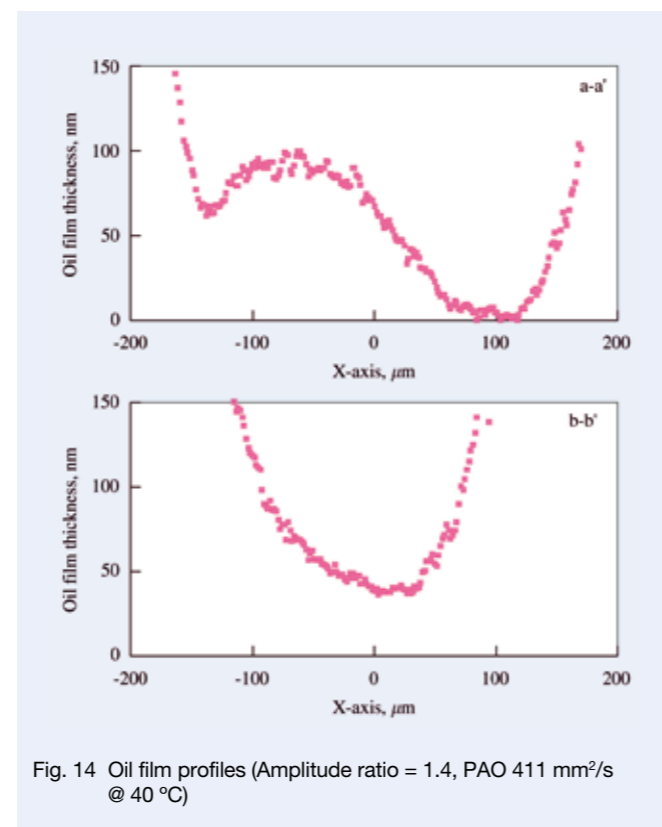


Fig. 14 Oil film profiles (Amplitude ratio = 1.4, PAO 411 mm²/s @ 40 °C)

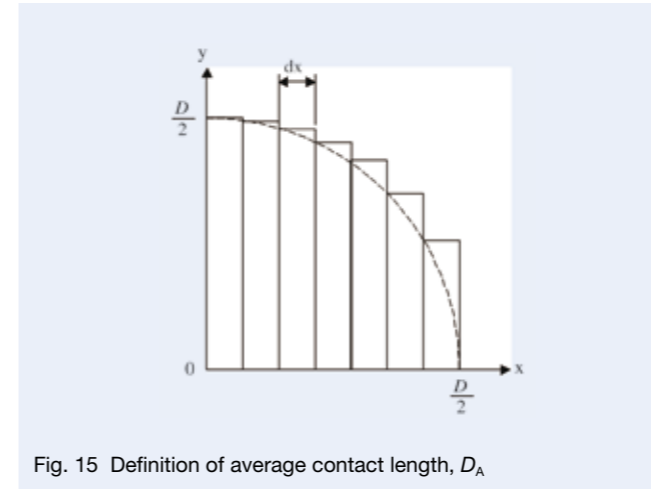


Fig. 15 Definition of average contact length, D_A

5. Conclusion

The results of investigations that have been presented in this paper verify the existence of a critical amplitude ratio at which point an oil film begins to form under pure sliding EHL point contacts with minute vibrating movements. The findings obtained in this research are summarized as follows:

1. A critical amplitude ratio exists at which point an oil film will form under conditions of minute vibrating in EHL. In other words, the oil film collapses or disappears when the amplitude is less than 1.6.
2. When exceeding the critical amplitude ratio, the oil film can appear because it can be introduced to whole contact area. And then, the oil film is retained as a result of the squeeze film effect even when the ball specimen is halted at the end of a cycle where sliding speed is 0 mm/s.
3. The critical amplitude ratio is 1.6 under sliding EHL point contacts irrespective of changes in the maximum vibrating speed, lubricating oil viscosity, or maximum contact pressure.
4. The critical amplitude ratio for a given point contact was determined by calculating the average contact length D_A , which changes according to the location of the point contact. The calculated result was nearly equivalent to our test results.

References

- [1] Ichimaru K, Optimization of Reynolds equation and application of CIP method for analysis of mixed elastohydrodynamic lubrication. *Jpn J Tribol* 2006; 51(4): 461–74.
- [2] Ikeuchi K, Fujita S, Ohashi M, Analysis of fluid film formation between contacting compliant solids. *Tribol Int* 1998; 31(10): 613–8.
- [3] Kalin M, Vizintin J, The tribological performance of DLC coatings under oil-lubricated fretting conditions. *Tribol Int* 2006; 39(10): 1060–7.

- [4] Kaneta M, Takeshima T, Togami S, Nishikawa H, Stribeck curve in reciprocating seals, In: *Proceedings of the 18th International Conference on Fluid Sealing*; 2005. p. 333–47.
- [5] Sugimura J, Okumura T, Yamamoto Y, Spikes HA, Simple equation for elastohydrodynamic film thickness under acceleration. *Tribol Int* 1999; 32(2): 117–23.
- [6] Glovnea RP, Spikes HA, Elastohydrodynamic film collapse during rapid deceleration: part 1—experimental results. *Trans ASME J Tribol* 2001; 123: 254–61.
- [7] Glovnea RP, Spikes HA, Elastohydrodynamic film collapse during rapid deceleration: part 2—theoretical analysis and comparison of theory and experiment. *Trans ASME J Tribol* 2001; 123: 262–7.
- [8] Wang J, Hashimoto T, Nishikawa H, Kaneta M, Pure rolling elastohydrodynamic lubrication of short stroke reciprocating motion. *Tribol Int* 2005; 38(11–12): 1013–21.
- [9] Jang S, Transient elastohydrodynamic lubrication film thickness in sliding and rolling line contacts. *J Mech Sci Technol* 2008; 22: 946–56.
- [10] Messé S, Lubrecht AA, Approximating EHL film thickness profiles under transient conditions. *Trans ASME J Tribol* 2002; 124: 443–7.
- [11] Izumi N, Tanaka S, Ichimaru K, Morita T, Observation and numerical simulation of oil-film formation under reciprocating rolling point contact. *Tribol Interface Eng Series* 2003; 43: 565–72.
- [12] Johnston GJ, Wayte R, Spikes HA, The measurement and study of very thin lubricant films in concentrated contacts. *Tribol Trans* 1991; 34(2): 187–94.

Development of ROBUSTSLIM Series of Low-Profile Angular Contact Ball Bearings for Swivel Units in Machine Tools

Mitsuho Aoki
Industrial Machinery Bearing Technology Center

ABSTRACT

Machine tools with swivel units, such as five-axis machining centers and multi-tasking CNC lathes, have increased in order to process complicated works. In recent years, with the use of direct-drive motors, processing systems with a higher degree of accurate control for swivel units have been put into practical use.

Typically, crossed roller bearings had been mounted to conventional swivel units, but such bearings were insufficient for direct-drive systems in terms of frictional torque and runout accuracy.

At a recent JIMTOF trade show, NSK released the ROBUSTSLIM series of low-profile angular contact ball bearings (ROBUSTSLIM) for use in swivel units used in machine tools. The features of this new product are high runout accuracy, high moment rigidity, and low frictional torque. Runout accuracy of the ROBUSTSLIM has been improved to one-third and dynamic frictional torque of the ROBUSTSLIM is 20 % less in comparison with conventional crossed roller bearings.

The ROBUSTSLIM is expected to contribute to higher accuracy and greater performance of five-axis machining centers and multi-tasking CNC lathes.

1. Introduction

In recent years, five-axis machining centers and multi-tasking CNC lathes have been universally used for the purpose of processing complicated works and consolidating work processes.

In addition, as a result of performance improvements of CNC equipment or computer aided manufacturing (CAM), advanced processing such as processing with simultaneous five-axis control for the purpose of high-quality finishing of three-dimensional free-form die surfaces has been increasing.

NSK developed the ROBUSTSLIM of high-precision low-profile angular contact ball bearings (Photo 1) as bearings for swivel units of five-axis machining centers and multi-tasking CNC lathes, which were introduced to the market at JIMTOF 2008.

This article introduces the product concept and



Photo 1 The ROBUSTSLIM series of low-profile angular contact ball bearing

performance evaluation test results of the ROBUSTSLIM.

2. Background of Development

2.1 Technological trends of five-axis machining centers

When looking at the transition of five-axis machining centers exhibited at JIMTOF, their numbers have been notably increasing since 2000. In fact, their numbers have increased by approximately four times and their ratio to machining centers has increased by five times as of 2008. Another trend at JIMTOF 2010 was represented by an increase in the number of five-axis machining centers according to research conducted by NSK (Figure 1). Thus, five-axis machining centers are becoming more and more commonplace throughout the industry.

Large drive torque and locking functionality are required to endure the cutting loads acting on the swivel unit of five-axis machine tools and multi-tasking CNC lathes. Therefore, worms and worm wheels with high reduction ratios were typically adopted for the drive system of swivel units.

However, this mechanism faces accuracy issues when attempting to perform high-precision processing with simultaneous five-axis control because it suffers from generation of delay, deflection, and backlash within the transfer system; and because the mechanism uses indirect feedback control with an encoder that is located on the line of the servo motor shaft.

Therefore, swivel units combining direct drive motors (DD motors) and a brake mechanism have become practical in recent years because DD motors enable high-

precision control since they are free of any loss in the transfer system, and since they use direct feedback control of the encoder, which is integrated into the output shaft.

In addition, DD motors have enabled high-speed rotation of swivel units at speeds that are impossible to achieve with worm drives due to their large reduction ratio. Therefore, many new types of multi-tasking machining centers have been featured, which have an additional functionality of turning of the main spindle by a method of high-speed rotation of the rotary table (Figure 1).

2.2 Functions required of bearings for swivel units

Crossed roller bearings have been generally used for swivel units of five-axis machining centers. These bearings are well suited for supporting swivel units on one side because of their compact size and high moment rigidity. Crossed roller bearings also have been widely adopted for the tilting shaft of the table used in five-axis machining centers with trunnion units because they offer greater compactness although their high moment rigidity is not as important since the tilting shaft can be supported on both sides.

However, crossed roller bearings have large frictional torque and a large irregular deviation of torque due to high sliding speeds generated on the rolling contact surface because of their structure. Bearings for DD motors are desirable for the smoothest possible rotation and their bearing torque should be as low as possible for maintaining high-accuracy positioning control since drive torque of a DD motor is less than that of worm-type drive systems.

In addition, since cylindrical rollers are used as the rolling elements in crossed roller bearings, they have limitations in terms of runout accuracy. DD motor bearings for swivel units require higher runout accuracy when such motors are used for the purpose of obtaining higher accuracy.

2.3 Product development of the ROBUSTSLIM

We considered that angular contact ball bearings were

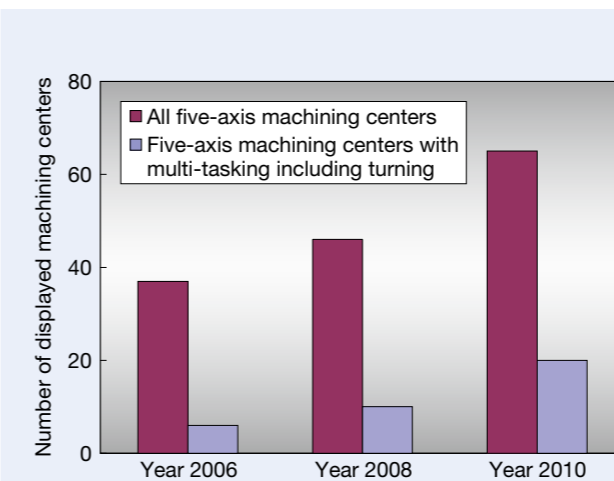


Fig. 1 Transition of five-axis machining centers displayed at JIMTOF

most suitable for bearings of future swivel units based on the background information discussed previously, resulting in the development of the ROBUSTSLIM high-precision low-profile angular contact ball bearings.

The swivel unit with a DD motor corresponds to a main spindle with an integrated internal motor found among main spindles. Gear drive systems or belt drive systems were previously the mainstream drive systems for the main spindle, but direct-drive units (also referred to as built-in motors) have become the mainstream drive unit for many spindles with higher speed and higher accuracy. Basic functions required of main spindle bearings are high runout accuracy, sufficient rigidity to bear cutting loads, low heat generation as a result of low-torque performance, and high rotational speed capability. The most suitable type of bearing for satisfying these requirements is the angular contact ball bearing, and it is commonly used in current applications.

Anticipating that the swivel unit would technologically trace the same trends of the main spindle in regard to improved performance and cost reductions of the DD motor in the future, NSK developed the ROBUSTSLIM as the most suitable bearing for swivel units of highly accurate five-axis machining centers.

3. Features

3.1 High runout accuracy

3.1.1 Runout accuracy required for swivel units

It is known that the quality grade of a worked surface deteriorates if non-repetitive runout (NRRO: asynchronous radial runout: deviation of each shaft center trace per each cycle of rotation) of a bearing is large in the case of main spindles for milling and for turning²⁾. This is because theoretical geometry of the roughness of a worked surface loses shape as the trace point of the tool or work per cycle does not always pass through the same position, and as a result, the turning surface becomes uneven (Figure 2).

Meanwhile, runout accuracy of a swivel unit is not necessary for swivel units in a five-axis machining center if the work is processed after being positioned and clamped.

However, simultaneous processes using five axes have been increasing recently for the purpose of improving

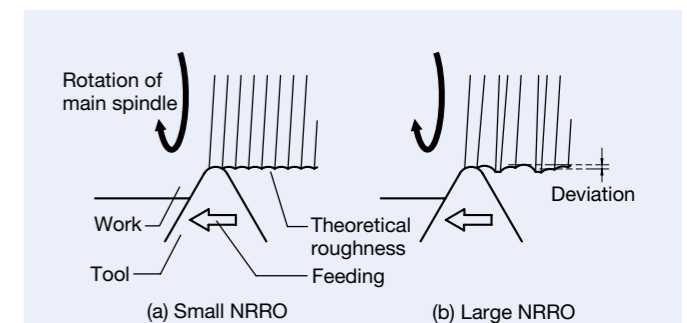


Fig. 2 Relationship between surface roughness of work and NRRO

the quality grade of a worked surface by maintaining the ball-end mill at a constant attitude against the worked surface. When processing with a rotating swivel unit, the higher the runout accuracy of the swivel unit, the better; especially regarding NRRO, the smaller the better. The reason is the same for main spindles; especially when aiming for higher processing accuracy after adopting a DD motor for the drive system, runout accuracy of the bearing becomes increasingly critical.

3.1.2 Runout accuracy of the ROBUSTSLIM

Runout accuracy of the bearing depends on raceway surface accuracy of the inner and outer rings, diameter variation in each rolling element set within a bearing, and any deviation from the spherical or circular form of each rolling element, and the extent of uneven distance during operation between rolling elements next to each other. Among them, accuracy of the rolling element highly influences NRRO.

With crossed roller bearings, it is difficult to improve accuracy of diameter variation in a rolling element set and accuracy of roundness (deviation from a circular form) of each rolling element, which greatly influences NRRO, since cylindrical rollers were used as rolling elements for crossed roller bearings that are commonly used for swivel units.

The newly developed ROBUSTSLIM has therefore adopted the same high-precision balls as balls used for main spindles as rolling elements. As these high-precision balls are used for many bearings for main spindles, it was easy to adopt them and manufacture various sizes of balls as rolling elements for the ROBUSTSLIM.

This was one critical advantage of adopting the balls for

the rolling elements.

We built a test rig specifically for measuring radial runout accuracy as illustrated in Figure 3, and measured radial runout accuracy of the ROBUSTSLIM. Measuring conditions are listed in Table 1.

Measuring results of radial runout accuracy are shown in Figure 4 as Lissajous figures. The ROBUSTSLIM showed a 1/3 improvement of less runout, and a 1/5 improvement of less NRRO in comparison with those of crossed roller bearings.

3.2 High moment rigidity

3.2.1 Rigidity features required for swivel units

There are various types of five-axis machining centers according to positioning of the two swivel axes in five axes. Machining centers are classified mainly into three types: two swivel axes on the work side; two swivel axes on the main spindle side; and one swivel axis on the work side with one swivel axis on the main spindle side. Furthermore, there are two types of support structures used for the swivel unit: the single type, where shaft support is positioned at one end, and the double support type, where shaft support is positioned at both ends. Rotary tables for machining centers generally have a single-type support structure (Figure 5).

Whereas the bearing for a single-type support of a swivel unit is subjected to moment load, the bearing requires high moment rigidity performance. This is the advantage of crossed roller bearings, which have commonly been used for swivel units.

Table 1 Measuring conditions

Bearing type		The ROBUSTSLIM	Crossed roller bearing
Bearing dimensions	Outside diameter × Bore × Width	∅215 mm × ∅170 mm × 27 mm	∅206 mm × ∅130 mm × 30 mm
	Pitch circle diameter of rolling element	∅192.5 mm	∅190 mm
Rotational speed when measuring		15 rpm (outer ring rotation)	
Number of rotations during measuring		8 rotations	
Distance between bearing and measuring point		80 mm	

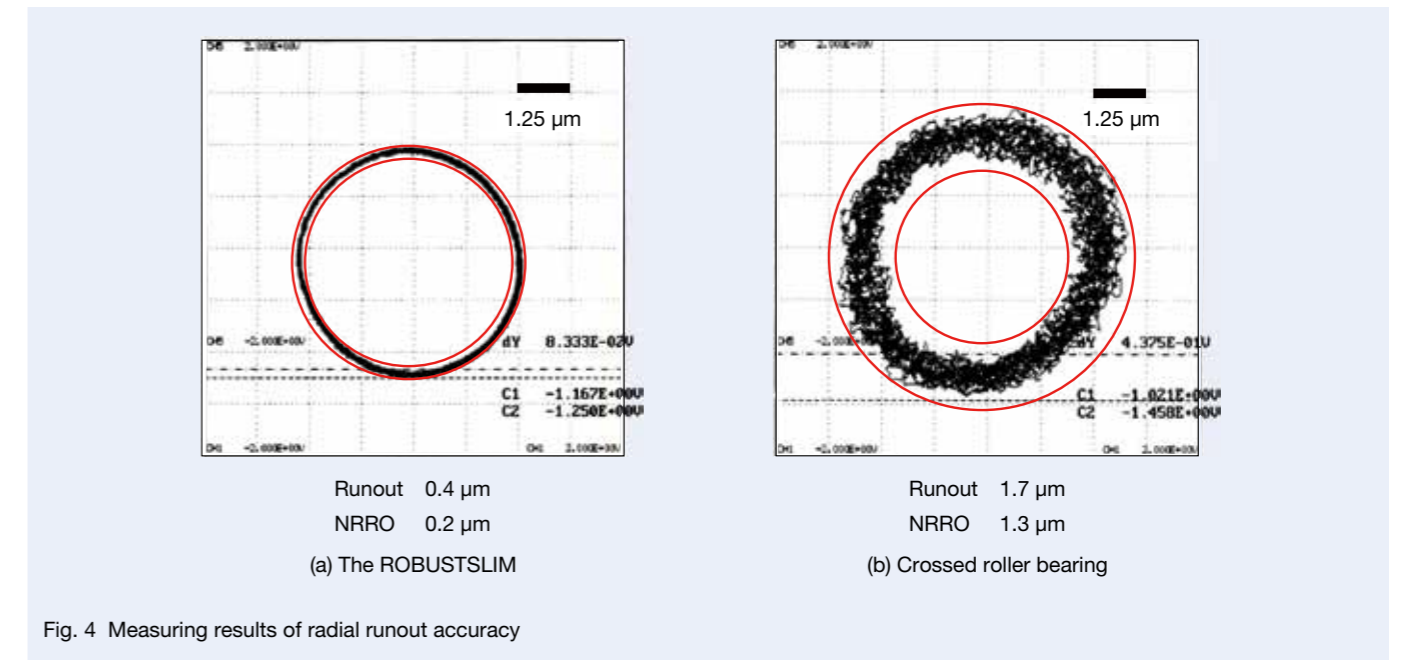


Fig. 4 Measuring results of radial runout accuracy

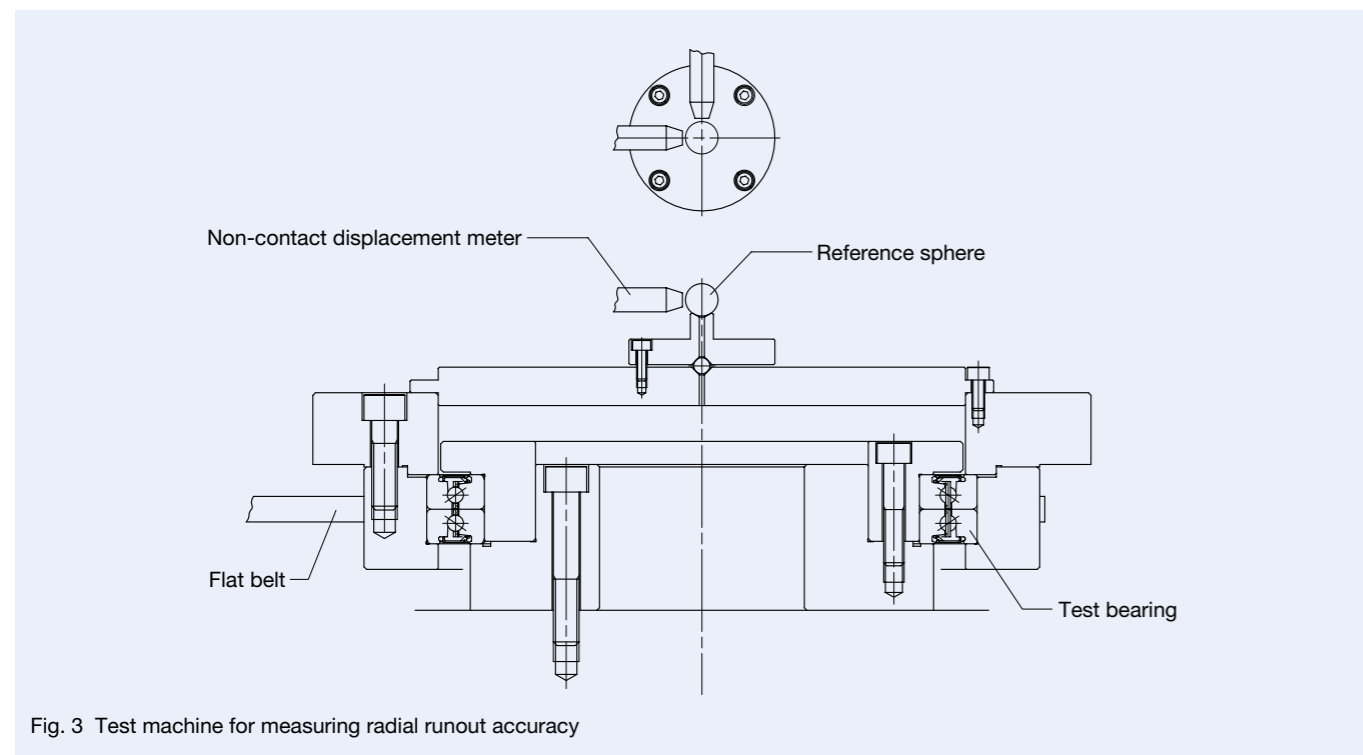


Fig. 3 Test machine for measuring radial runout accuracy

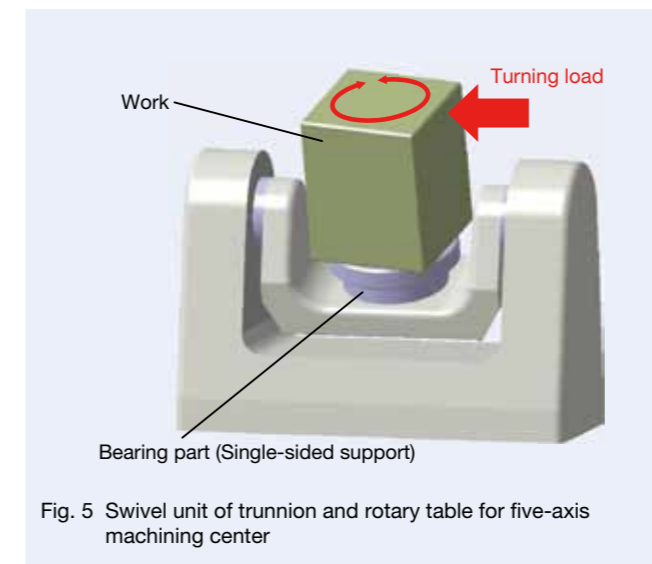


Fig. 5 Swivel unit of trunnion and rotary table for five-axis machining center

3.2.2 Moment rigidity of the ROBUSTSLIM

In designing and developing the ROBUSTSLIM, we aimed for an equivalent level of moment rigidity as

crossed roller bearings. Whereas moment rigidity of the ROBUSTSLIM is insufficient in terms of general designs, a back-to-back arrangement of angular contact ball bearings has been applied to the ROBUSTSLIM in order to improve runout accuracy. Therefore, we reduced the diameter of the balls and more than doubled the number of balls used in the bearing.

These changes in diameter and number of balls resulted in achieving a level of moment rigidity on a par with crossed roller bearings based on calculations. Moment rigidity was then measured to confirm the influence of moment load on deformation of the inner and outer rings.

Figure 6 shows the structure of the testing machine for measuring moment rigidity, and Photo 2 shows the testing machine. The bearings used for testing were the same as the bearings listed in Table 1. Because rigidity in design could not be generated without preloading the bearing, measurements were taken with the bearing mounted to a spindle and housing. The amount of deformation of the spindle and housing was measured beforehand, and that amount of deformation was eliminated from the calculations.

Figure 7 shows the measured results of moment rigidity of the bearing obtained by the means previously

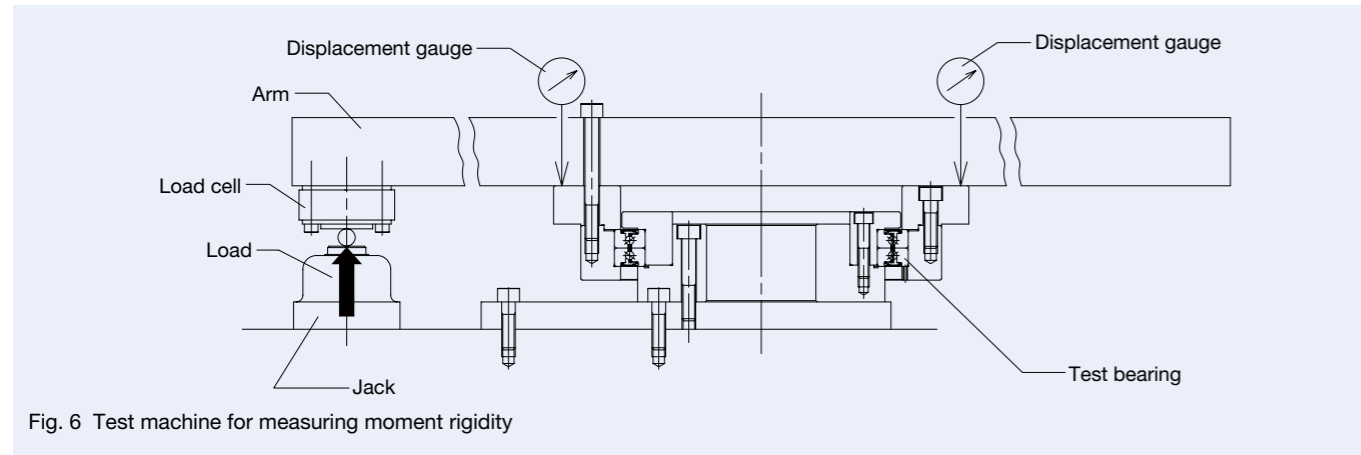


Fig. 6 Test machine for measuring moment rigidity

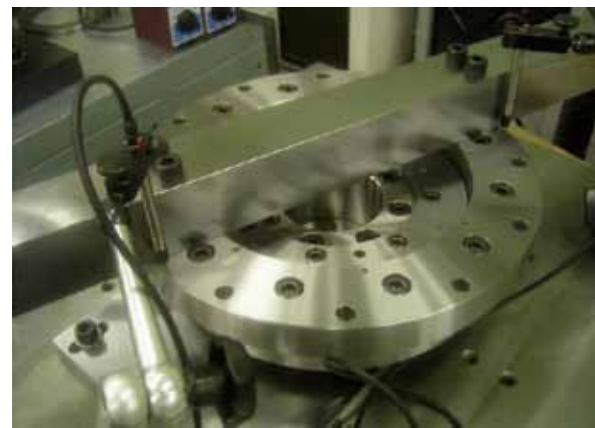


Photo 2 Test machine for measuring moment rigidity

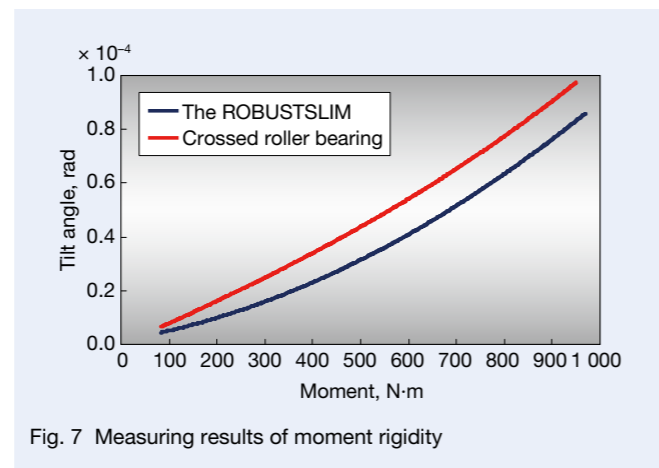


Fig. 7 Measuring results of moment rigidity

mentioned. As a result, it was confirmed that the moment rigidity of the ROBUSTSLIM is on a par with that of the crossed roller bearing as we had aimed for.

3.3 Low frictional torque

3.3.1 Frictional torque of bearings for swivel units

Reducing frictional torque of bearings has been essential to swivel units used in five-axis machining centers due to the growing application of built-in DD motorized swivel units.

Very large drive torque is obtainable where the swivel unit serves as the output shaft in conventional drive systems using worms and worm wheels because the reduction ratio is large in those systems. Therefore, frictional torque of the bearing for the swivel unit has not been a problem to be addressed. In addition, servomotor control for countering fluctuation of applied torque is simple since cutting forces acting on the output shaft do not act on the motor shaft as reactionary forces because of the self-locking function of the worm gear. When processing with simultaneous five-axis control using a DD motor, positioning control with higher precision and a higher degree of responsiveness became mandatory as the applied torque is received directly from the DD motor.

Therefore, any uncertainty such as fluctuations in bearing frictional torque should be eliminated from the system to the greatest degree possible.

3.3.2 Frictional torque of the ROBUSTSLIM

Since the ROBUSTSLIM is an NSK subset of angular contact ball bearings, they have a slower sliding speed within bearings than that of crossed roller bearings. As a result of slow sliding, frictional running torque of the ROBUSTSLIM is theoretically low; however, irregular deviation of this torque is difficult to predict theoretically.

We thus built a testing machine for evaluating frictional running torque as shown in Figure 8, and measured frictional running torque of the ROBUSTSLIM. The table part of a processing machine was represented by the construction of only test bearings, which were directly connected to a motor with flexible couplings through a dynamic-torque measuring instrument. The same bearings as listed in Table 1 were used as the test bearings. Rotational speed was set at 100 rpm.

According to the test results, it was found that frictional running torque of the ROBUSTSLIM was approximately 20% less and irregular deviation of torque was significantly improved compared with those of crossed roller bearings, as shown in Figure 9.

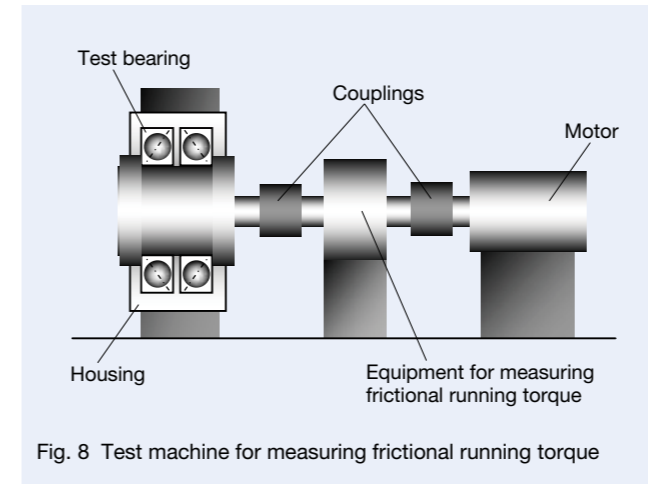


Fig. 8 Test machine for measuring frictional running torque

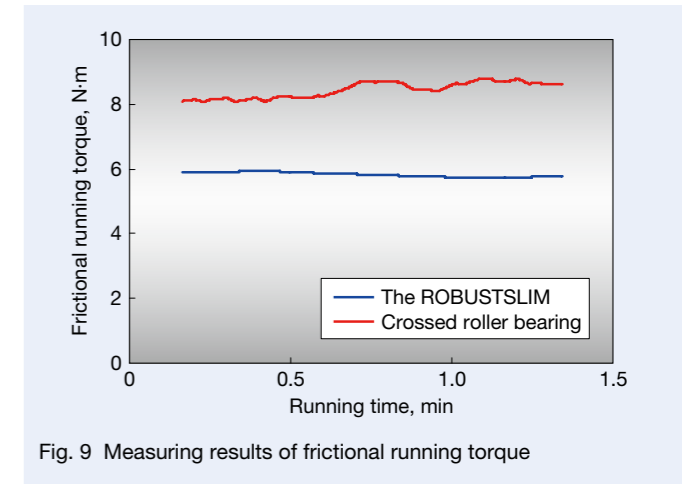


Fig. 9 Measuring results of frictional running torque

3.4 Compact design

Adopting a design that uses plural bearings and widens the span between them for ensuring moment rigidity is not an option for a swivel unit as the size of this spindle cannot extend in the axial direction, although it is possible with a main spindle. Therefore, crossed roller bearings are often used for swivel units because crossed roller bearings facilitate increased moment rigidity without widening the size in the axial direction with alternating and reversed locating of roller contact angles in a single row groove.

Considering this, and utilizing small ball diameters, the axial-direction width of a single row of the ROBUSTSLIM is approximately 35% less than that of a standard design. As a result, the ROBUSTSLIM with two rows is capable of facilitating nearly the same width in the axial direction as that of a single row of crossed roller bearings (Figure 10).

Regarding bore and outside diameters, the 78 series of bearings are conventionally used as the minimum dimensional series within regularly specified dimensional series. The 78 series of bearings are a so-called thin cross-section type and are very compact, but the rigidity of the inner and outer rings is relatively low. The ratio of cross-section thickness and diameter of the ROBUSTSLIM inner and outer rings achieves the same ratio as that of

the 79 series, which is one degree larger in size than the 78 series, by means of designing the ball diameter to be smaller. This design ensures the necessary accuracy and rigidity of the bearing.

4. Conclusion

It is considered that the precision of five-axis machining centers will be improved to even higher levels in the future through the use of DD motors for swivel units. The ROBUSTSLIM series of low-profile angular contact ball bearings introduced in this article is the most suitable bearing for this type of application.

Meanwhile, it is anticipated that the number of five-axis machining centers with multi-tasking capability including turning will increase by means of increased rotational speeds, which is another advantage of the DD motor. In this case, it is a big challenge for bearings to ensure the features of both high rigidity and high-speed rotation.

The ROBUSTSLIM is a duplex bearing of angular contact ball bearings and has the advantage of being preloaded for ensuring control in a relatively simple way. We will continue to develop new bearing products that respond to the future needs of users by incorporating these superior points.

References

- 1) S. Shimizu, H. Sakamoto, S. Yaoi, "New technological trend of cutting machine tools," *Machines and Tools*, 53-1 (2009) 28-29.
- 2) Y. Katsuno, S. Yoshikawa, O. Iwasaki, "Super Precision Cylindrical Roller Bearings," *NSK TECHNICAL JOURNAL* No. 673 (2002) 49-53.

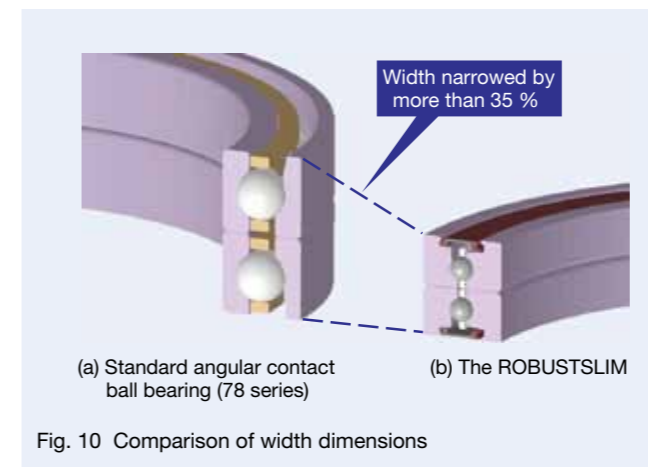


Fig. 10 Comparison of width dimensions



Mitsuho Aoki

Smear-Resistant Spherical Roller Bearings for Papermaking Machinery

Generally, spherical roller bearings are widely adopted for the rolls used in the papermaking process of papermaking machinery. The operating environment of these bearings exposes them to water, high temperatures, high speeds, and sudden changes from light loads to heavy loads; that is, they are used under severe operating conditions. Major types of damage involving bearings include wear, smearing (initial stage of seizure), flaking, and fracture. Though the types of damage like wear and smearing are mild, if a bearing with such damage is not dealt with, the damage will occasionally lead to flaking or fractures that significantly reduce bearing performance.

NSK has newly developed a smear-resistant spherical roller bearing that remarkably prevents the generation of smearing, which poses a risk that could lead to serious bearing trouble.

1. Smear-Resistant Properties

(1) Adopting originally developed DLC^{a)} coating

The newly developed smear-resistant spherical roller bearing is treated with NSK's originally developed diamond-like carbon coating (NSK DLC coating) on the rolling contact surface of the rollers (Photo 1).

DLC coating, which is a type of solid lubricant, has been regarded as superior in terms of its wear-resistant and seizing-resistant properties. However, DLC coating has had to face the challenge of durability with respect to its capability to adhere to the substrate since the application using bearings (Figure 1) is subjected to high pressures of several GPa.

A mid-layer is added in addition to a foundation layer and a composite carbon layer for the NSK DLC coating, and a structure that is gradually changed at the atomic



Photo 1 Smear-resistant spherical roller bearing for papermaking machinery

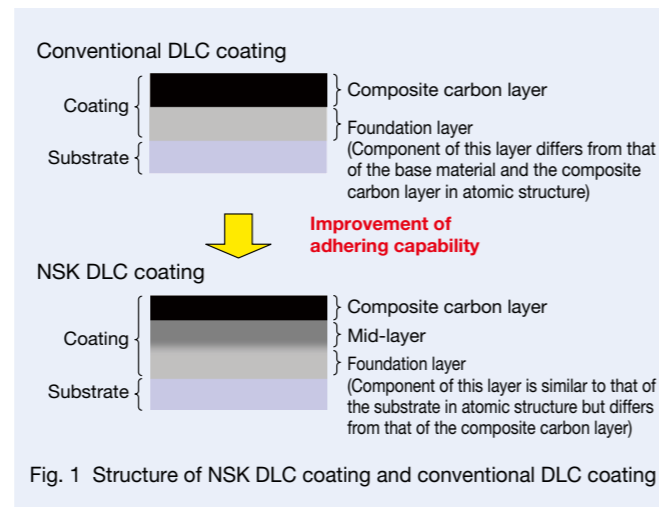


Fig. 1 Structure of NSK DLC coating and conventional DLC coating

level from the foundation layer to the composite carbon layer has been adopted for the mid-layer (Figure 1). Moreover, the component of the foundation layer is selected so as to be similar to the components of the substrate in atomic structure. As a result, adhering capability of this coating is highly advanced and the durability has been successfully improved to a remarkable degree.

(2) Improving smearing resistance

(a) Twin-disk test

A rolling-contact test was conducted under boundary lubrication conditions in addition to sliding contact conditions in which the speeds of two disk test pieces are set differently (Figure 2).

Figure 3 shows the test results. Smearing generates after approximately 1.5 hours in the test piece without NSK DLC coating. Conversely, smearing does not generate on the test piece with NSK DLC coating even after almost 200 hours of testing.

(b) Bearing rotating test

Figure 4 shows the structure of the bearing rotating test machine. Both types of spherical roller bearings, which included NSK DLC coating on the rolling contact surface of the rollers and a spherical roller bearing without NSK DLC coating on the rollers were used for the test in the bearing rotating test machine. Both bearings were tested under estimated conditions of light loads and boundary lubrication. Table 1 lists the test results. Smearing generated on the raceway of the outer ring and rolling contact surfaces of rollers in the bearing without NSK DLC coating. However, smearing was not generated on any surfaces of the inner ring, outer ring, or rollers in the bearing with NSK DLC coating.

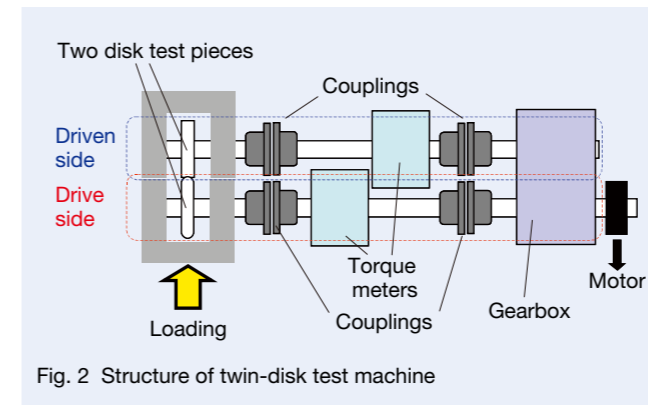


Fig. 2 Structure of twin-disk test machine

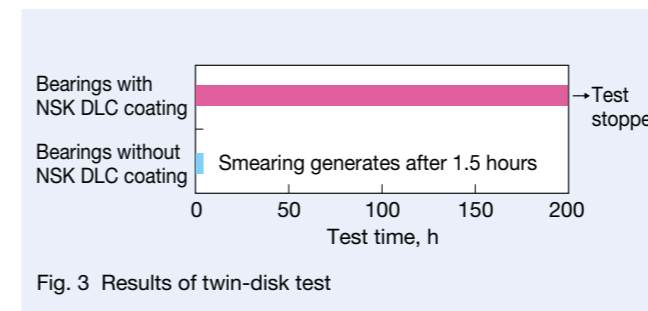


Fig. 3 Results of twin-disk test

2. Applications

This newly developed bearing is suitable for the following applications where the bearings have a high risk of smearing when they are used under light loads.

- (1) Inner side bearings for suction rolls in press process parts (Figure 5)
- (2) Bearings for soft calendar rolls in calendar process parts (Figure 6)

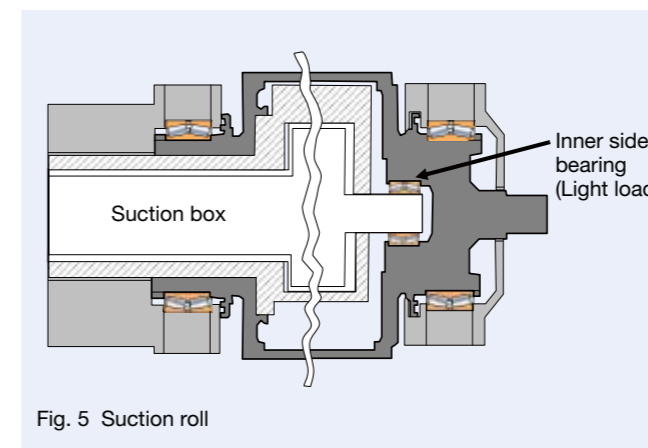


Fig. 5 Suction roll

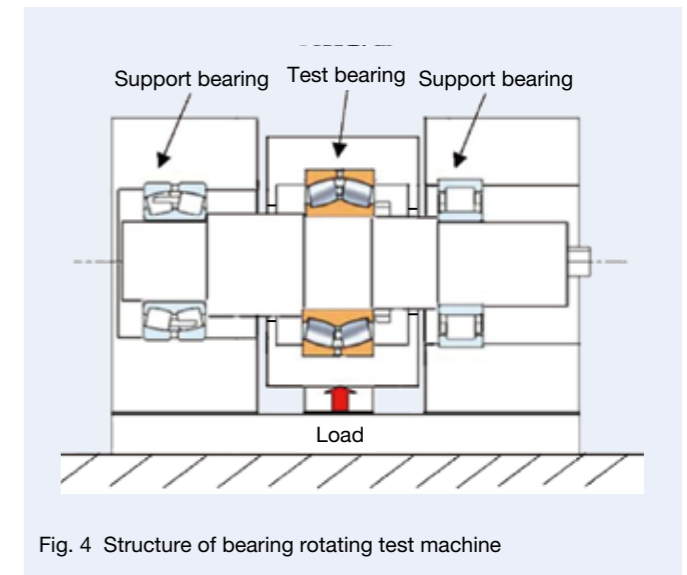


Fig. 4 Structure of bearing rotating test machine

Table 1 Results of bearing rotating test

	Outer ring raceway	Inner ring raceway	Rolling contact surface of rollers
Bearings without NSK DLC coating	Smearing occurred	No smearing	Smearing occurred
Bearings with NSK DLC coating	No smearing	No smearing	No smearing

3. Summary

Smear-resistant spherical roller bearings with NSK DLC coating are superior in durability and are expected to contribute to the stable operation of equipment of papermaking machinery and promote reduced maintenance requirements of such equipment.

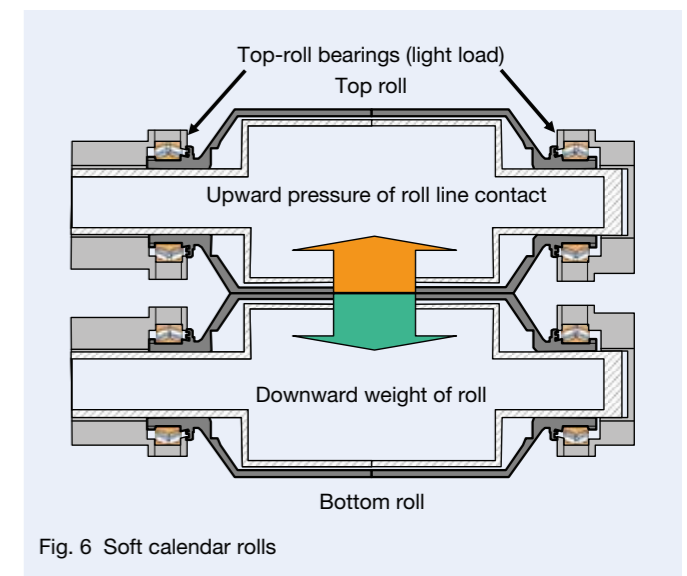


Fig. 6 Soft calendar rolls

^{a)} DLC: Hard coating mainly consisting of carbon (diamond-like carbon)

High-Performance Bearings for Satellite Attitude Control Reaction Wheels

The satellite attitude control reaction wheel is a device for controlling the attitude of a satellite by means of reaction torque that is generated when an inner rotating mass (flywheel) is accelerated or decelerated by a motor. Bearings used for satellite attitude control reaction wheels are one of the critical components that affect performance of the satellite attitude control reaction wheel. Such bearings are required to operate with minimal vibration and continuously perform stable rotation for a considerable length of time from 10 to 15 years while orbiting in space. In addition, the bearings are required to endure the vibration and shock during launch of the satellite from Earth and must endure extreme temperature fluctuations during orbit.

NSK has developed a high-performance bearing for satellite attitude control reaction wheels (Photo 1) that will contribute to lower vibrations, high-speed rotation, and high power torque transmission performance, in



Photo 1 A set of high-performance bearings for satellite attitude control reaction wheels

addition to higher reliability of conventional bearings. This newly developed bearing is the first product to be manufactured using Japanese technology.

1. Construction and Specifications

This high-performance bearing for satellite attitude control reaction wheels has achieved stable torque under conditions of minute amounts of lubricating oil using a highly reliable lubrication system. In addition, reduced vibration performance is ensured by adopting high-purity bearing material and high-precision balls with superior wear resistance.

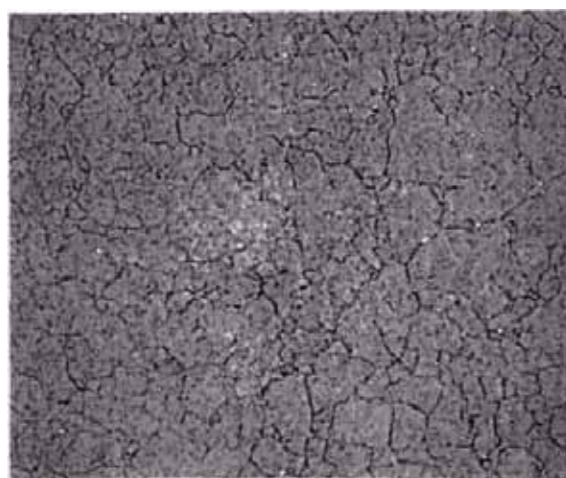
2. Features

(1) Technology towards high reliability

High-polymer synthetic oil is adopted as the lubrication oil. This oil is superior in terms of low evaporation properties, long-term stability, and lubrication properties. Additionally, the self-circulation lubrication system in which the proper amount of lubrication oil is impregnated to the cage makes it possible to supply a stable amount of lubrication oil in only minute quantities. Furthermore, a new cage has been developed with superior stability of ball motion as a result of optimizing cage dimensions and configuration.

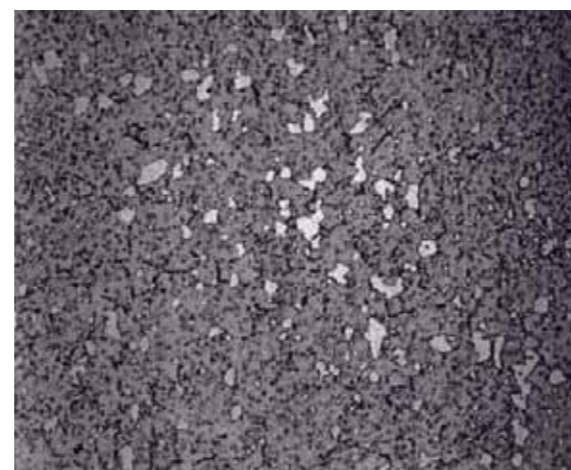
(2) Technology for reducing vibration

High-purity stainless steel with refined carbides is applied to the bearing rings, and an ultra-clean raceway surface is achieved by making full use of a proprietary, contaminant-free cleaning technology developed in-house for the raceway surfaces (Photo 2).



(a) High-purity stainless steel for newly developed bearings

25 μm



(b) Stainless steel for conventional bearings

25 μm

Photo 2 Micrographs of high-purity stainless steel and conventional stainless steel

In addition, balls with superior wear resistance have been improved using a special surface treatment process (Figure 1).

3. Applications

This high-performance bearing is intended for use as a support bearing (Figure 2) for the rotating mass of satellite attitude control reaction wheels.

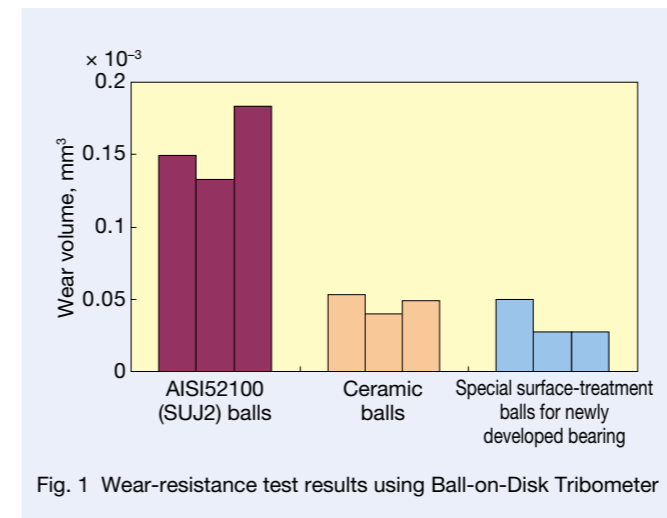


Fig. 1 Wear-resistance test results using Ball-on-Disk Tribometer

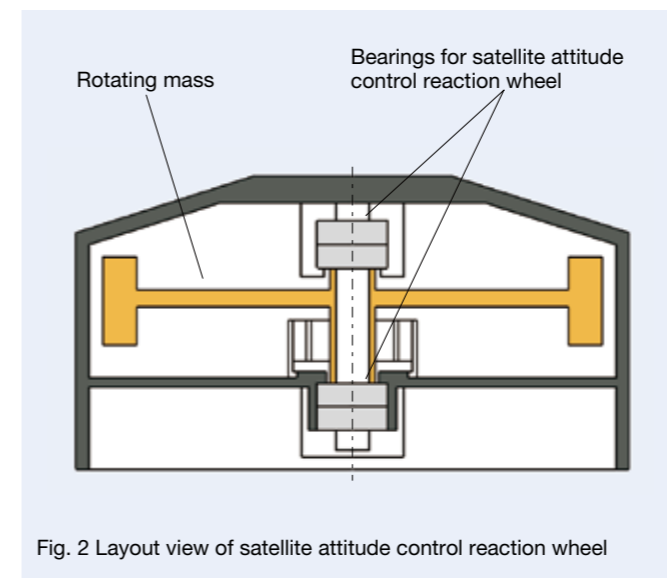


Fig. 2 Layout view of satellite attitude control reaction wheel

4. Summary

Mass production of the high-performance bearing for satellite attitude control reaction wheels has already reached the manufacturing stage. In the future, NSK will continue to work toward the development of bearings with lower costs and higher levels of performance based on technologies that have been cultivated through achievements made in the development of bearings for satellite attitude control reaction wheels using Japanese technology.

Slight-Preload Type RA Series Roller Guides of NSK Linear Guides

RA series roller guides were developed and commercialized in 2004 in response to the requirement of longer service life and higher rigidity of linear guides for equipment centering on machine tools. The RA series roller guide is the one series of NSK linear guides using rollers for the rolling elements of the linear guide. The RA series roller guide offers high-load capability and high rigidity that far exceed those of a ball guide. Therefore, because machinery such as liquid crystal display manufacturing equipment and carrier devices also require longer service life, the switch to roller guides from ball guides for these applications has progressed in recent years.

External loads of these applications are not as high as the loads of machine-tool applications, while the fluctuating loads are small. Thus, the need for rigidity is not as high as that of a machine tool. Preloading is applied to the roller guides in order to increase rigidity;



Photo 1 Slight-preload type RA series roller guide

however, excessive preload affects the service life of the roller guides. Furthermore, prolonging service life for such applications is also required because the required running distance of these applications is long compared with that of machine-tool applications.

Therefore, in optimizing the preload of roller guides, NSK developed the slight-preload roller guide in order to respond to the needs of further prolonging the life of liquid crystal display manufacturing equipment and carrier devices, and added this roller guide to the RA roller guide series (Photo 1).

1. Features

(1) Optimizing preload and achieving longer service life

If the external load is small, excessive preload conversely results in a shorter service life. By adopting an optimum preload, it is possible to achieve longer service life.

Table 1 lists the preloads of the slight-preload roller guide for the RA series. In addition, Figure 1 presents examples of calculated results for service life of slight-preload products and medium-preload products when external load is relatively small.

(2) Easy mounting to machinery tables

The slight-preload roller guide of the RA series has a large mounting tolerance, which facilitates ease of mounting the slight-preload roller guide to the table of machinery compared to the medium-preload product. This is especially suitable for applications such as carrier devices that require high-load capability but do not require high rigidity.

Table 2 lists the mounting tolerance of the slight-preload roller guide together with the medium-preload product.

Table 1 Preload for series lineup

Unit N

Type	High-load type		Super high-load type	
	Slight preload (Z1)	Medium preload (Z3)	Slight preload (Z1)	Medium preload (Z3)
RA25	880	2 920	1 060	3 540
RA30	1 170	3 890	1 430	4 760
RA35	1 600	5 330	2 020	6 740
RA45	2 780	9 280	3 480	11 600
RA55	3 870	12 900	5 040	16 800
RA65	6 300	21 000	8 640	28 800

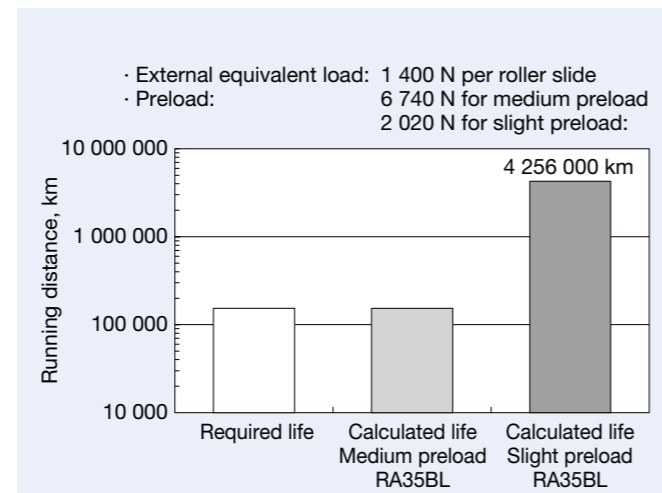
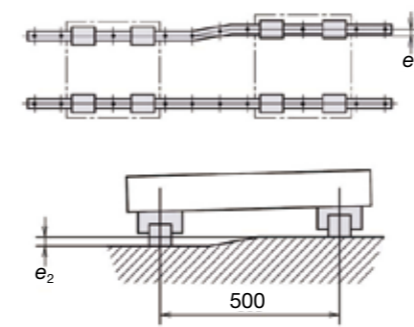


Fig. 1 Comparison of calculated service life

Table 2 Mounting tolerance of RA roller guide series



Unit μm

Type	Parallelism tolerance of two roller guides e_1		Height tolerance of two roller guides e_2	
	Slight preload (Z1)	Medium preload (Z3)	Slight preload (Z1)	Medium preload (Z3)
RA25	14	9	290 μm / 500 mm	150 μm / 500 mm
RA30	18	11		
RA35	21	13		
RA45	27	17		
RA55	31	19		
RA65	49	30		

Note: Mounting tolerance is determined according to calculation results and conditions. If an operating life were calculated to be more than 10 000 km when the load per roller slide is 10 % of the basic dynamic load rating, and the mounting error is assumed to be of a certain value, the value of the mounting error at that time is set as the mounting tolerance (rigidity of the machinery table is assumed to be infinite).

2. Specifications and Description of Model Number

Figure 2 shows an example of a model number of the slight-preload roller guide of the RA series.

In addition, Figure 3 shows the outline of specifications.

Example of model number: RA 35 1000 AN C 2 - ** P5 1

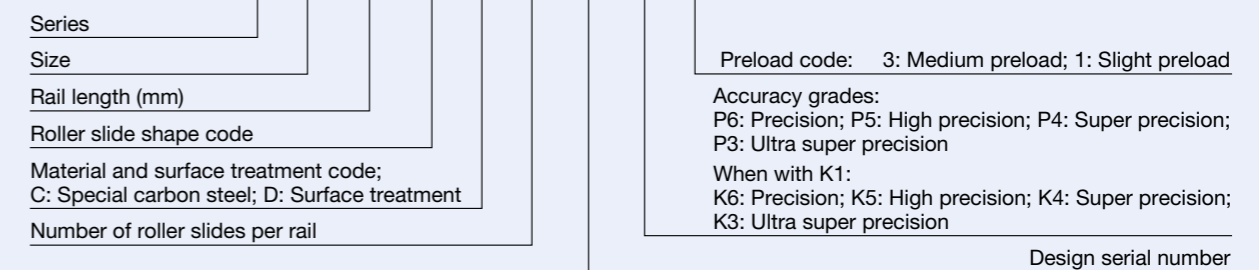


Fig. 2 Description of roller guide model number

Size: RA25, RA30, RA35, RA45, RA55, RA65
Roller slide type: AN, AL, BN, BL, EM, GM
Accuracy: P6, P5, P4, P3

	AN/AL	Square and high-load type
	BN/BL	Square and super high-load type
	EM	Flange and high-load type Available for tapped and drilled holes
	GM	Flange and super high-load type Available for tapped and drilled holes

Fig. 3 Specifications

The slight-preload roller guide of the RA series is available in a sufficient lineup of 6 models: RA25, RA30, RA35, RA45, RA55, and RA65, and is available in a total of 34 types. This lineup ensures that the slight-preload roller guide of the RA series is capable of responding to the needs of a wide range of applications.

3. Summary

At present, the RA series roller guide is used not only for machine tools but also for liquid crystal display manufacturing equipment, carrier devices, and general-purpose machinery. Selection of a more suitable roller guide for each application has become possible by the contribution of this newly developed slight-preload product.

NSK will continue to develop and increase the number of random matching products that enable any combination of rail and roller slide in the future. Managing the available stock of rails and roller slides in single component quantities will become possible upon further developments related to this product, which will better respond to customer needs by achieving quicker and more timely delivery.

Motion & Control

No. 24 December 2014

Published by NSK Ltd.



NSK used environmentally friendly printing methods for this publication.

CAT. No. ETJ-0024 2014 C-12 Printed in Japan ©NSK Ltd. 2014